THE UNIVERSITY OF OKLAHOMA

GRADUATE COLLEGE

CONCURRENT TWO-PHASE FLOW OF LIQUIDS AND GASES IN HORIZONTAL PIPING

A DISSERTATION

SUBMITTED TO THE GRADUATE FACULTY

in partial fulfillment of the requirements for the

degree of

DOCTOR OF PHILOSOPHY

BY

WILLIAM EVERETT BRIGHAM

Norman, Oklahoma

1962

CONCURRENT TWO-PHASE FLOW OF LIQUIDS AND GASES

IN HORIZONTAL PIPING

APPROVED BY

A L Huntington

Wm K Kerr

John E Powers

C M Slepcevich

E R Wilson Jr

DISSERTATION COMMITTEE

ACKNOWLEDGMENT

There are many people who materially aided the author in this investigation. Their willing help is gratefully appreciated. Dr. R. L. Huntington was the research director in this work, and his sage advice was a steadying influence. Other members of the Chemical Engineering faculty who added valuable suggestions were: Dr. O. K. Crosser, Dr. J. E. Powers and Dr. C. M. Sliepcevich.

Mr. R. L. Howard, now deceased, helped construct the experimental equipment. Mr. E. D. Holstein helped design the test apparatus, also Mr. Holstein and Mr. A. L. Coldiron assisted with most of the experimental data.

Miss Peggy Townsley and Mr. John Sievert of the Continental Oil Company helped with the intricacies of data processing on the IBM 650 and 1401 equipment. All the repetitive calculations, analysis of correlations, and table listings were done on these machines. The excellent typing was by Mrs. Jane Rega.

The Celanese Corporation provided financial assistance through a fellowship fund.

To my wife, Carol, goes the bulk of the thanks. Hers was the thankless job of being both mother and father to our children, remaining in good cheer when her husband was in the dumps and constantly prodding without becoming a termagant; all without losing her own equilibrium. She did an admirable job.

William Everett Brigham

TABLE OF CONTENTS

LIST OF TABLES

LIST OF ILLUSTRATIONS

CONCURRENT TWO-PHASE FLOW OF LIQUIDS AND GASES IN HORIZONTAL PIPING

CHAPTER I

INTRODUCTION

The General Field of Two-Phase Flow. The mechanics of motion between two fluids and the interplay of forces at the interface between these fluids have been the subject of much theoretical and experimental effort by engineers, mathematicians, and physicists. The complexities brought about by the simple addition of a fluid property discontinuity (the interface) are manifold; and thus the problem is intriguing to the theorists. These same complexities are rather more disconcerting than intriguing to the design engineer; for he finds that the theoretical studies, although interesting, do not give him the answers he needs to design his equipment. For this reason, there have also been many purely empirical attempts to get the badly needed answers.

The motion of two phases is a broad subject. For instance, this field includes the studies of wind on a surface of water such as reported by Russell (65) in 1844, later by Jefferys (46), and thoroughly treated by Lamb (51). There has been much work on the transportation of solids by fluidization, a fairly recent notable example

being Vogt and White (74). An offshoot of this problem is in the air drilling of oil wells, recently treated by Scott (69), Gray (36), and Angel (3). Also the interest has been high on gas-liquid and liquid-liquid flow in porous reservoir media, this interest sparked largely by the work of Buckley and Leverett (2). But the widest interest, and the greatest problems, arise with the simultaneous flow of fluids in piping.

Two-Phase Flow in the Production of Oil and Gas. Even when narrowing this subject to the multiphase flow of fluids through pipes one finds a wide area of interest. In the production division of the oil industry for instance, the simultaneous flow of oil and gas is the commonplace operation rather than the exception.

One common problem is in production tubing where several thousand feet of vertical distance are usually involved. Thus the pressure and sometimes the temperature are greatly different from bottom to top, and there is an appreciable change in all the fluid properties as the flow proceeds up the tubing. In addition, gas is often injected at the bottom of the tubing string to help increase the oil flow rate. The basic problem here is either to get the maximum oil rate or to get a certain production rate with a minimum volume of gas. Although the problem is easy to define, it is hard to solve, as can be seen by studying the pioneering work on this problem by Uren et. al. (72) and Gilbert (35), and later efforts by Poettman and Carpenter (61), Baxendall (12), and McAfee (57).

Once the oil and gas are on the surface, the flow is horizontal rather than vertical, but still it is often in two phases. Particularly this is becoming true in automated gathering, test, and custody transfer systems with their accompanying centralized batteries. With the recent

tremendous expansion of off-shore production, the two-phase flow problem always arises. Here the problem is one of balancing economics. A larger line costs more money to buy and lay; but to balance this, a larger pressure drop increases the subsequent compression costs. To perform an adequate economic balance, one must be able to predict the pressure drop accurately. There have been many attempts to make this prediction, as will be noted in the later chapters.

A rather interesting off-shoot of the horizontal two-phase flow problem has recently received attention in Canada. It is found that, when flowing a highly viscous crude oil, the pressure drop may be reduced by the addition of water in the line. This result is contrary to that usually found by the addition of a second phase; but it is highly advantageous to anyone faced with the practical problem of transporting viscous crude in a pipeline. Some recent experimental and theoretical treatments of this important two-phase flow problem can be found in the work by Charles, et. al. (26,27), and by Russell and Charles (66).

Flow Problems in Plant Processing. In the processing industries, two-phase flow is most commonly found in association with the exchange of heat and/or chemical reaction. Whenever there is boiling, condensation or evaporation two-phase flow is involved in the equipment. Often there are limitations as to the allowable pressure drop, so a good method of prediction is required. This phase of the problem was recognized and investigated some 20 years ago. In fact, the first serious study of two-phase pipe flow was directed toward the combination with heat transfer; for example, the work by Benjamin and Miller (15), Dittus and Hildebrand (31), and McAdams, et. al. (56).

If in addition there is a chemical reaction involved the volume of each fluid in place in a two-phase system is also of great importance, for the residence time in the reactor is always an important variable in the over-all reaction kinetics. Although there has been a multitude of data reported on the shut-in (or in-place) ratios, the only accepted generalized correlation is that by Lockhart and Martinelli (52).

A further complication arises when the two-phase pipeline flow includes appreciable hills and valleys. A report on the extra pressure drop to be expected due to hills was published by Brigham, Holstein, and Huntington (21) based on their laboratory data; and by Baker (6,7) and Flanigan (32) on field data. From these papers one can see the pronounced effects that hills may have on pressure drop in two-phase pipe lines.

Scope of Present Investigation. It is apparent from the above that there is a large array of two-phase flow problems which, at best, are only partially solved. The immediate question, then, becomes one of narrowing down the scope of an investigation to only a small facet of the total problem.

In reviewing the literature on two-phase flow and considering the needs of industry, it appears that the greatest occurrence of two-phase phenomena is in the simultaneous horizontal pipe flow of liquid and gas. Also this facet of the problem is among the less well understood although it has received a large amount of attention in the literature.

The investigators of gas-liquid pipe flow can be divided into two classes. A small group, has attacked the problem with a theoretical

approach. The larger group, by far, has attempted to correlate their data using empirical means with a minimum of theoretical reasons for their correlations.

The results of these two types of investigations have not been entirely satisfactory. So far the empiricists seem to have the edge over the theorists (largely due to weight of numbers). The theoretical treatments have in no case lead to a workable correlation of two-phase flow phenomena. The empiricists have produced a multitude of correlations, each one fitting the data presented; however as is often true with empirical approaches, these correlations lose their validity when the range of variables is extended. Some of these are being used today for the predictions the engineer must make, but their accuracy leaves much to be desired.

The purpose of this investigation of two-phase flow is to attempt to weld the theoretical and the empirical methods. The approach used was to study the visual flow phenomena; and, from these visual studies, to develop a theoretical model which matched the observed flow characteristics. With this approach it was possible to predict which variables are important in two-phase flow, and to a large extent the quantitative importance of these variables. The theory is extended as far as possible toward the desired correlations, and then empiricism is introduced where necessary to determine constants of multiplication or exponentiation in the correlations. This approach is successfully used in later chapters to predict both the horizontal two-phase pressure drop and the ratios of fluids in place.

CHAPTER II

PREVIOUS INVESTIGATIONS

Correlations by Martinelli and Coworkers

In any treatise on simultaneous gas-liquid pipe flow, one is drawn to the pioneering efforts of Martinelli, et. al. (53). The correlations presented in that paper and in later papers by Martinelli, Putnam and Lockhart (54), by Lockhart and Martinelli (52), and by Martinelli and Nelson (55) have been the standard for comparison of subsequent investigators. Let us briefly review this work.

Although never stated directly in any of the above papers, there are two basic assumptions underlying the theory in these correlations. The first assumption is that the friction factor equation is valid in two-phase flow; and that the functional relationship between the friction factor and the Reynolds' Number remains the same in two-phase flow as in single-phase flow.

The second assumption is that the gas flows through a constant cross sectional portion of the pipe and the liquid through the remainder. This assumption eliminates the commonly found flow patterns of Plug and Slug Flow, wherein the liquid and gas alternate their positions in a portion of the pipe. In spite of being eliminated in the theoretical analysis, however, these types of flow are included in the data correlated by Martinelli, et. al.

The pressure drop in two-phase flow is greater than in single-phase flow. The magnitude of this increase is covered in the Martinelli correlations by the use of the hydraulic radius, and by recognizing the fact that the available cross-sectional area to flow of either phase is reduced by the presence of the other phase. These basic tenets lead to the following equation,

$$\left(\frac{\Delta P}{\Delta L}\right)_{TP} = \left(\frac{\Delta P}{\Delta L}\right)_G \left[1 + \alpha^{1/4}\left(\frac{\mu_L}{\mu_G}\right)^{0.083}\left(\frac{\rho_G}{\rho_L}\right)^{0.416}\left(\frac{W_L}{W_G}\right)^{0.75}\right]^{2.4} \quad (1)$$

where $(\Delta P/\Delta L)_{TP}$ is the actual two-phase pressure drop; $(\Delta P/\Delta L)_G$ is the pressure drop one would expect if only gas were flowing through the pipe with no liquid present; and α is a dimensionless hydraulic radius term which accounts for the non-circular (actually crescent shaped) nature of the liquid cross section. The other terms are density, ρ, viscosity, μ, and mass flow rate, W. Notice that there is no gas hydraulic radius term corresponding to the liquid term, α. Martinelli, et. al., from their visual data, reasoned that the actual cross section available to gas flow was close to being circular, and further felt that any slightly non-circular nature of the gas cross section would be accounted for in the liquid term. By trial-and-error they determined what variables best correlated $\alpha^{1/4}$ against the measured pressure drop. The best fit was found by correlating $\alpha^{1/4}$ against its multiplier, $(\mu_L/\mu_G)^{.083} \times (\rho_G/\rho_L)^{0.416} \times (W_L/W_G)^{0.75}$.

In one of their later papers, Martinelli, et. al. (42), realized that the correlating term (the term containing the μ's, ρ's, and W's) was actually the ratio of the pressure drop if only liquid were flowing,

over the pressure drop if only gas were flowing. Thus the final correlations could be greatly simplified by relating the increase in pressure drop to the all-liquid/all-gas pressure drop ratio.

What of the theoretical validity of the Martinelli correlations? There are two basic points in the logic leading to their correlations that are open to considerable doubt. The first is in the use of the hydraulic radius. The hydraulic radius, according to its definition is the cross-sectional area divided by the wetted perimeter, where the wetted perimeter is the plane along which the shear forces act with a decelerating force on the fluid. This results in a pressure drop in that fluid. But in two-phase flow, at the interface between the gas and liquid, there is an accelerating force on the liquid rather than a decelerating force; so this interface cannot be properly considered part of the wetted perimeter. It is so considered in the correlations.

The second, and probably the greater flaw is in the assumption that $\alpha^{1/4}$ can be correlated properly against its multiplier, $(\mu_L/\mu_G)^{0.083} \times (\rho_G/\rho_L)^{0.416} \times (W_L/W_G)^{0.75}$. There is no theoretical or logical basis for this assumption. This is undoubtedly the reason for the banding of data around Martinelli's correlation, as was pointed out by Gazley and Bergelin (34). Gazley and Bergelin (17) also mentioned that the correlation is not as accurate as it first appears, since the data were plotted proportional to the square root of the pressure drop, rather than to the first power. Thus an apparent error of 25 per cent is really an error of 55 per cent on pressure drop.

In spite of these faults, the Martinelli correlations have remained the most commonly used of those available in the two-phase flow

literature, and they have been commonly used as a basis for revision and extension. In addition, Martinelli's is the only generalized correlation available for the prediction of shut-in (or in-place) gas/liquid ratios.

Revisions and Extensions of the Martinelli Correlations. Many people have taken Martinelli's basic correlations and extended them to include other ranges of pressure, pipe diameter, and flow rate. For instance, Begell and Hoopes (14) showed that in a boiling mixture the expected pressure drop should be higher than predicted, due to acceleration and gravitational effects. They show how to calculate these extra terms. Johnson and Abou-Sabe (48) found that the amount of liquid in place in the pipe was less than predicted by Martinelli. Alves (2) reported that the flowing mixtures exhibited various types of flow patterns (Slug, Plug, Stratified, etc.) and found that the pressure drops and the validity of the Martinelli correlations depended on the pattern of flow. This was also expressed by Bergelin and Gazley (16,17,34), d Hoogendorn (42). Rogers (63) used the Martinelli correlation to calculate pressure drops for two-phase flow of hydrogen, but presented no data.

Baker in several articles (6,8,9,10) has made some major revisions of Martinelli's basic pressure drop correlation. These are based on a combination of field and laboratory data. The correlation was empirically "fudged" using various parameters depending on the flow pattern. He also correlated flow patterns based on Alves' (2) descriptions. Baker's empirical correlations have been widely used in the pipeline branch of the petroleum industry for the prediction of two-phase pressure drops, and have been found to be particularly useful in

the Slug Flow region (5). Another test of Martinelli's correlation was made by van Wingen (73) on oil and gas gathering systems. He found at low gas rates that the correlation was too low; and at high gas rates, too high. He presented new curves which came closer to matching his data.

Another important extension of the Martinelli form of correlation was made by Chenoweth and Martin (29). Their correlation was based on the ratio of the actual two-phase pressure drop to the pressure drop predicted if all the flowing material were liquid. They included correlation parameters of liquid volume fraction in addition to the Martinelli ratio of the all-liquid to the all-gas pressure drops. However, in their pressure drop ratio they used the total mass rate, rather than the mass rate of each phase separately, as used by Martinelli, et. al. Their correlation fits data at greater ranges of pressure and pipe diameter than Martinelli's. Reid, et. al. (62) took data in 4-inch and 6-inch piping and also found that the Chenoweth and Martin correlation was more accurate than Martinelli's. Also they tested their data against Baker's correlation (10) and found that there was very poor agreement.

Pseudo Friction Factors

A number of investigators have attempted to correlate horizontal two-phase pressure drops using a modified friction factor equation or a modified Reynolds Number correlation. For instance, Bertuzzi, et. al. (19), calculated a friction factor using the total volumetric liquid and gas rate and the total mass rate. Their Reynolds Number was a combination of the liquid and gas Reynolds Numbers to various powers, depending on the relative amounts of liquid and gas flowing. Tek (70,71) recently

has used this same correlating technique on vertical flow. In these correlations, the exponents on the Reynolds Number were adjusted so that when only one fluid is flowing, the correlating parameters reverted to the proper single-phase Reynolds Number and friction factor. The authors seemed to feel that this put the correlation on a sound theoretical basis. They neglected to mention, however, that the correlation itself does not revert to the single-phase values—only the parameters do. Briefly then it is not difficult to see that this approach is also largely empirical.

Schneider, White, and Huntington (68) have also used a pseudo-friction factor, this based on the gas flow rates. It was correlated against the ratios of the gas to liquid mass rates and the gas to liquid viscosities. This correlation has found some application in the petroleum pipeline industry.

Baxendall (12,13) in two papers has shown a horizontal two-phase correlation of friction factor using a modified Reynolds Number in which the viscosity is not included. This correlation is based on Poettmann and Carpenter's (61) original work on vertical flow. It closely predicts the horizontal pressure drop for Baxendall's specific field conditions. However, it is somewhat limited, since the flow rates were high and the gas-oil ratios were quite low. Hoogendorn (42) has presented a variety of pseudo-friction factor correlations, each differing depending on the flow pattern. His data are also compared against the Martinelli correlations, and were generally not found to agree with them.

Empirical Correlations

All the above-mentioned work, although empirical to a large

degree, was at least partially based on established single-phase flow relationships. However, in addition to these, there are a number of correlations that are strictly empirical. The most noteworthy is the one presented by White and Huntington (77). This correlation consistently fits the low pressure laboratory data in the Wavy and (Semi) Annular flow patterns. For instance, it has been tested against the data of Schneider (67) Green (37) Martinelli (53) and Jenkins (47), and it is remarkably accurate. However, it does not fit the pressure drop data at larger diameters or higher pressures. This, of course, is a common fault of a purely empirical correlation. It must necessarily be viewed with distrust for conditions outside the range of data on which it is based.

A recent correlation has been presented by Chavez (28). A design engineer should be skeptical about using this correlation which is supported by only a small amount of data. Berry and Moreau (18) have presented a correlation relating the pipeline efficiency of a gas condensate line to the gallons per MMSCF of condensate carried in the line. No data are presented, so there is no adequate test of its validity. Flanigan (32) has also presented a pipeline efficiency correlation for condensate lines. This is based on gas velocity as well as the gallons per MMSCF used by Moreau and Berry. The correlation appears adequate for the rather narrow range of data used. Baker (10) has shown a "rule of thumb" method of approximating two-phase line sizes. He calculates the diameter needed to carry only the liquid, and the diameter to carry only the gas. The diameter of the line needed to carry them both is merely the sum of these two. Campbell (25) has also mentioned a "rule of thumb" for condensate gathering lines and gasoline plants wherein he

calculates the gas pressure drop and multiplies this by three for the two-phase pressure drop. He states this method has been quite successful for this limited application.

Fundamental or Theoretical Work

Gazley (33) has attempted a fundamental approach by investigating the energy transfer and losses at the gas-liquid interface, and also measuring the regions of interfacial stability. This work was limited to Stratified Flow. No generalized or unified theory has come of this work. Similar data were taken by Hanratty and Enzen (40) in a horizontal rectangular conduit flowing water and air. Excellent velocity profile data were taken along with data on the character of the water surface waves, but no generalized "truths" concerning the mechanics of the two-phase motion were apparent.

Govier and Omer (39) recently have taken some careful shut-in, pressure drop and flow pattern data of water-air pipe flow. Their data show the extra pressure drop expected due to the addition of the second phase and in general agree with the data of Johnson and Abou-Sabe (48), and Schneider (68). Aziz (4) attempted a theoretical treatment of annular flow of liquid and gas. This was based on the single phase theories of von Karman (75). He introduced a ratio, "K", which compares the actual two-phase pressure drop with that predicted using von Karman's "universal velocity profile". However, no generalized relationship was found for the value of "K".

The excellent work by Calvert and Williams (23) should be mentioned. These authors investigated the annular vertical flow of

water and air; however, their method of analysis is quite basic, and much of the theoretical work is equally valid in horizontal flow. Using an analogy to single-phase flow, they were able to predict the pressure drops for all but the highest rates where entrainment is an important factor. The only attempt to use this same technique in horizontal flow (see Aziz above) has not been successful. Abramson (1) investigated horizontal annular flow in terms of interfacial turbulence. He found that the points of onset of interfacial instabilities fit remarkably well with the accepted single-phase theories (11,75) of a laminar boundary layer and a turbulent core. However, he made no attempt to relate his findings to a correlation of pressure drops or shut-in ratios. Wicks and Dukler (78) have also studied annular flow, directing their efforts toward the amount of entrainment as well as the pressure drop. Their work indicates that the entrance section design and length will affect these flow variables; and they point out the erroneous results that may be reported by the use of too short a stabilizing section and test section. The entrainment data were best fit by a Martinelli type correlation. Isbin, et. al., (44) were also interested in volumes in place. They reported data at wide ranges of temperature and pressure, but were not able to arrive at a general correlation.

Summary

The ultimate desire of any investigator of two-phase flow is the understanding of the flow mechanism such that he can predict the pressure drop and the in-place ratios of fluids, and also present a clear picture of the flow behavior within the pipe. In reviewing the

above investigations it becomes apparent that the most successful prediction work has been done by those who have relied on largely empirical means for their prediction methods. These empirical methods, however, are limited in their applicability to a rather narrow range of data. Further, they add little to the basic understanding of the problem. The theoretical investigations, on the other hand, have contributed to the understanding of the flow behavior; but in no case have they been successful in making the necessary predictions in horizontal flow. The desire of this writer is to use the advantages of both approaches for the problem.

It should be mentioned that the references cited in this chapter represent only a small fraction of the total available literature on the concurrent two-phase flow of fluids. Only the articles the writer felt were most significant were included in this discussion. Particular stress was put on the more recent literature except in the cases of older articles which have played a decidedly important role. For the more interested reader, excellent bibliographies of all but the most recent literature can be found in the writings of Isbin, et. al., (43,45) Campbell (24) and White (76).

CHAPTER III

EXPERIMENTAL EQUIPMENT AND PROCEDURE

In brief, the equipment used was a double loop of clear plastic pipe through which air and various liquids could flow simultaneously. The tubing was fitted with pressure taps such that the pressure drop could be measured over portions of the tubing as well as over the entire test section. In addition, other necessary auxiliary equipment such as orifices, displacement meters, and thermometers were included to measure the flow rates, temperatures and the differential and static pressures of the flowing fluids. Quick-closing valves were installed at the inlet and outlet to help measure the ratios of the fluids in place. A diagram of the test loop is shown in Figure I.

Test Section

It was felt that good visual data on the flowing fluids was a highly important item to consider in this experimental program. Clear plastic piping seemed to be made to order to fit this need. A butyrate tenite plastic made by Tennessee-Eastman, sold under the trade name, Kraloy, fit the requirements of strength, transparency, and ease of handling. The tubing, nominally 2 inches in diameter, was found to have an internal diameter of 1.975 inches.

The tubing was equipped with tightly fitting bell joints. By

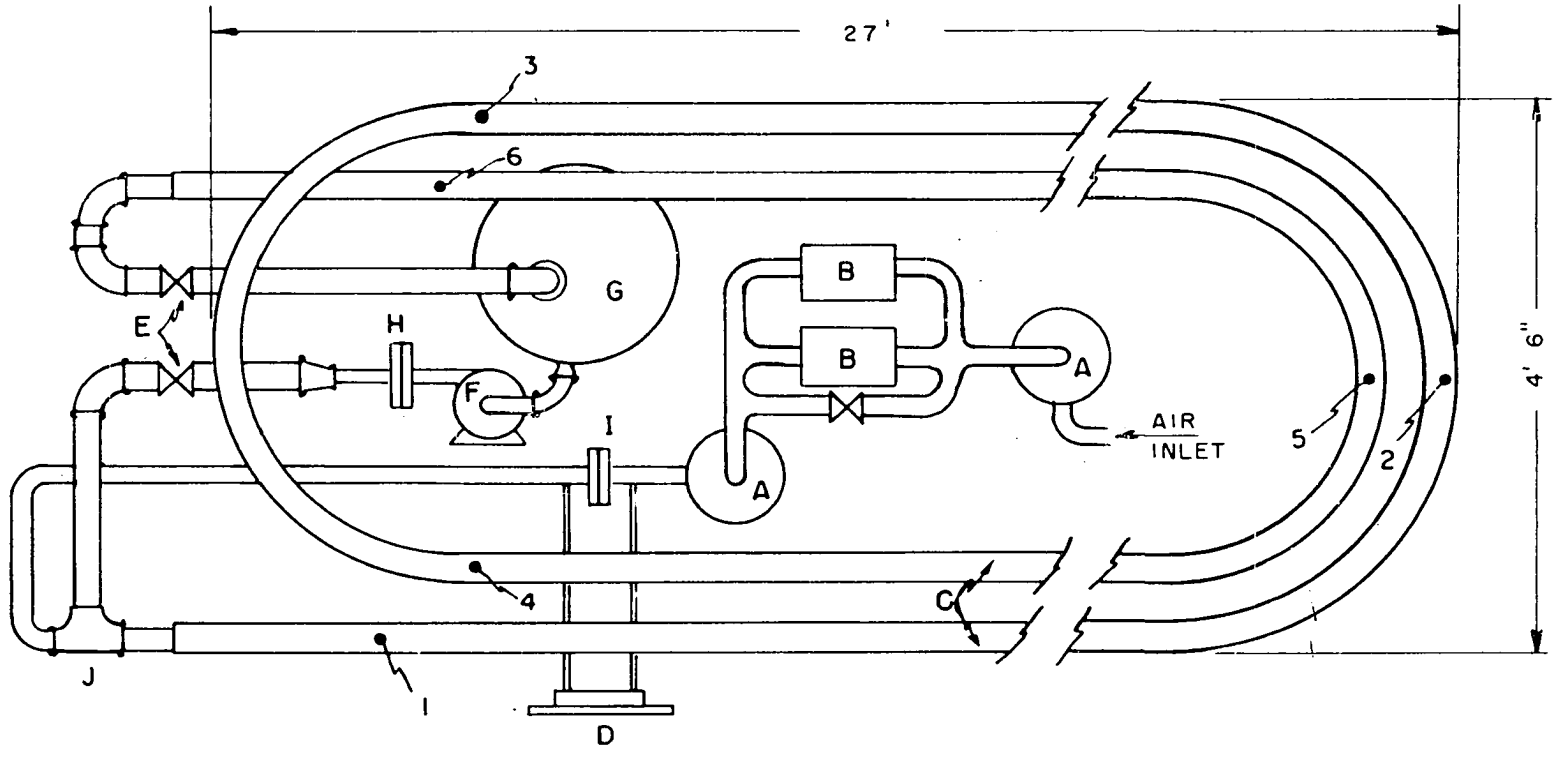

ARABIC NUMBERS 1 THROUGH 6 INDICATE MANOMETER TAPS

A = AIR SEPARATORS
B = POSITIVE DISPLACEMENT METERS
C = 2-INCH PLASTIC TUBING TEST SECTION
D = AIR FLOW RECORDER
E = QUICK CLOSING VALVES
F = LIQUID PUMP
G = LIQUID STORAGE DRUM
H = LIQUID ORIFICE METER
I = AIR ORIFICE METER
J = LIQUID-AIR MIXING "TEE"

FIG. I FLOW DIAGRAM OF TEST SECTION

trial-and-error it was found that better connections for this purpose could be made by cutting off the belled ends and butting the joints. This type of bond was more easily repaired in case of leaks and also presented a smoother internal surface to the flowing fluids. Cement for joining the pipe sections was made by dissolving chips of the tubing in ethylene dichloride. Leaks could be detected by pressuring the piping with air and spreading a soap solution on the joints.

The test section was a double loop so that an effectively longer section could be contained in the space available. Attempts were made to heat and bend the tubing to make the three required "U" bends, but to no avail. Eventually each "U" bend was fabricated from 9 short straight pieces of tubing cut at a 9° angle at each end. This made acceptably smooth return loops. The overall test section was approximately 4 1/2 feet wide and 27 feet long. This included 120 feet of straight tubing and 16 feet in the three "U" bends.

At the inlet and outlet ends, plastic sleeves were cemented in the piping and internally threaded for 1 1/2 inch standard pipe. The entrance mixing "tee" was made from a standard 1 1/2 inch pipe tee with a copper tubing inserted in the run of the tee to introduce the air from a flexible hose into the test section. The side outlet of the tee, faced downward, was used for the liquid entrance. On all runs there were 26 inches of plastic piping for a calming section between the end of the air entrance tubing and the first pressure tap. A cross-section sketch of the entrance "tee" is shown in Figure II. Three bleed-off taps were installed in the test section to collect liquids for the shut-in data.

Pressure taps were placed at six locations on the test section.

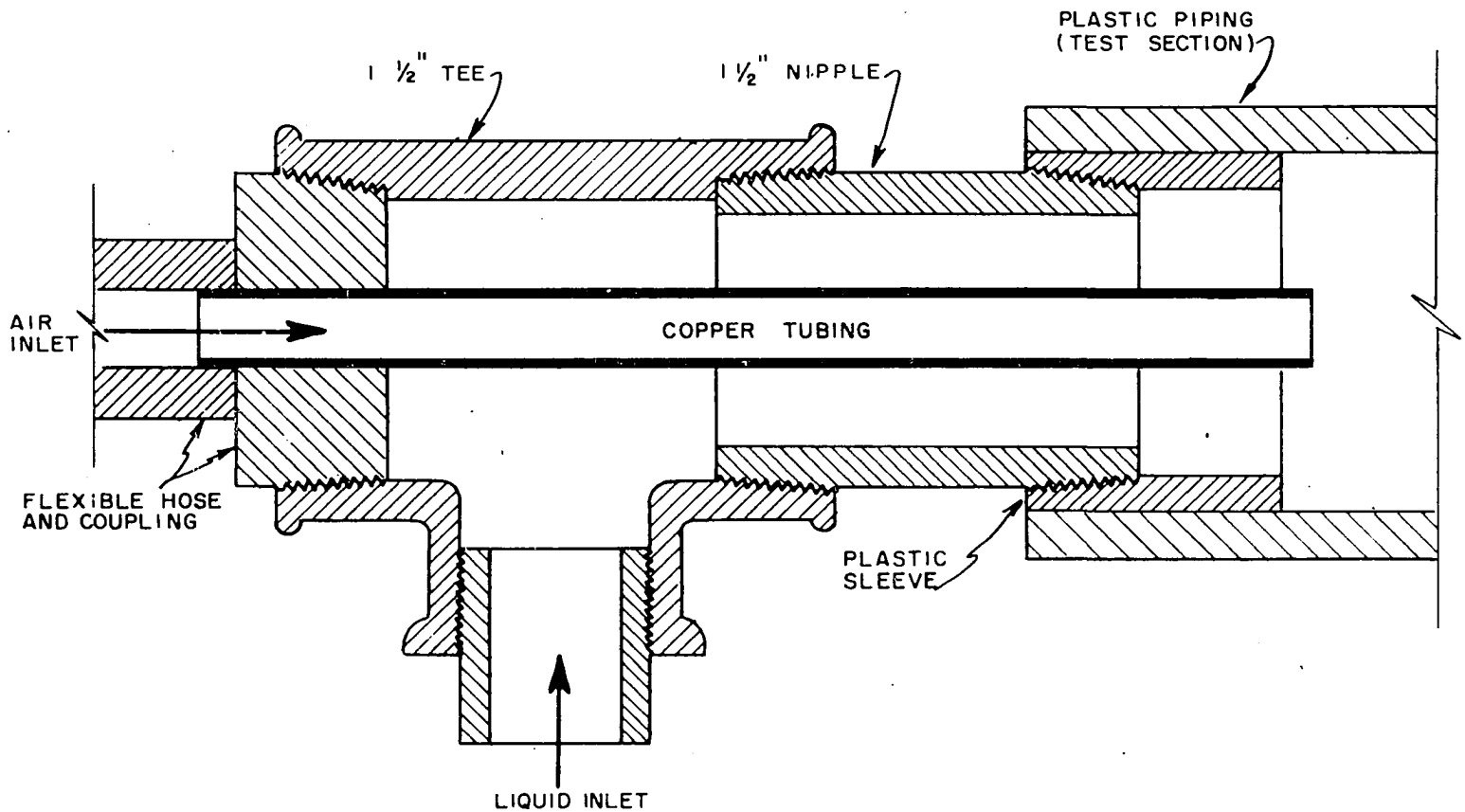

FIG. II INLET TEE

Their approximate location is shown in Figure I. Taps No. 3 and No. 4 were at each end of a "U" return bend. Thus the pressure drop across this "U" bend could be compared to the total pipe pressure drop to get the equivalent length of a bend. The pressure taps were 3/16 inch holes drilled in the top of the test pipe. A short piece of 1/2 inch I.D. Kraloy tubing was cemented over the hole to act as a liquid-gas separator to keep liquid from carrying over into the pressure lines. For greater strength a back-up plate, with a hole cut for the separator tubing, was cemented to the test pipe wall. A brass adaptor was fitted into the top of the separator tubing and from there the line went to the appropriate manometer(s). A sketch of this pressure tap set-up is shown in Figure III.

In some of the flow patterns the pressure fluctuations were extremely high. In fact, in Slug Flow sometimes the variation in the readings was greater than the average reading. After a few runs were made it became apparent that some method was needed to minimize the pressure fluctuation in the manometer lines. The system finally selected was a combination of large buffer cylinders and a packing inserted in brass fittings. The buffer cylinders acted as reservoirs to absorb the pressure fluctuations and the packed fittings acted as a highly resistive flow path. At the beginning the brass fittings were packed with steel wool, but it was found that these packings gradually rusted, closing off the manometer lines completely. Later, glass wool was used and it was found to be excellent. It was necessary to try various degrees of "tightness" in the packing until the fluctuations were suitably damped out without impairing the readings. To help adjust the packing, a number

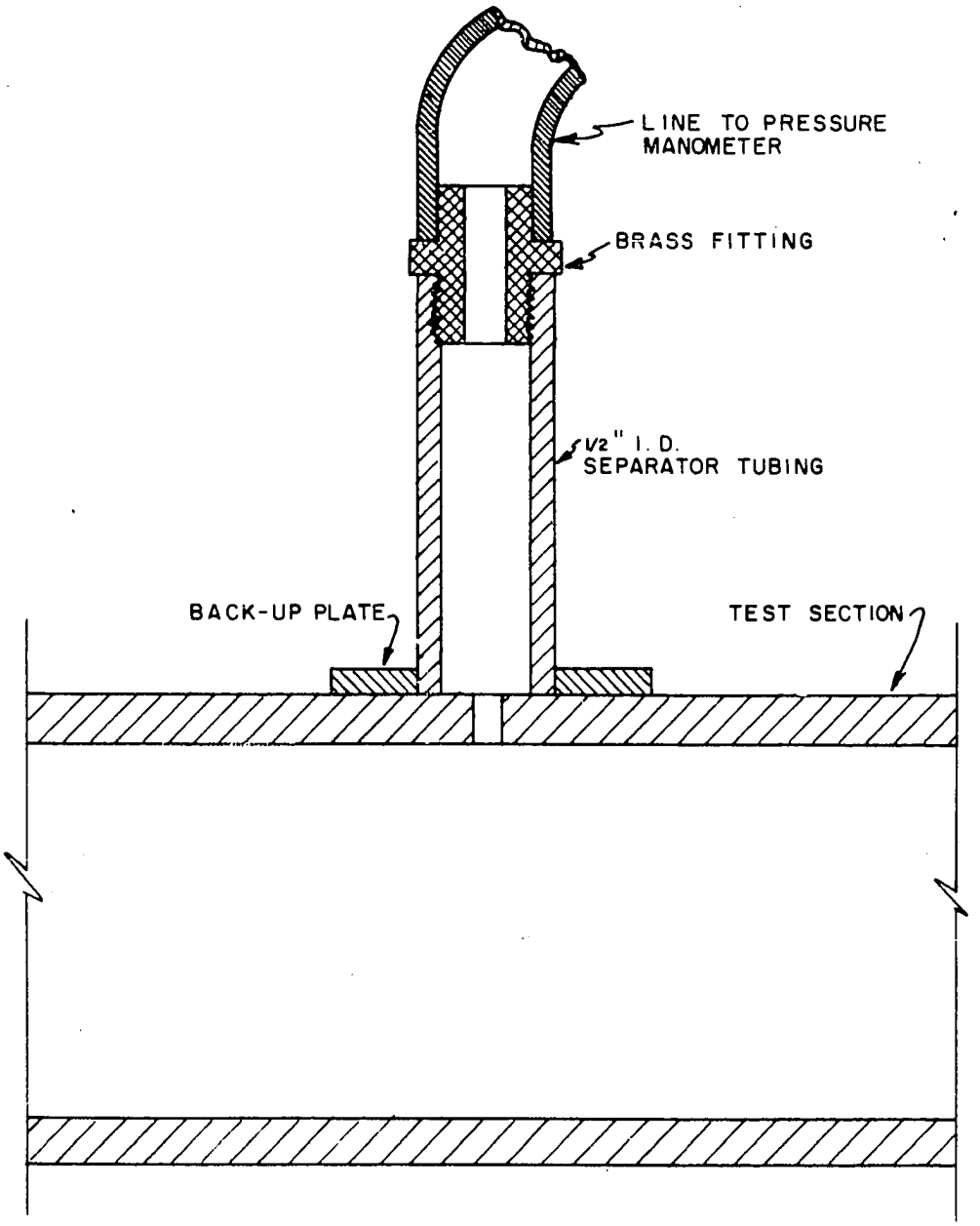

FIG. III PIPE PRESSURE TAP

of comparisons were made between readings with and without packing for those types of flow which had little pressure fluctuation.

A sketch of a typical manometer connection is shown in Figure IV. The reader will notice that this combination of buffer-plus-packing is very similar to the common filter circuit used in radios, television sets, and other electronic equipment to eliminate the A. C. component of a D. C. voltage supply. There is a direct analogy to the result desired in these experiments, in that it is desirable to filter out the "A. C." component of the pressure.

During some of the runs, the manometers were all connected to read static pressure, with the exception that one manometer read the differentail from tap No. 3 to No. 4 across the return bend. With this set-up, any pressure differential reading across a given portion of the test section could be obtained by subtracting the two appropriate manometer readings. Later the lines and manometers were changed so that all manometers read differential readings: that is, from tap No. 1 to No. 2, tap No. 2 to No. 3, etc. In addition, a static reading was made at tap No. 3 to get the average pressure in the test tubing. In this case any desired differential reading over a larger portion of the pipe could be calculated by adding the appropriate manometer readings.

The manometer fluids used were water mercury or tetrabromoethane (Sp. Gr. 2.964), depending on the specific pressure range needed. Of course with either manometer set-up, the pressure differentials could be read over the entire pipe or only a portion of the pipe as desired; however, it was found that even with buffers present in the line, the pressure fluctuations were too great for the intermediate pressures to be

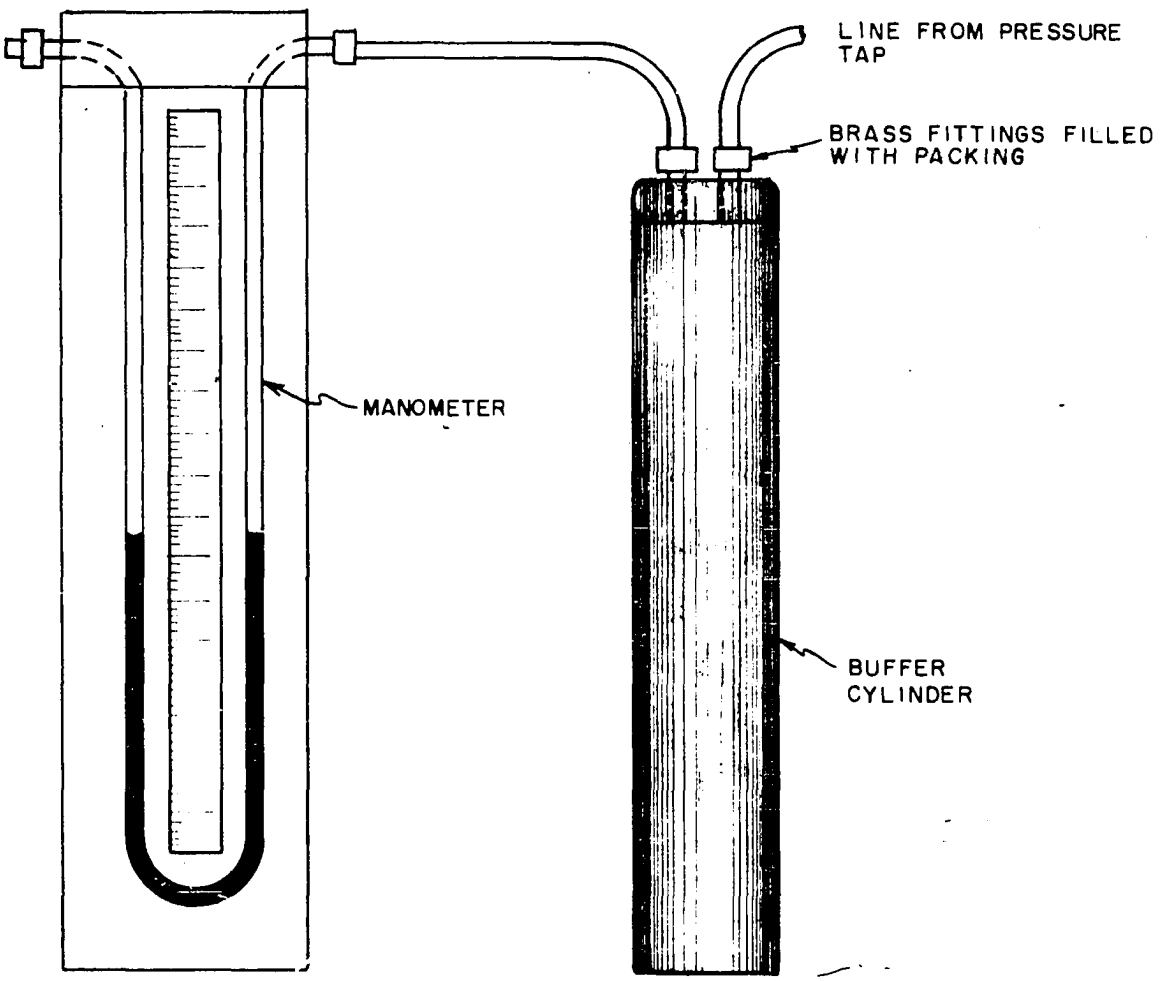

FIG. IV TYPICAL MANOMETER CONNECTION

meaningful. For this reason only the overall pressure drops are reported.

The overall test section was mounted on a 1-inch by 1-inch angle iron frame with several angle iron cross bars to support the tubing. The tubing sagged somewhat between the cross bars, but the deviation was judged to be no more than 1/2 inch from the horizontal. In addition the frame was designed so that it could be raised to any desired angle for the inclined data reported by Brigham (22) Holstein (41) and Coldiron (30). Since this dissertation is not directly concerned with inclined data, the details of the construction will be omitted. These details may be found in any of the above references, including pictures showing the elevating tees.

Metering and Auxiliary Equipment

The test liquids were stored in a 55-gallon drum which acted both as the reservoir for the liquid supply and as a separator for the outlet stream of liquid and air. Four inches of wire mesh screen were placed in the top of the drum. This effectively eliminated entrainment of the liquids in the exit air stream. For some of the data a centrifugal pump equipped with a by-pass line was used for liquid circulation. Later the centrifugal pump was replaced by a positive displacement pump for greater stability against pressure fluctuations and for a higher output. The liquids were metered in a 1-inch vertical meter run using 0.25-inch and 0.54-inch orifice plates and a mercury manometer. The orifice plates were calibrated directly by weighing the output from a pump over a timed interval.

The air supply was tapped from the University of Oklahoma

compressed air lines. After about half the runs had been made, the air supply arrangement was modified because the on-off action of the University air compressor caused a pressure fluctuation from about 120 psig to 100 psig. A Kimray pressure regulating valve was installed in the line which held the downstream constant at 70 psig.

The air was metered with an Emco orifice meter recorder to read differential pressure. Orifices of 0.672-inch and 0.872-inch diameter were used in a 2-inch horizontal meter run to give the desired range of air rates. A 0-60 pound Reid gauge was mounted on the recorder and gave the flowing pressure on the downstream side of the orifice. The gauge pressure could be read to the nearest 0.1 pound. The Emco meter was adjusted by a representative of the Phillips Petroleum Company.

Two positive displacement meters were used to calibrate the Emco meter. Their maximum capacities were 1800 and 2500 cubic feet per hour. Even in parallel this was somewhat short of the maximum range of rates used in the experiments, so the calibration curves later had to be extrapolated. Separators were installed both upstream and downstream of the positive displacement meters, thus no liquid could carry over and ruin the readings. Also a by-pass line was piped around these meters so that, once the Emco meter was calibrated, no air flowed through them. For the data at very low air rates, only the positive displacement meters were used for flow measurements since the Emco meter was not accurate at low rates.

Temperature measurements were made on incoming air, on the liquid reservoir drum, and on the effluent as it came from the test section. These temperatures could all be measured within 1°F. Generally,

once the flow rates had stabilized, the thermometer readings did not differ from each other by more than 5°F, which showed that the fluid properties were effectively constant during a run.

Equipment Calibration

The liquid orifice calibrations were plotted on log-log paper as flow rate versus manometer reading. As expected, the plot was a straight line with a slope very close to 0.50, indicating a nearly constand orifice coefficient. A typical example of a liquid orifice calibration is shown for glycol in Figure V.

The air orifices were calibrated against the positive displacement meters. The results of these calibration runs can be seen in Figure VI. In this graph the Emco orifice reading in inches of water is plotted against a pseudo orifice coefficient, K, which is equivalent to the air rate in pounds per minute divided by the term $\sqrt{P(\Delta P)/T}$. In this square root expression, P is in pounds per square inch, T is in degrees Rankine, and ΔP is in inches of water. One can see that this pseudo coefficient is based on the usual orifice equation; except that, rather than being in its correct dimensionless form, all the dimensional conversion factors have been included in the constant, K. This was done merely for convenience in later runs when making direct calculations of air flow rates from the meter readings.

Notice also that for the 0.872-inch orifice, there are no calibration points reading above 30 inches of water. No calibration could be made at this high an air rate due to the maximum limitation on the positive displacement meters (1800 cu ft/min plus 2500 cu ft/min). However,

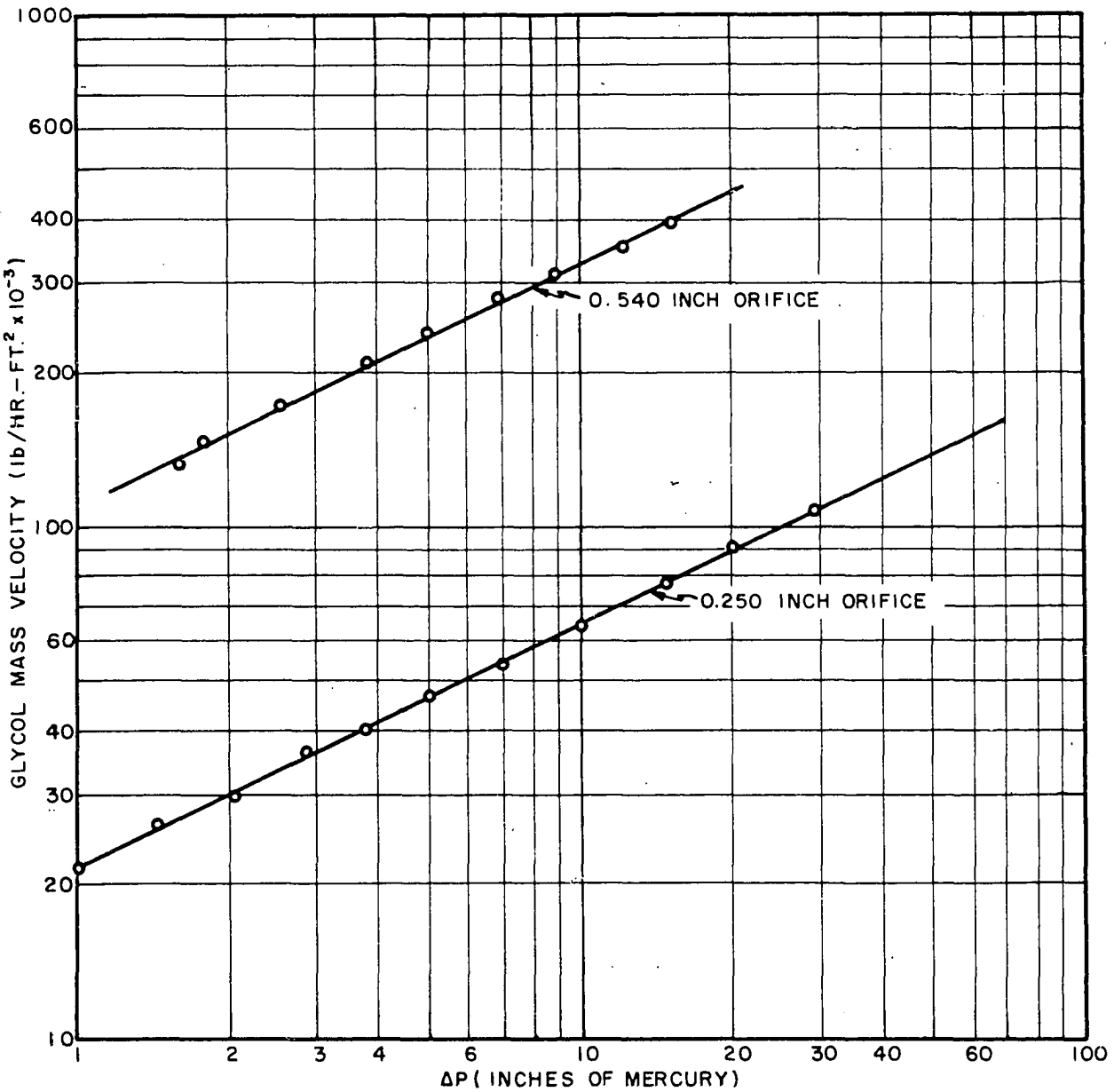

FIG. V GLYCOL CALIBRATION

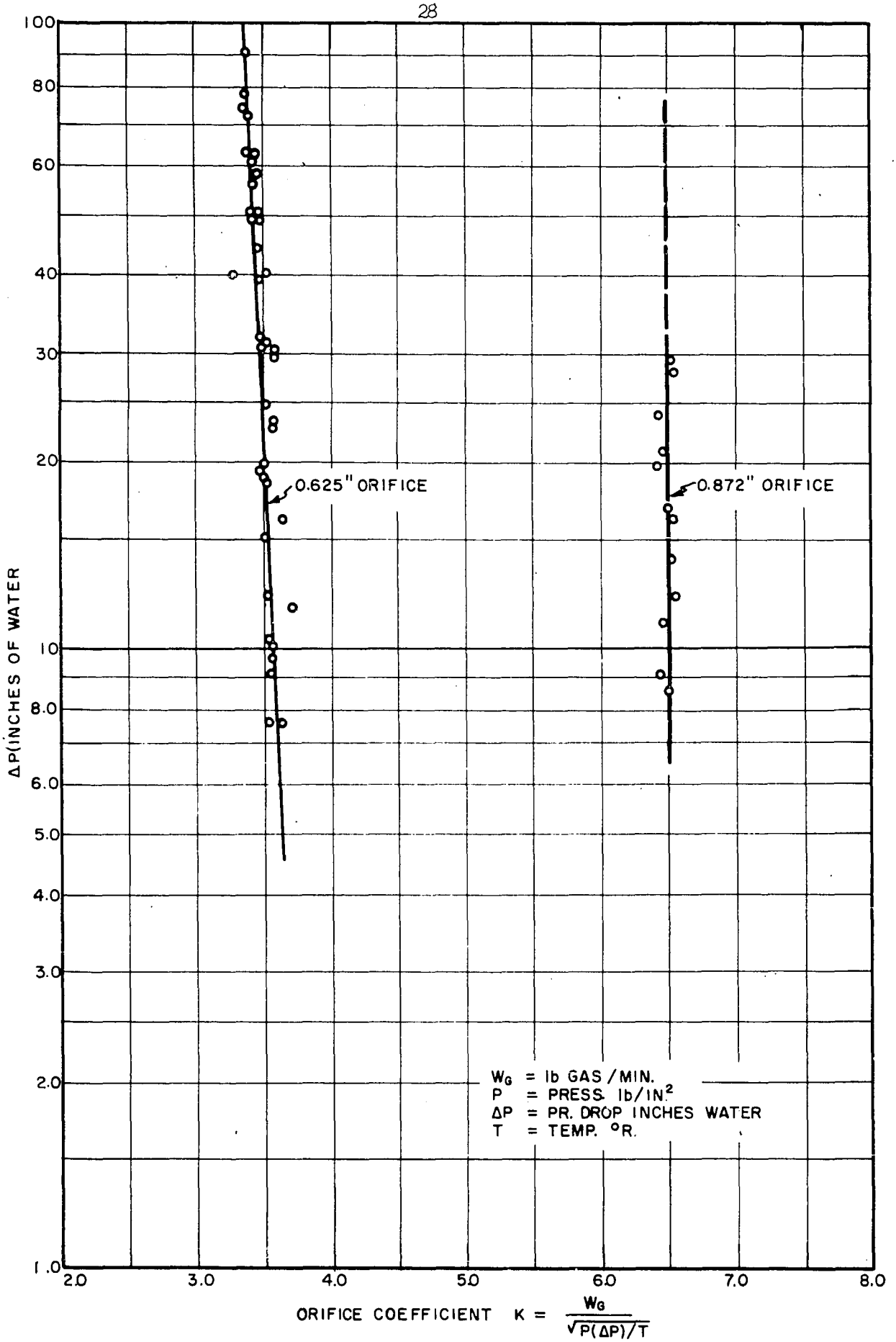

FIG. VI CALIBRATION OF AIR ORIFICES

within the accuracy of the data, it appeared that the coefficient, K, was constant at 6.50 at lower rates; so this value was assumed at the higher rates, as implied by the extrapolated dashed line in Figure VI.

The test loop itself was also calibrated: that is, pressure drops were measured with air flow only in the loop to determine its equivalent length and also to find the best fit of Moody friction factor versus Reynolds Number for this type of pipe material. For some of the calibration runs the actual length of the test section was 112 feet, with an equivalent length of 125.5 feet due to the somewhat greater pressure drop around the bends. Later, the test loop was lengthened slightly with revisions in the exit section, and the equivalent length was increased to 128.4 feet. These equivalent lengths were calculated by comparing the pressure drop around a bend (from pressure taps No. 3 and No. 4) to the total pressure drop in the test section when flowing air through the tubing.

The calibration data relating the experimental friction factor with the Reynolds Number for the flow of air are shown in Figure VII. A least squares fit of the data gave the following equation for the friction factor.

$$f = \frac{0.134}{(Re.\ No.)^{0.187}} \qquad (2)$$

This plastic tubing gave slightly lower friction factors than Von Karmans' (75) equation for smooth tubing.

Test Fluids

It was desirable to use liquids that varied widely in physical

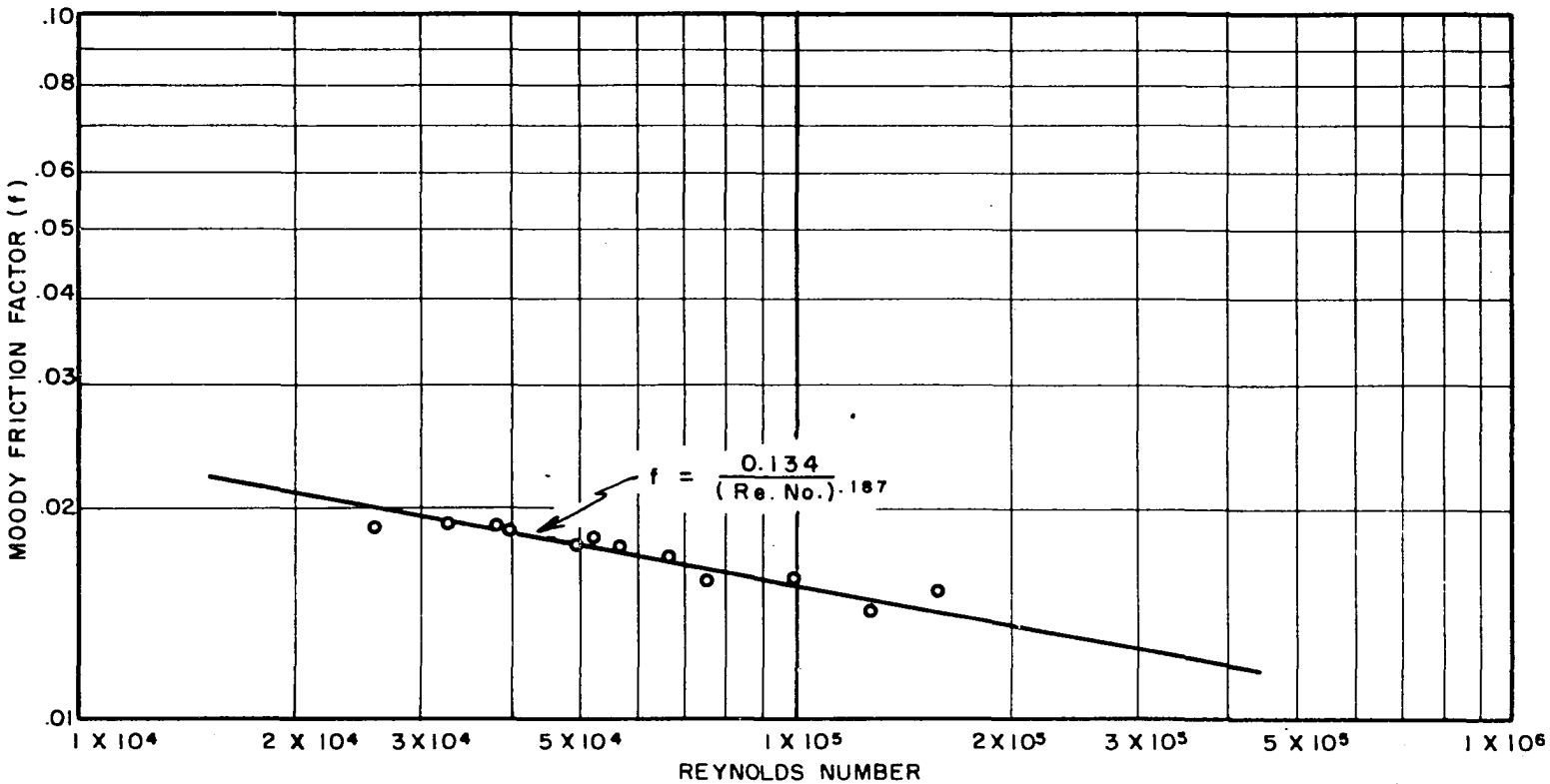

FIG. VII EXPERIMENTALLY DETERMINED FRICTION FACTORS FOR KRALOY TEST PIPE

properties, but still would be inexpensive in bulk quantities. Water, of course, was a natural choice; and the other two liquids were No. 10 S.A.E. oil and commercial 95 per cent diethylene glycol. The properties of liquids do not change greatly with temperature, so it was sufficiently accurate to use average values of density and viscosity of each liquid.

For some of the water runs the average temperature was 72°F. The viscosity and density of water at this temperature were found in Perry (60) to be 0.958 centipoise and 62.29 lb/cu ft. Some later runs were at an average temperature of 75°F. At this temperature the viscosity of water (from Perry) is 0.916 centipoise and density 62.26 lb/cu ft. The viscosity and density of the glycol and oil were measured with an Ostwald viscometer and a pycnometer. The glycol had an average temperature of 82°F at which the viscosity was 19.4 centipoise and density was 69.3 lb/cu ft. The average oil temperature was 78°F and the measured properties were: viscosity, 70.4 centipoise, and density, 53.8 lb/cu ft.

The air properties (excepting temperature and pressure) were not measured. The viscosity of air, like that of the liquids, was assumed constant at the average temperature of a given set of data; and it was read from the gas viscosity chart in Perry (60). This showed only a variation from 0.0180 to 0.0182 centipoise in the temperature range of the runs. The density of the air was calculated using the average pressure in the pipe for each run and the average temperature of each run. Ideal gas laws were assumed to hold for air. This is quite a good assumption. For instance, at room temperature and 25 atmospheres, the density of air is only about 2 per cent greater than predicted by the ideal gas laws; and the error is correspondingly smaller at the lower pressure of these runs.

Procedure for Taking Data

Several test runs were made to determine the best method for taking data and the proper flow rates to use to cover the broadest range of data possible within the limitations of the equipment. Liquid rates ranged from 18,500 lb/hr-sq ft to 345,000 lb/hr-sq ft of open tubing. Air rates ranged from 73 lb/hr-sq ft to the maximum the University system could supply (about 45,000 lb/hr-sq ft).

Before each day's observations, the barometric pressure and room temperature were recorded. The air and test liquid were allowed to flow through the line until they had reached fairly constant temperatures. These temperatures were recorded periodically during the day's runs.

A run consisted of setting the rate of air and liquid; allowing them to run until steady state conditions were reached; noting the pattern of flow; and recording the pressure, temperature, orifice and manometer readings. The pattern of flow was most important. As will be seen in the next chapter, the visual studies lead to a logical theoretical approach to predicting the pressure drop and shut-in ratios. It was recognized that various visual flow phenomena may be interpreted differently by different viewers, so movies (both normal and slow motion) were made of the flowing fluids, and these are available through Dr. R. L. Huntington of the Department of Chemical Engineering.

Before the constant-pressure valve was installed in the air supply line, there was a continuous pressure fluctuation during each run, due to the on-off action of the University air compressor. For these runs the fluids were allowed to flow for enough time to cover several cycles of

fluctuation, and the values recorded were at the midpoint of a cycle. To make the data easier to analyze, the liquid rates were set to a predetermined value and a series of runs then covered many gas rates at a constant liquid rate. The air rates could not be set exactly since it was not possible to know the air mass rate until appropriate calculations had been made.

Shut-in data were taken at periodic intervals chosen to cover the range of rates studied. They were not observed for all points since they were so time consuming. For the shut-in runs, the procedure in the above paragraphs was followed; the quick closing valves were snapped shut, and then the air supply valve, and the liquid pump and valve were quickly closed to avoid building up pressure. The test loop was lifted so the trapped liquid could flow toward the taps. It took 10 to 15 minutes for the liquid to drain completely from the piping.

Run numbers, liquid flow rates, gas flow rates, average pressures and temperatures, recorded pressure drops, and predicted pressure drops are listed in Appendix C for all three liquids. The data at an incline are also reported along with the horizontal data though the theoretical analysis and correlative effort of this dissertation is only directed toward horizontal flow behavior. The inclined data are included since it was found that Brigham and Holstein had made a small error in their original calibration of gas flow rates (30), and they were incorrectly recorded. This writer later found that Coldiron (30) also made an error in his gas rate calibration. So it was felt that the correct rates of all these data should be on record. The water-air data are recorded in Table I of Appendix C, the oil-air data in Table II, and the

glycol-air data in Table III. Rather than recording the data in the order it was taken, the constant liquid rates are grouped together for easier interpretation by any subsequent investigator. On many of the inclined data, no predicted pressure drop is recorded, for these points exhibited an increase in pressure drop due to the inclines, and no attempt was made to predict this effect.

In Appendix D the shut-in data are presented. The water-air data are presented in Table IV of Appendix D, the oil-air data in Table V and the glycol-air data in Table VI. The tables include the run numbers, the air and liquid mass velocities, the Kinetic Liquid Fractions, the Reynolds Numbers, the actual fraction shut-in and the shut-in fraction predicted from the correlation presented in the later chapters.

CHAPTER IV

DEVELOPMENT OF CORRELATION PARAMETERS

Introduction. This chapter contains the author's explanations of the observed flow phenomena combined with conclusions about the theoretically important variables in two-phase flow. It is a potpourri of experimental visual observations, logical inferences from this observed flow behavior, and data gleaned from the literature references to back up these inferences. The purpose of this chapter is to try to understand the mechanism of two-phase flow and the visual two-phase phenomena by relating them back to our concepts of single-phase flow; and by this route to have a sound basis for correlating two-phase behavior.

The first step is an understanding of the flow patterns. It is shown that the two-phase flow behavior can be divided logically into three regions. The first is Plug Flow, which occurs when the liquid is the predominant fluid in determining the flow mechanism. Second is Intermediate (or Slug) Flow, which occurs when the liquid and the gas are more or less equally important. Third is Continuous (or Annular) Flow, which occurs when the gas is the predominant flowing fluid, with the liquid being of secondary importance.

This description eliminates the Stratified Flow pattern commonly reported in laboratory work. It is shown that Stratified Flow is primarily a laboratory phenomenon, caused by the short lengths of piping

usually used in laboratory investigations. The remainder of the chapter develops the theories of two-phase flow from these basic descriptions.

In Continuous Flow the liquid is primarily carried as an annulus along the pipe wall by energy transfer from the turbulent core of gas. An analogy with the single-phase theories of Prandtl and von Karman is used to show that the pressure drop is related to the flowing kinetic energies of the liquid and gas. The liquid can be changed to an equivalent gas (or vice versa) by the use of a square root relationship between the densities and velocities. These relationships are used to determine the proper terms in the two-phase friction factor. The two-phase Reynolds Number should contain both the liquid and the gas viscosities with the liquid viscosity predominating. The Froude Number is also expected to be of some importance in Continuous Flow, with a higher Froude Number causing a greater pressure drop.

A simplified picture of Continuous Flow is used to predict the in-place ratios when the flowing ratios are known. It is shown that the in-place ratio should be a function of the Reynolds Number and the relative kinetic energies of the flowing fluids. The inherent errors in this simplified model are described, and the direction of the error is predicted.

In Plug Flow the liquid is the predominant flowing fluid and the gas is primarily carried by the action of the liquid. Two simplified models are presented to predict the pressure drop in this flow regime. The first model assumes that the liquid and gas flow as a homogeneous mixture; the second assumes the flow is in alternate plugs of gas and liquid. These two models are quite close in their predictions, and the

actual flow behavior should lie between the two extremes.

No theoretical treatment is attempted for Intermediate (or Slug) Flow. It is the transition region between Continuous Flow and Plug Flow. A simple interpolation between the Continuous and the Plug equations seems to offer the most hope for predicting the pressure drop in this region.

Flow Patterns

When studying the flow patterns described and pictured in the literature, the first point that becomes apparent is the bewildering and (sometimes) conflicting descriptions used by various authors. For instance Alves (2) referred to a flow type sequence of Bubble, Plug, Stratified, Wavy, Slug, Annular and Spray Flow as the ratio of gas to liquid flowing increased. Martinelli, et. al. (53) did not name the flow types but sketched them as they appeared at various gas/liquid flowing ratios. Bergelin and Gazley (16) refer to Stratified, Wave, Slug and Annular Flow. White (76) uses Stratified, Ripple, Slug, Wave, Cresting and (Semi) Annular Flow as the gas/liquid flowing ratio increases. Further, he states that the pattern he calls Ripple Flow is the same as that referred to as Wave Flow by Bergelin and Gazley. Govier and Omer (39) use the term Film Flow rather than Annular Flow, but otherwise they generally agree with the terminology of Alves. Most other references closely follow the nomenclature of one of the above authors.

An intensive study was made of the data presented by these authors and of the flow patterns described. It became apparent that the data did not exactly follow the above descriptions. The described flow patterns all existed at one time or another in their experimental

programs, but the patterns did not necessarily occur in the order described. The writer's own visual data were also studied, and from these data and the above references a simpler picture of two-phase flow behavior emerged.

Modified Flow Description. Let us consider a pipe filled with flowing liquid and describe what occurs as gas is introduced. When there is only a relatively small amount of gas, it flows along with the liquid as separate plugs. Also, the liquid will have some gas bubbles entrained. The alternate plugs of gas will have approximately the same velocity as the liquid. In this type of flow the liquid is the predominant flowing fluid. This will be called Plug Flow. It is the same as Bubble, or Froth or Plug Flow described variously by other authors. The only differences between these descriptions are the size and shape of the gas plugs.

Now let us look to the other end of the liquid/gas flow spectrum and consider what happens when some liquid is added to a flowing gas stream. We find that the liquid is carried along as a continuous stream at the pipe wall by energy transfer at the interface from the rapidly moving gas. Much of the liquid is flowing in a continuous phase on the bottom; but to some extent, depending on the violence of this energy exchange, the liquid flows as a film along the walls and also as entrained droplets through the open cross section. In this type of flow the gas is the predominant fluid. This will be called Continuous (or Annular) Flow, for the gas flows as a continuous phase in the interior of the pipe and the liquid phase is continuous along the bottom and walls. This flow region is the same as Wavy, (Semi) Annular, Cresting, Spray and Film Flow

described by other authors. The various crests and waves are merely manifestations of this interfacial energy exchange, and the film and spray are always present to a greater or lesser extent, depending on the violence of the energy exchange.

Between the two extremes of Plug Flow and Continuous Flow is a region that will be called Intermediate (or Slug) Flow. This region is the same as the Slug Flow patterns described by all authors. It is also referred to as Intermediate Flow here so as to emphasize the fact that the mechanism is intermediate between the Plug and Continuous Flow regions. In this type of flow there are alternate gas-liquid slugs along the top of the pipe, and in that respect the flow is similar to Plug Flow. However, these slugs move appreciably faster than the main body of the liquid. Since the gas flows faster, there is considerable energy transfer at the interface to the bottom liquid layer; thus, in this respect, the flow is similar to Continuous Flow. In Intermediate Flow both fluids are important in determining the flow mechanism and some aspects of both Plug and Continuous Flow are always present.

Stratified Flow. It is most important to realize that the stratified flow pattern is not included in the above descriptions. This was deliberate. In fact, understanding the nature of stratified flow was the key to simplifying the two-phase flow to three major regions.

In stratified flow, the liquid is flowing in a quiescent layer on the bottom and the gas on the top. In this superficial respect the flow behavior looks like Continuous Flow; but there is an outstanding difference. The liquid is flowing primarily because of the gravitational forces, rather than from the energy received from the gas. In fact, even

if no gas were flowing, the liquid would still flow along the bottom of the pipe in a smooth stratified layer. This is open channel flow, not pipe flow. The fact that gas is also present is incidental to the nature of the process.

This description of stratified flow is well validated by the data. For instance Gazley (33) refers to the interfacial gradient present in stratified flow. This, of course, is caused by the action of gravity on the liquid. It is flowing under the influence of its own gravity head. The stratified pressure drop data of White (76), Schneider (67) and Govier and Omer (39) were also investigated. In no case did the pressure drop exceed the liquid head in the pipe. Thus the gravity head is the major force causing fluid motion in stratified flow.

The length of the tubing has a marked effect on whether stratified flow exists. In short laboratory tubing, where the gravity head often is large compared to the total pressure drop, stratified flow may be often encountered. But in the long tubing usually found in industrial applications, such as flow lines or multipass exchangers, the gravity head is almost always small compared to the total pressure drop, and stratified flow seldom exists. These are very small pressure drops. In the three-inch pipe, for instance, the water head is only equal to 0.11 psi.

Summary. To summarize, the two-phase flow mechanism can be divided into three major regions, which (as the gas/liquid flowing ratio increases) are:

1. Plug Flow - This is the flow region where the liquid is the predominant flowing fluid. The gas is carried along near the top of the pipe as a discontinuous phase in plugs and

mixed with the liquid in bubbles.

2. Intermediate (or Slug) Flow - This is the transition between the first and third regions. Part of the liquid flows in slugs alternating with the gas as in (1) above and part flows in a continuous layer due to the energy transfer at the interface as in (3) below.

3. Continuous (or Annular) Flow - This is the flow region where the gas is the predominant flowing fluid. The gas flows as a continuous phase through the interior, and the liquid flows as a continuous phase at the walls due to the energy it receives from the gas. In addition some liquid is entrained as droplets.

A pictorial sketch of these three major flow regions is shown in Figure VIII. This triad of flow regions is considerably easier to comprehend than the multiplicity of flow patterns generally used in the literature on two-phase flow.

The next step is to develop flow models which compare closely with the major flow regions outlined above, and then to develop equation forms which fit these modes.

Flow Equation -- Continuous Flow

In the flow region labeled Continuous, the gas flows as a continuous phase primarily above the liquid in the central portion of the piping. The liquid also flows as a continuous phase, primarily along the bottom and walls. Some of the liquid flows as entrained droplets in the gas. The flow is also turbulent in the classical Reynolds sense in both phases.

This point of "turbulence" should be enlarged a bit. In many of

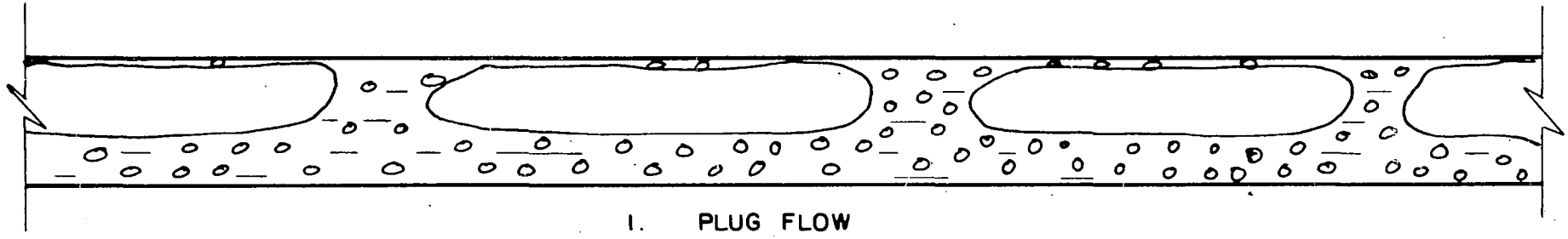

1. PLUG FLOW

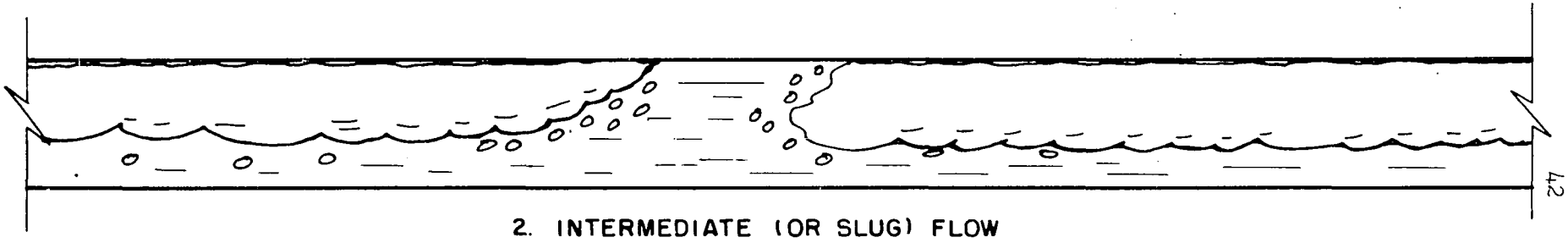

2. INTERMEDIATE (OR SLUG) FLOW

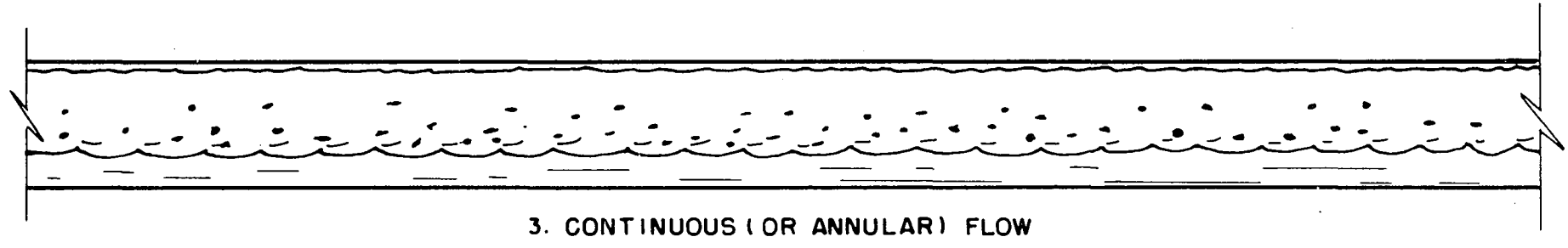

3. CONTINUOUS (OR ANNULAR) FLOW

FIG. VIII THREE MAJOR FLOW REGIONS

the data, the liquid, if flowing alone, would have been in laminar flow. However, the liquid was not flowing by itself, and its average velocity was considerably greater due to the presence of the gas. In no case was the flow in the liquid found to be along the classical "stream lines" of laminar flow except very near the pipe wall. This could be seen clearly from the movement of the tiny entrained air bubbles in the liquid.

The basic theories of single phase turbulent flow will be used as the foundation for developing the Continuous Flow equation, so it seems appropriate to cover briefly the salient features of the single phase theories of Prandtl and von Karman. For most of this discussion, the writer has borrowed freely from the excellent book by Bahkmeteff (11).

Single Phase Turbulent Flow. In single phase turbulent flow the tangential shear stresses, which oppose the flow and give rise to the pressure drop, are caused by a continuous interchange of fluid "particles" between neighboring flow layers. The momentum of the fluid coming from the faster layer imparts an accelerating force to the slower layer, and vice versa. The velocity difference between any two layers will be labelled , u'; the interchange velocity (or eddy velocity), v'; and the fluid density, ρ. The shear stress, (τ), on each layer is then:

$$\tau_{gc} = \rho v' u' \qquad (3)$$

Prandtl devised the concept of the "mixing length," l, and deduced that the velocities v' and u' would both be proportional to the mixing length and the local velocity gradient. This results in the Prandtl equation,

$$\tau_{gc} = \rho l^2 (du/dy)^2 \qquad (4)$$

If accurate data are taken on the velocity profile and the pressure drop, it is possible to calculate the mixing length by using

Equation (4) and graphically differentiating the velocity profile. Nikuradse (59) did this and found that, for fully developed turbulent flow, the ratio l/r_o (mixing length over pipe radius) is a unique function of the relative distance from the pipe wall, y/r_o. It does not depend on the fluid properties, the pipe material, the volume of flow or the size of pipe. This remarkable result has been known for several years, but it should be kept in mind for later reference to two-phase flow.

Near the pipe wall the mixing length approaches a constant slope, k, so in this region Equation (4) becomes,

$$\tau_o g_c = \rho k^2 y^2 (du/dy)^2 \tag{5}$$

where τ_o = shear stress at the wall,
k = the constant slope of the mixing length.

The shear stress and density are often combined into the term $\sqrt{\tau_o g_c/\rho}$ called the friction velocity u*. Using this term, Equation (5) becomes,

$$du/dy = u^*/ky \tag{6}$$

which is valid near the wall. Prandtl, however, made the broad assumption that Equation (6) is valid over the entire pipe. This result upon integration is

$$u/u^* - u_w/u^* = (1/k) \ln (y/y_w) \tag{7}$$

where u_w = "wall" velocity, the velocity at the point where the laminar layer ends and the turbulent core begins.
y_w = thickness of the laminar layer.

In fully developed turbulent flow, the thickness of the laminar layer, y_w, has been found to be proportional to the wall roughness height, e.

$$y_w = m e \tag{8}$$

So with proper substitution and rearranging, Equation (7) becomes:

$$u/u^* = u_w/u^* - (1/k) \ln m + (1/k) \ln (y/\epsilon) \qquad (9)$$

Equation (9) is the accepted "universal" velocity profile equation for turbulent single-phase flow in rough pipes. Nikuradse (59) found that the terms u_w/u^* and $(1/k)\ln m$ are constants, so the equation can be simplified to,

$$u/u^* = A_r - (1/k) \ln (y/\epsilon) \qquad (10)$$

Consider now a special case of turbulent single-phase flow through a particular given pipe. In this case Equation (10) can be written as follows,

$$u = \sqrt{\tau_o g_c/\rho}\,(A + B \ln y) \qquad (11)$$

and the terms A and B are constants depending on the properties of the particular pipe used. Let us assume a fluid (labelled 1) is flowing through this pipe with a given pressure drop (or shear stress, τ_o). The equation is

$$u_1\sqrt{\rho_1} = \sqrt{\tau_o g_c}\,(A + B \ln y) \qquad (12)$$

If later a different fluid (labelled 2) is flowing through the pipe in single-phase flow with the same pressure drop (or τ_o), the equation is

$$u_2\sqrt{\rho_2} = \sqrt{\tau_o g_c}\,(A + B \ln y) \qquad (13)$$

Notice that the right hand sides of Equations (12) and (13) are identical. So the left sides can be equated.

$$u_1 = u_2 \sqrt{\rho_2/\rho_1} \qquad (14)$$

Equation (14) is interesting to consider. It shows that if the two fluids are flowing at the same pressure drop, the velocities at every point in the pipe are inversely proportional to the square root of their

densities. For example: Assume fluid 1 has a density 100 times as great as fluid 2. At different times they are flowing through the same pipe with the same pressure drop. If the velocity of fluid 1 is 3.0 ft/sec at a certain point in the pipe, then, when fluid 2 is flowing through the pipe, its velocity must be 30 ft/sec ($3.0\sqrt{100} = 30$) at that same point. Since the average or bulk velocity is the normalized summation of the point velocities, the same square root relationship holds for the bulk velocity.

$$U_1 = \sqrt{\rho_2/\rho_1}\ U_2 \qquad (15)$$

Equations (14) and (15) are the result found in single phase flow when first one phase is flowing, then another. The next step is to extend this concept to simultaneous two-phase flow.

Two-Phase Turbulent Flow. In the region called Continuous Flow the gas and liquid flow adjacent to each other as continuous phases. In single-phase flow the turbulent pressure drop is postulated to be caused by the interchange of fluid (eddies) between adjacent flow layers. Does it seem reasonable to assume that this interchange also occurs in two-phase flow? Does it further seem possible that these eddies could consist of different phases — that is, eddies of gas moving from a gas layer toward the bulk of the liquid and back again, and eddies of liquid performing the same maneuver in the reverse direction? This assumption seems quite reasonable. In fact, the crests, waves, and other surface disturbances discussed in the two-phase literature follow this description exactly. So we have a two-phase analogy to equations (3) and (4).

Can we assume the mixing length is not affected by the presence of two fluids? Referring to Nikuradse's work in single-phase flow, the

mixing length is independent of fluid properties. This result would tend to make Equations (5) through (11) acceptable. It appears then, that the "square root of density" relation of equations (14) and (15) will also be valid; for this relation is based on equation (11). The next step then is to put equations (14) and (15) into a usable form for two-phase flow.

Two-Phase Friction Factor Equation. Liquid and gas are flowing through a tubing in Continuous Flow. Call the volumetric liquid rate V_L. This liquid is flowing through only a partial cross section of the pipe A_L. These are related as follows,

$$V_L = \int_0^{A_L} u_L \, dA \tag{16}$$

If gas had been flowing (at the same shear stress) through the area containing liquid, its velocity, from Equation (14), would have been greater by the ratio $\sqrt{\rho_L/\rho_G}$. Let us replace the liquid with an equivalent amount of gas, labeling this equivalent gas $V_{L\to G}$.

$$V_{L\to G} = \int_0^{A_L} u_L \sqrt{\rho_L/\rho_G} \, dA = \sqrt{\rho_L/\rho_G}\, V_L \tag{17}$$

The actual liquid flowing has now been changed to an equivalent volume of gas. The remainder of the pipe actually contains flowing gas, so the total equivalent gas (which will be labeled $V_{G,eq.}$) is merely the sum of the two gas terms.

$$V_{G,eq.} = V_G + V_{L\to G} = V_G + \sqrt{\rho_L/\rho_G}\, V_L \tag{18}$$

Equation (18), for convenience, can be changed to the more common engineering units of bulk velocity by dividing by the total cross sectional area.

$$U_{G,eq.} = U_G + U_{L\to G} = U_G + \sqrt{\rho_L/\rho_G}\, U_L \tag{19}$$

where U = the bulk velocity of a phase based on the total cross sectional area.

Thus in Equation (19) the total two-phase flow has been changed to an equivalent volume of gas.

The Moody (58) friction factor equation for horizontal single phase flow at constant velocity is,

$$f = \frac{2g_c D}{U^2 \rho} \frac{dP}{dL} \tag{20}$$

The only terms in this equation which relate to the flowing fluid are the velocity, U, and the density, ρ. To use Equation (20) for two-phase flow, the total equivalent gas velocity (Equation (19)) and the gas density would be proper to use. The result is,

$$f_{TP} = \frac{2g_c D}{(U_G\sqrt{\rho_G} + U_L\sqrt{\rho_L})^2} \left(\frac{dP}{dL}\right)_{TP} \tag{21}$$

Equation (21) is the friction factor equation resulting when the flowing liquid was changed to an equivalent amount of gas from Equation (17); and it should be valid for two-phase flow.

It is quite interesting to note that the flowing gas could have been changed to an equivalent amount of liquid rather than the converse. In so doing, an expression analogous to Equation (17) would be the result. By adding the two equivalent terms, as in Equation (18), and inserting them into the friction factor, the resulting expression will be identical with Equation (21). Thus it makes no difference whether one calculates the total fluid as an equivalent gas or as an equivalent liquid; the result is the same. In fact, the total kinetic energy of the flowing system is the term being calculated. This is the same as in single-phase flow; for the term $U^2\rho$ in Equation (20) is equal to the

kinetic energy of the flowing fluid.

Often, because of the nature of the experimental data, it is more convenient to use the superficial mass velocity, G, rather than the linear velocity. In this case Equation (21) becomes,

$$f_{TP} = \frac{2 g_c D}{(G_L\sqrt{\rho_L} + G_G\sqrt{\rho_G})^2}\left(\frac{dP}{dL}\right)_{TP} \qquad (22)$$

for the friction factor in two-phase flow.

Kinetic Liquid Fraction. As stated above, the kinetic energy of the flowing fluids is the term which determines either the single-phase or the two-phase pressure drop. It seems logical, when referring to the fraction of liquid flowing or the liquid/gas flowing ratio, to use the most important properties of these flowing fluids — their relative kinetic energies. For this reason, when referring to the fraction of liquid flowing, the term used will be the Kinetic Liquid Fraction (K.L.F.). It can be defined either from Equation (21) or Equation (22),

$$K.L.F. = \frac{U_L\sqrt{\rho_L}}{U_L\sqrt{\rho_L} + U_G\sqrt{\rho_G}} = \frac{G_L\sqrt{\rho_L}}{G_L\sqrt{\rho_L} + G_G\sqrt{\rho_G}} \qquad (23)$$

It seems likely that the K.L.F. will be useful in predicting which of the three major flow regions can be expected in a given flow situation. With a K.L.F. near 1.0, the liquid is the predominant fluid and Plug Flow should occur; and with a K.L.F. near 0.0, the gas is the predominant fluid and Continuous Flow should be seen.

Validation of the Two-Phase Equations. In searching the literature, the writer found experimental evidence that tends to corroborate the above equations. Abramson (1) in an excellent paper presented data on the surface waves of the liquid-gas interface in annular two-phase flow.

In his experimental work, liquid was introduced at the annulus with gas in the center. He measured the flow rates at which surface waves were just beginning to be formed.

Abramson used von Karman's (75) universal velocity profile for smooth pipe,

Laminar Layer	$u^+ = y^+$	For $0 < y^+ \leq 5$	(24a)
Transition Zone	$u^+ = 3.05 + 5 \ln y^+$	For $5 < y^+ \leq 30$	(24b)
Turbulent Core	$u^+ = 5.5 + 2.5 \ln y^+$	For $30 < y^+$	(24c)

where $u^+ = u/u^*$
$y^+ = yu^*\rho/\mu$

and the same "square root of density" relation derived in Equations (14) and (15). With these equations he could calculate the thickness (y and y^+) of the annular layer of flowing liquid. The values of y^+ at which the liquid first became disturbed by surface waves ranged from $12 < y^+ \leq 21$. This is an excellent fit with Equation (24b).

From these data and calculations there are two possible conclusions. Either the "square root of density" relation is valid and the universal velocity profile holds for two-phase flow; or neither of these two assumptions is valid, and the apparent agreement of y^+ is merely a fortuitous set of circumstances. Note the word apparent, for y^+ was not measured, but rather calculated using these two assumptions.

However, we are almost forced to rule out the hypothesis of fortuity. Abramson used various liquids, including water at two different temperatures (to change viscosity), water with varying amounts of wetting agents (to change surface tension), and water with varying amounts of glycol (to change density and viscosity). There was no discernable

effect from these changes in variables, and the range of variables seems too broad for the results to be considered accidental. Thus the assumptions appear valid, at least near the wall.

Two-Phase Reynolds Number. In deriving Equations (14) and (15) the equation for fully developed turbulent flow in rough piping was used. This equation assumes that the friction factor is a constant. Although this is a good first approximation, particularly at high Reynolds Numbers, it is not exact. The friction factor is a function of Reynolds Number; and thus it is necessary to decide on the proper terms to use for the Reynolds Number in two-phase flow.

Here the two-phase visual data can be used. These data show that the liquid wets the pipe walls even if only a small amount of liquid is present in the flowing mixture. Thus one would tend to use the liquid properties for the Reynolds Number, viz.

$$Re.No. = \frac{DG_{L,eq}}{\mu_L} \qquad (25)$$

At low rates of flow the visual data show that the liquid gas interface along the upper wall of the pipe is quite smooth. Thus the laminar sublayer must extend into the gas phase; and the gas phase viscosity would be expected to have a minor effect. At very high rates of flow, the liquid/gas interface is definitely disturbed throughout the pipe wall, and in this case the laminar sublayer lies wholly within the liquid.

It seems then that a good empirical approach is to include both viscosities in the Reynolds Number, thus,

$$Re.No. = \frac{DG_{L,eq}}{\mu_L^{n}\,\mu_G^{1-n}} = \frac{DG_{L,eq}}{\mu_L}\left(\frac{\mu_L}{\mu_G}\right)^{1-n} \qquad (26)$$

At fairly low rates of flow it looks as if the gas viscosity would have some effect, although the liquid viscosity is still predominant; and the exponent, n, would likely be somewhat less than 1.0 but somewhat more than 0.5. At very high rates of flow it appears that the liquid laminar film is controlling and "n" should increase to 1.0. Thus the exponent, n, is very likely not a constant. However, it may be possible to use a constant "n" and be sufficiently accurate for the total range of data; for at high Reynolds Numbers the friction factor becomes virtually a constant, and it will make little difference what exponent is used. The best "n" will have to be found empirically from the experimental data.

Froude Number in Two-Phase Flow. In turbulent flow, there is a continuous interchange of fluid between flow layers. This is the eddy velocity which gives rise to the turbulent shear stresses. In two-phase turbulent flow, the eddies consist of liquid moving into and out of the gas stream and vice versa with the gas. However, due to the density difference between liquid and gas, this type of movement will be affected by the gravitational forces. This is an extra effect which does not exist in the flow of a single phase.

What would be the expected effect of the gravitational forces? Under conditions of low velocity they would tend to keep the fluids more nearly separated into distinct layers and thus "buck" to some extent the turbulent forces. On the other hand, under conditions of high velocity, the kinetic (or turbulent) forces would be expected to largely override the gravitational forces.

A dimensionless grouping comes immediately to mind which characterizes the kinetic and gravitational forces — the Froude Number. It is

often used for ship models when worrying about dimensional similitude, also it is the criterion for various modes of flow behavior in open channels, canals, weirs, dam spillways and the like. For the length term in this system, the pipe diameter is the logical choice, and the equivalent gas velocity of Equation (19) seems the proper choice for the velocity term. Using these terms the Froude Number is,

$$Fr.No. = \frac{U_{G,eq.}}{\sqrt{Dg}} \qquad (27)$$

The Froude Number has been used only once before (30b), to the author's knowledge, in the prediction of two-phase pressure drop, and in this one reference it was used in vertical flow. But it should be possible to make some intelligent guesses as to the effects of the Froude Number. For instance, the gravity forces (characterized by g) tend to make the interface more quiescent and this will lower the pressure gradient. At high velocities the turbulent forces would tend to be stronger, and also, a greater portion of the liquid would be carried as a spray — increasing the pressure drop. So, looking at Equation (27), the pressure gradient is expected to be higher with a higher Froude Number.

This reasoning can be justified to some extent by published data. Chenoweth and Martin (29) presented data on equivalent length of three different pipe fittings. The data on a globe valve and an orifice showed a greater equivalent length of these fittings under two-phase flow conditions than under single-phase flow. This is predicted in Equation (27) for the restrictions result in higher velocities in these fittings. Around a 180° return bend, the equivalent length in two-phase flow was less than in single-phase flow. Again this result is anticipated in

Equation (27), for the angular acceleration around a bend has the same effect as an increase in the gravitational acceleration, g.

Summary of Continuous Flow Equations. The equations for pressure drop prediction in Continuous Flow can be summarized as follows. The bulk flow of the two phases can be reduced to an equivalent single phase for the friction factor equation by using Equation (22).

$$f_{TP} = \frac{2 g_c D}{(G_L\sqrt{\rho_L} + G_G\sqrt{\rho_G})^2}\left(\frac{dP}{dL}\right)_{TP} \qquad (22)$$

The Reynolds Number should contain both the liquid and the gas viscosities as follows:

$$Re.No. = \frac{D G_{L,eq.}}{\mu_L^{n} \mu_G^{1-n}} = \frac{D G_{L,eq.}}{\mu_L}\left(\frac{\mu_L}{\mu_G}\right)^{1-n} \qquad (25)$$

The Froude Number should affect the pressure gradient, and the Froude Number can be expressed as in Equation (27).

$$Fr.No. = \frac{U_{G,eq.}}{\sqrt{D g}} \qquad (27)$$

The relative importance of each phase to the flow mechanism is related to the kinetic energy of each phase. To characterize this importance, the term Kinetic Liquid Fraction (K.L.F.) is used, as defined in Equation (23).

$$K.L.F. = \frac{U_L\sqrt{\rho_L}}{U_L\sqrt{\rho_L} + U_G\sqrt{\rho_G}} = \frac{G_L\sqrt{\rho_L}}{G_L\sqrt{\rho_L} + G_G\sqrt{\rho_G}} \qquad (23)$$

The K.L.F. is also expected to be the criterion that determines which of the three flow regions is present.

Shut-In Ratio — Continuous Flow

The single-phase flow theories have been used to predict the probable correlating parameters for pressure drop in Continuous Flow. This same approach should also be valid for prediction of the liquid/gas

shut-in ratios for Continuous Flow.

In turbulent flow the velocity of the flowing fluid is not everywhere constant; it increases from zero at the wall to a maximum at the center. For this reason a greater percentage of the total flow is coming from the center of the pipe. So, if we are comparing the interior portion of the pipe with the portion near the wall, the flowing volumetric ratio is not the same as the shut-in ratio.

Refer to the "universal velocity profile" Equation (24). It can be seen that the transition zone is rather narrow, so it is permissible to simplify the equation into two regions — the laminar layer and the turbulent core. When so doing, the laminar-to-turbulent transition takes place at a y^+ of 11.62.

Laminar Layer $u^+ = y^+$ $y^+ < 11.62$ (28a)

Turbulent Core $u^+ = 5.5 + 2.5 \ln y^+$ $y^+ > 11.62$ (28b)

Equation (28) can be used to calculate the variation in the velocity from the wall to the center.

Developing Simplified Equations. Referring to the flow description in Continuous Flow, the liquid, being the wetting phase, flows primarily along the bottom and walls. The gas flows primarily in the central core; but some liquid is also entrained as droplets in the gas. Let us simplify this description, and state as a first approximation, that the liquid flows only in a symmetrical annular ring. The gas flow is then in a cylindrical core centered on the axis. With this description the gas/liquid interface can be defined as being at some radius, r_i, and the liquid fraction shut-in (F.S.I.) is,

$$F.S.I. = 1 - (r_i/r_o)^2 \tag{29}$$

where r_i = interface radius,
r_o = pipe radius.

The volume of gas flowing in the central core is,

$$V_c = \int_0^{r_i} 2\pi r u \, dr \tag{30}$$

where r = radius,
u = local velocity of the gas at radius r,
V_c = volumetric flow rate of gas in the central core.

To integrate Equation (30), the local velocity, u, must be expressed as a function of radius. For this, Equation (28) is used. The equation is then directly integrable.

To determine the total flow, V_T, the equation must be integrated over the total pipe radius

$$V_T = \int_0^{r_o} 2\pi r u \, dr \tag{31}$$

Again the velocity, u, is substituted from Equation 28. Notice in this calculation that the same velocity is used for the liquid portion of the pipe as for the gaseous portion. This is valid because of the basic definition of the K.L.F., wherein the liquid has been converted to an equivalent volume of gas. The "square root of density" relation of Equations (14) and (15) is the key to this conversion. This can also be seen in Equation (28); for the term $u\sqrt{\rho}$ is contained in the dimensionless velocity, u^+.

In Appendix B the above substitutions and integrations are covered in detail. The results of these integrations are shown in Figure IX where the K.L.F. is plotted against the theoretical liquid fraction shut-in (F.S.I.). These were calculated at three different values of

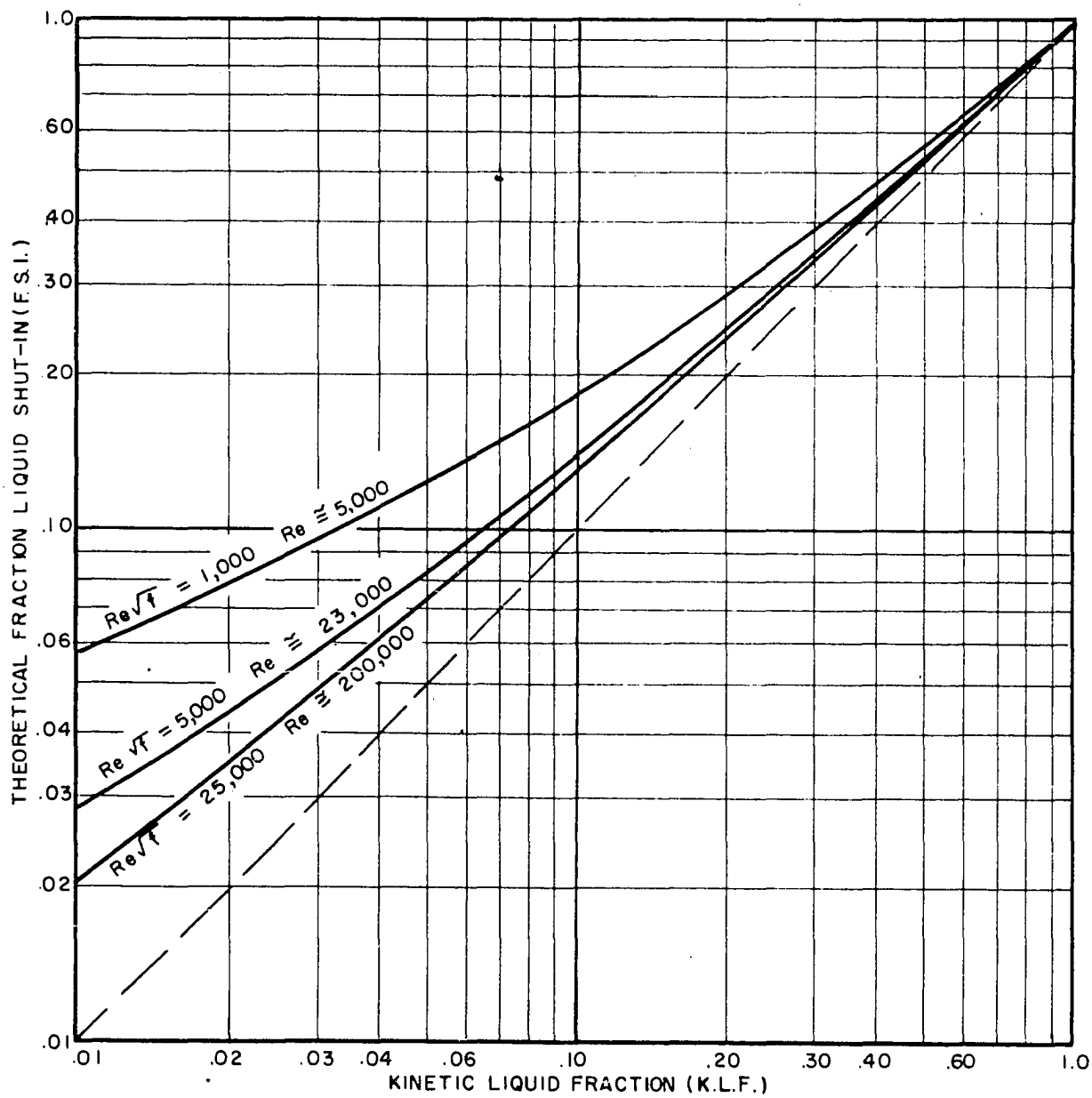

FIG. IX THEORETICAL FLOWING VS SHUT-IN RATIOS AS A FUNCTION OF REYNOLDS NUMBER

Reynolds Number.

There are several features of Figure IX which are worthy of mention. First, the F.S.I. is always greater than the K.L.F. Second, it is seen that the greatest difference between K.L.F. and F.S.I. is when only a small portion of the flowing fluid is liquid. These results are to be expected, for the liquid is flowing at the walls where the velocity is less than average. Third, is the effect of changing Reynolds Number. At high Reynolds Numbers the F.S.I. more nearly equals the K.L.F. This result is due to the change in the velocity profile with Reynolds Number. At higher Reynolds Numbers the velocity remains more nearly constant until near the wall, where it plunges rapidly toward zero; while at lower Reynolds Numbers the velocity changes more gradually throughout the pipe.

Effects of Errors in the Assumptions. The curves of Figure IX are based on the simplifying assumption that the liquid flows in a symmetrical annulus between the interface at r_i and the pipe wall r_o, and the gas flows in the central core. This flow picture is sketched in Figure X. Notice that the actual liquid velocity is less than the gas velocity by the "square root of density" ratio. With this assumption, there is an abrupt "jump" in velocity at the liquid/gas interface. This concept is somewhat idealized, however, since there must be an interchange of momentum at the interface for turbulent flow to exist. This means there must be a mixing zone wherein eddies of gas move into the liquid and eddies of liquid into the gas to achieve this interchange. The result of such a mixing zone is sketched in Figure XI. There is no longer a sudden jump in the velocity profile.

How will the presence of such a mixing zone affect the shut-in

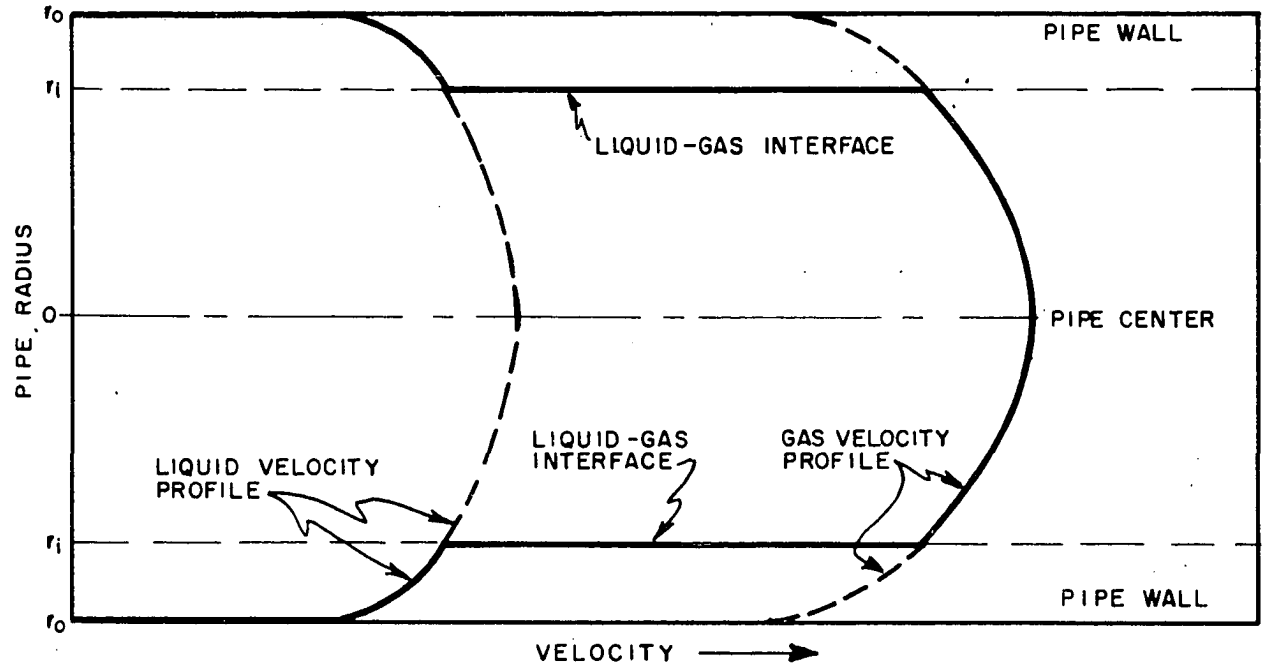

FIG. X "IDEAL" TWO-PHASE VELOCITY PROFILE

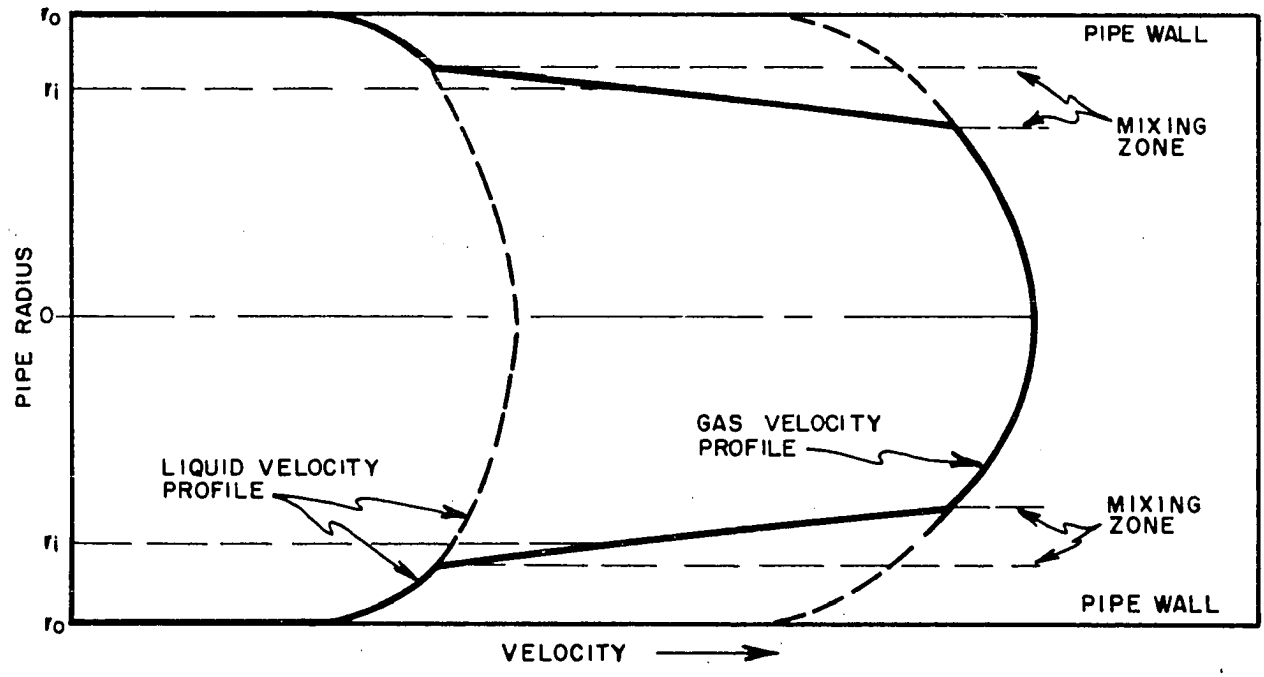

FIG. XI TWO-PHASE VELOCITY PROFILE SHOWING MIXING ZONE

and flowing fractions? It is apparent from Figure XI that some of the liquid is flowing faster than predicted by the liquid velocity profile equation. Therefore one would expect that, with a given flowing fraction, the shut-in liquid fraction will be less than predicted by the curves of Figure IX.

There are some further characteristics of the flow which will cause the curves of Figure IX to be erroneous. First, we know that some of the liquid is continuously being carried as droplets within the central core of gas. Second, it can be seen that the liquid is not actually flowing in a concentric annular ring. A larger percentage is flowing along the bottom due to the gravitational forces. The effect of these assumption errors is the same as before. The actual shut-in fraction will be smaller than predicted by Figure IX; that is, the actual liquid velocity will, on the average, be higher than predicted in Equation (28). However, it seems reasonable to suggest the correlating parameters of Figure IX can be successfully used to correlate the actual liquid F.S.I. versus the K.L.F.

Flow Equation — Plug Flow

In Plug Flow the liquid is the predominant flowing fluid. The gas is being carried along by the liquid, either in alternate plugs or as bubbles entrained in the bulk of the liquid. From this description it is possible to make two differing assumptions about the character of the flow, and these will lead to two differing equations for predicting the pressure drop. These alternate assumptions are, (1) the liquid and gas flow as if they are a completely mixed homogeneous fluid, and (2) the liquid and gas

act as completely separate entities — that is, plugs of liquid followed by plugs of gas, followed by liquid and so on. Equations are derived to represent these two assumptions.

Assumption (1) — Liquid and Gas Mixed. If the liquid and gas are completely mixed, the proper mass velocity to use in the Reynolds Number is merely the total mass velocity, G_L plus G_G. The visual data shows the liquid is definitely the wetting fluid in this type of flow, so the liquid viscosity, μ_L, should be used. The resulting Reynolds Number is,

$$Re.No. = \frac{D(G_L+G_G)}{\mu_L} \tag{32}$$

In the expression for the friction factor the mass velocity also appears. This, too, will be the sum, G_L plus G_G. The density will have to be the average mass per unit volume, which is the sum of the superficial mass velocities (G_L plus G_G) divided by the sum of the superficial bulk velocities (U_L plus U_G). And the resulting Moody (58) friction factor is,

$$f = \frac{2g_c\rho_{ave.}}{(G_L+G_G)^2}\left(\frac{dP}{dL}\right)_{TP} = \frac{2g_cD}{(G_L+G_G)(U_L+U_G)}\left(\frac{dP}{dL}\right)_{TP} \tag{33}$$

If the assumption of completely mixed flow is correct, Equations (32) and (33) can now be used to predict the pressure drop. That is, knowing the Reynolds Number from Equation (32), the Karman or Blazius (64) equation, or other suitable single-phase correlation is used to calculate the friction factor; then the pressure gradient is calculated from Equation (33).

Assumption (2) — Liquid and Gas in Separate Plugs. If the liquid and gas are flowing as completely separate entities with plugs of liquid alternating with plugs of gas, the pressure gradients can be

calculated separately in each phase then added together to get the total pressure drop.

To calculate the liquid Reynolds Number it must be remembered that the liquid is flowing faster than it would if no gas were present. The amount of this velocity increase can be expressed as a ratio of the superficial velocities of the phases flowing. Thus the liquid Reynolds Number, $(Re.\ No.)_L$, becomes

$$(Re.No.)_L = \frac{DG_L}{\mu_L}\left(\frac{U_L+U_G}{U_L}\right) \tag{34}$$

Since the velocity is squared in the friction factor equation, the velocity ratio term, $((U_L + U_G)/U_L)$, must also be squared, and the friction factor is as follows,

$$f_L = \frac{2g_c D P_L U_L^2}{G_L^2 (U_L+U_G)^2}\left(\frac{dP}{dL}\right) \tag{35}$$

Equation (35) gives the expression for the pressure gradient within a liquid plug. It would be more convenient to express this as an average pressure drop per length of pipe. This is done simply by dividing by the volumetric flowing ratio of liquid and gas; and the result is,

$$f_L = \frac{2g_c D P_L U_L}{G_L^2 (U_L+U_G)}\left(\frac{dP}{dL}\right)_L = \frac{2g_c D}{G_L (U_L+U_G)}\left(\frac{dP}{dL}\right)_L \tag{36}$$

For the gas plugs it is possible to get expressions analogous to Equations (34) and (36) for the friction factor and the Reynolds Number. The expression for the friction factor is simply,

$$f_G = \frac{2g_c D P_G U_G}{G_G^2 (U_L+U_G)}\left(\frac{dP}{dL}\right)_G = \frac{2g_c D}{G_G (U_L+U_G)}\left(\frac{dP}{dL}\right)_G \tag{37}$$

The Reynolds Number must be modified somewhat for the gas plugs. When a gas plug is flowing, the walls are completely liquid wet. This means

the liquid viscosity must be used in the Reynolds Number. Also, the gas flow rate must be changed to an equivalent liquid. Here the "square root of density" relation of Equation (15) is in order. So the resultant gas Reynolds Number (Analogous to Equation (34)) is,

$$(Re.No.)_G = \frac{DG_G}{\mu_L}\sqrt{\frac{\rho_L}{\rho_G}}\left(\frac{U_L+U_G}{U_G}\right) \tag{38}$$

The total pressure drop of the system is merely the sum of the liquid and gas components. So adding Equations (36) and (37), the predicted two-phase pressure drop per foot of pipe is,

$$\left(\frac{dP}{dL}\right)_{TP} = \left(\frac{dP}{dL}\right)_L + \left(\frac{dP}{dL}\right)_G = \frac{f_G G_G (U_G+U_L)}{2g_c D} + \frac{f_L G_L (U_L+U_G)}{2g_c D} \tag{39}$$

Comparison of the Equations. Two equations have been derived. Equation (33) is based on the assumption that the fluids are mixed; Equation (39) assumes the fluids are in completely separate plugs. The actual flow conditions appear to lie somewhere between these extremes, so it seems apropos to compare the two equations.

First consider Equation (39). In calculating the Plug Flow data, the writer found the gas term was always less than 5 per cent of the liquid term. Thus we can neglect the gas term; and Equation (36), which is for liquid only, will be used rather than equation (39). Also the Blazius (64) form of the friction factor equation will be used rather than the more awkward Karman Equation. The Blazius Equation is,

$$f = A/(Re.No.)^m \tag{40}$$

When substituting Equations (32) and (40) into Equation (33) and rearranging, the result is,

$$\left(\frac{dP}{dL}\right)_{TP} = \left(\frac{A}{D(G_L+G_G)}\right)^m \frac{\mu_L^m (U_L+U_G)(G_L+G_G)}{2g_c D} \tag{41}$$

for liquid and gas flowing mixed. Substituting into Equation (36) the result for liquid and gas separated into plugs is,

$$\left(\frac{dP}{dL}\right)_{TP} = A\left(\frac{\mu_L U_L}{D G_L (U_L + U_G)}\right)^m \frac{G_L (U_L + U_G)}{2 g_c D} \tag{42}$$

We wish to make a comparison of the two equations, so Equation (41) will be divided by Equation (42) and the result labeled, R, to signify a ratio of predicted pressure drops. Note in dividing that the term, $A(\mu_L/D)^m (U_L + U_G)/2gcD$, is common to both equations. So the result is,

$$R = \left(\frac{G_L + G_G}{G_L}\right)^{1-m} \left(\frac{U_L + U_G}{U_L}\right)^m \tag{43}$$

It was stated that the gas portion of Equation (39) was always less than 5 per cent of the liquid portion and so it was neglected. For the same reason we can see that G_G will be negligible compared to G_L. This will eliminate the first term in Equation (43) leaving only,

$$R \cong \left(\frac{U_L + U_G}{U_L}\right)^m \tag{44}$$

Now consider Equation (44) which presents a picture of the two theoretical equations and their differences. First, notice that, as the volume of gas becomes small compared to the liquid volume, the ratio R approaches unity — both equations predict the same pressure drop. Actually, as can be seen from Equations (41) and (42), both equations correctly predict the all-liquid pressure drop at this condition. Second, it is seen that, with an appreciable gas rate, the ratio R in Equation (44) is always greater than unity. This means that the assumption of completely mixed flow (Equation (33)) always predicts the greater pressure drop. Third, it can be seen that the ratio R is greatest when the gas volume

is greatest. So the two equations differ most widely when the system pressure is low and the gas volume is high.

Maximum Difference in Equations. It should be possible to calculate approximately the maximum range of the pressure drop ratio, R. From the visual data the author found that in Plug Flow the gas bulk velocity never exceeds about six times the liquid bulk velocity. The exponent, m, in Equation (44) is the Reynolds Number exponent in the Blazius Equation. It is somewhat variable, but generally doesn't exceed 0.25. Using these numbers, the maximum value for the pressure drop ratio, R_{max}, becomes

$$R_{max} = \left(\frac{U_L+U_G}{U_L}\right)^m = \left(\frac{1+6}{1}\right)^{0.25} = 1.63 \qquad (45)$$

So it is seen that Equations (33) and (39) are never very far apart in their pressure drop predictions, even at their maximum difference. In correlating the data, the measured drop should lie between these two predictions, since the assumptions leading to these equations cover the extremes within which the actual flowing system seems to lie.

Flow Equation — Intermediate (or Slug) Flow

As pointed out earlier in this chapter, Intermediate (or Slug) Flow is the transition region between the Continuous and the Plug Flow regions. Part of the liquid is flowing as a continuous phase along the bottom and walls of the tubing due to energy transfer from the gas, as in Continuous Flow; and part of the liquid is flowing along the top of the pipe in slugs alternating with the gas, as in Plug Flow. It seems reasonable to expect that, as the gas/liquid flowing ratio increases, the pressure drop will gradually change from that predicted by the Plug Flow

equations to that predicted by the Continuous Flow equations. It is extremely difficult, however, to suggest a theoretical analysis which is deeper than this rather elementary premise.

In the next chapter it is shown that a simple interpolation between the two basic flow correlations (Plug and Continuous) is quite adequate for predicting the Slug Flow pressure drop.

CHAPTER V

RESULTS AND CONCLUSIONS

The theoretical prognoses of the last chapter are tested in this chapter. Correlations are presented to predict the pressure drop in all three flow regions, and also to predict the shut-in ratios. The correlations are tested for accuracy using the author's laboratory data as well as other laboratory and field data. Before presenting these results, however, a comment should be made on the data used for correlating.

At the time this study was begun, Messrs. Chenoweth and Martin (29) of the C. F. Braun Co. presented a study of air-water flow in 1 1/2-inch and 3-inch piping at atmospheric pressure and 100 psia. These data well complemented the writer's program of study, so Chenoweth and Martin were contacted concerning the use of their data. They graciously agreed to release it.

Thus the following correlations are based on a large range of operating conditions and fluid properties. The Chenoweth and Martin data, since they were taken at widely varying pressure, show the effects of gas density variation. When combined with the writer's data, they were ideal for the study of the effects of diameter. The writer's data were well suited to cover a range of liquid densities and viscosities; also this study includes the shut-in data, and presents the visual observations

that were so necessary before an adequate understanding of the flow behavior was possible.

Pressure Drop Correlation — Continuous Flow

In the preceding chapter, the theory led to the following relationships for Continuous Flow. First, the friction factor for two-phase flow should include the properties of both fluids according to their respective kinetic energies,

$$f_{TP} = \frac{2 g_c D}{(G_L\sqrt{\rho_L} + G_G\sqrt{\rho_G})^2}\left(\frac{dP}{dL}\right)_{TP} \qquad (22)$$

Second, the two-phase Reynolds Number should be,

$$Re.No. = \frac{D G_{L,eq.}}{\mu_L^{n}\mu_G^{1-n}} = \frac{D G_{L,eq.}}{\mu_L}\left(\frac{\mu_L}{\mu_G}\right)^{1-n} \qquad (26)$$

Third, the Froude Number should be included, where the Froude Number is defined as follows,

$$Fr.No. = \frac{U_{G,eq.}}{\sqrt{Dg}} \qquad (27)$$

Fourth, a dynamic ratio, the Kinetic Liquid Fraction (K.L.F.), was defined. It is expected to be of importance in defining the flow regions, and the shut-in fraction. With these characteristics, it should also be important in determining the pressure drop. It is defined as follows,

$$K.L.F. = \frac{G_L\sqrt{\rho_L}}{G_L\sqrt{\rho_L} + G_G\sqrt{\rho_G}} \qquad (23)$$

These parameters should be sufficient to predict the two-phase pressure drop in continuous flow. The reader will notice that these parameters are all dimensionless, and that there are five in all — f_{TP}; $DG_{L,eq}/\mu_L$; μ_L/μ_G; Fr. No. and K.L.F. It is interesting that a simple dimensional analysis shows five dimensionless parameters are required to

characterize two-phase flow adequately. Although these parameters were not chosen by use of dimensional analysis, it is gratifying to find that they do match this necessary criterion.

The Exponent, n, on the Viscosities. Using the water, oil and glycol data, it was possible to determine empirically the value of the exponent, n, on the liquid and gas viscosities. The single-phase data on the Kraloy tubing showed the following relation between the friction factor and the Reynolds Number,

$$f = \frac{0.134}{(Re.No.)^{0.187}} \tag{2}$$

The two-phase data on water, oil and glycol were compared with each other using Equation (2) and various constants of exponentiation on the viscosities in the Reynolds Number (Equation (26)). When using an exponent, n, of 1.0 on the liquid viscosity it was found that the friction factors for oil-air were highest, glycol-air in the middle, and water-air lowest. When using an "n" equal to 0.50 the order was reversed; water was highest and oil lowest. By trial and error, the best value for the exponent was found to be 0.70. Many two-phase oil, glycol, and water runs were calculated and compared with each other; and the value of 0.70 for "n" was found to be valid for the entire range of mass velocities studied. Thus equation (26) becomes,

$$Re.No. = \frac{DG_{L,eq.}}{\mu_L^{0.70}\mu_G^{0.30}} = \frac{DG_{L,eq.}}{\mu_L}\left(\frac{\mu_L}{\mu_G}\right)^{0.30} \tag{46}$$

It should be emphasized that no experimental basis can be claimed for assuming that the proper exponent on the gas viscosity is 0.30. The only gas used in this correlation was air, which, over the range of data, had essentially a constant viscosity. The primary

argument for including the gas viscosity to the 0.30 power is for dimensional consistency. However, even if this is not correct, it will make little difference in the usual case, for most gases have roughly the same viscosity. If a gas is used whose viscosity differs from air by a factor of two, the resulting error would be only four per cent ($(2.0)^{.30} \times .187 = 1.04$) in the pressure drop.

Kinetic Liquid Fraction and Froude Number. Once the correct exponent was found on the viscosity, the remaining problem was to determine the importance of the Kinetic Liquid Fraction and the Froude Number. The Chenoweth and Martin data were included along with the writer's data in this phase of the correlation work, so it was necessary to calculate a least squares fit of the Chenoweth and Martin single-phase data. Their 1 1/2-inch pipe gave the following equation for the friction factor,

$$f = \frac{0.294}{(Re.No.)^{0.245}} \tag{47}$$

and the equation for the 3-inch pipe was

$$f = \frac{0.105}{(Re.No.)^{0.145}} \tag{48}$$

To correlate the two-phase data, the actual measured two-phase friction factors (f_{TP} from Equation (22)) were compared against the friction factors from the single phase equations (f from Equations (2), (47) and (48)). Plots and cross plots were made of the friction factor ratios (f_{TP}/f) as a function of the Kinetic Liquid Fraction (K.L.F.) and the Froude Number. A good correlation was evident. It was valid over the entire range of Froude Numbers and over a K.L.F. ranging from .001 to 0.500. Above a K.L.F. of 0.500 this type of correlation did not fit the data. There were no data below a K.L.F. of 0.001.

The correlation curves are shown in Figures XII and XIII. In Figure XII the friction factor ratio (f_{TP}/f) is plotted against the K.L.F. with Froude Number parameters. In Figure XIII the correlation is cross plotted to better show the effect of a variation in Froude Number.

Some Aspects of the Correlation. Notice the ordinate of Figure XII. The actual friction factor (or pressure drop) is always greater than that predicted using the single-phase equations (Equations (21), (47) or (48)). This ratio ranges from about 1.2 to 7.9 depending on the value of the Froude Number and the K.L.F. A higher Froude Number causes a higher friction factor ratio. This was predicted in the previous chapter. Also a high K.L.F. causes a higher friction factor ratio. The reason for this is discussed below.

The correlation parameters which lead to the curves of Figure XII are based on the assumption of Continuous Flow. In the analysis of this flow region it was assumed that none of the liquid is flowing in slugs. As the Kinetic Liquid Fraction increases, this assumption becomes erroneous; and, due to the high liquid slug velocity, the pressure drop becomes higher. The change from one type of flow to another is over a broad range of gas/liquid ratios rather than at one point; but, as close as could be determined, the beginning of Slug Flow occurred at about a K.L.F. of 0.15. Notice that this is also the same region in which the correlation curves of Figure XII begin to rise markedly.

Thus it is a simple matter to determine the flow regime. At a K.L.F. below about 0.15 the fluids are in Continuous Flow. Above 0.15 the mechanism is Intermediate (or Slug) Flow.

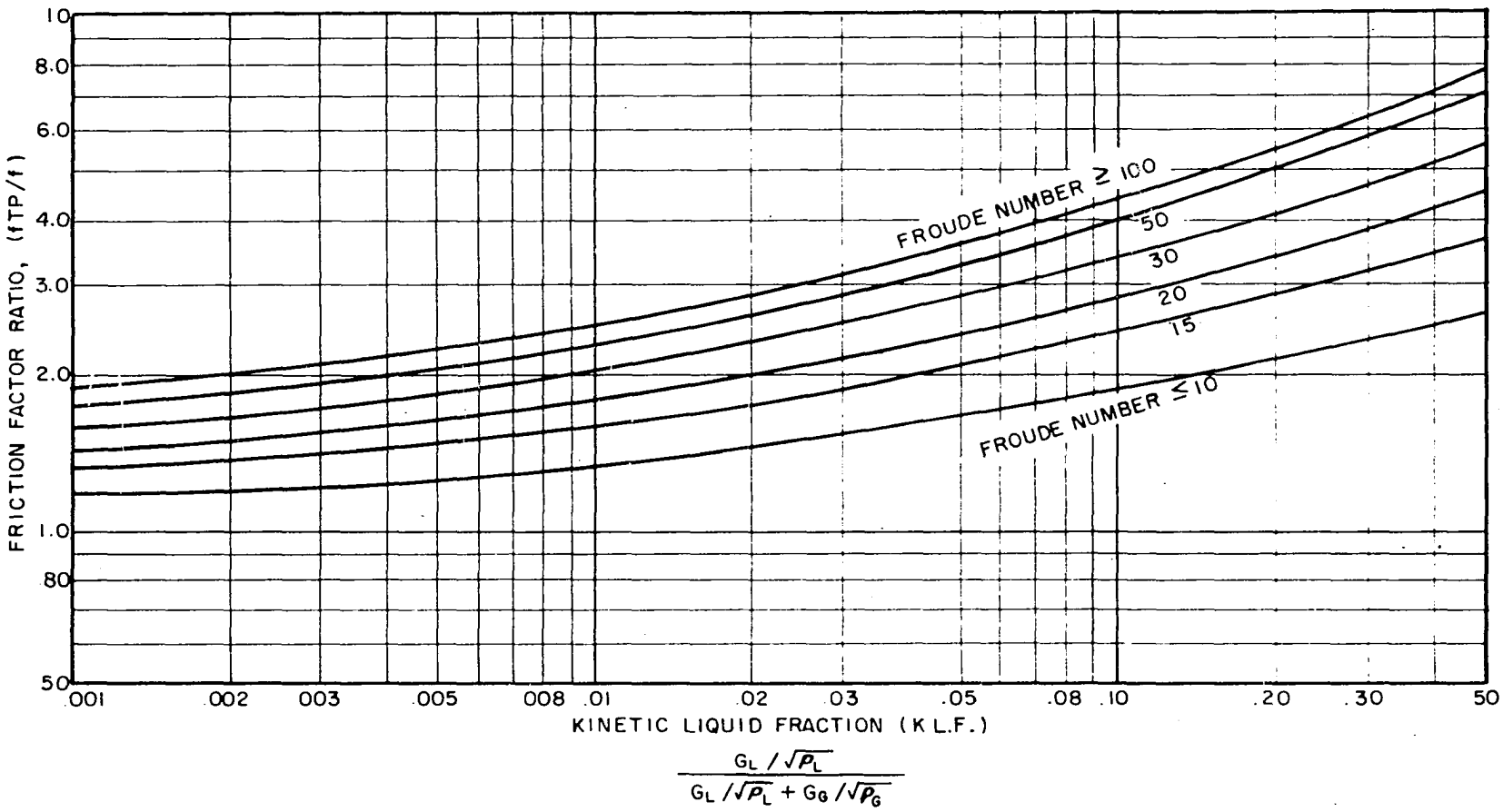

FIG. XII

CORRELATION OF TWO-PHASE PRESSURE DROP
Fraction Factor Ratio (fTP/f) As a
Function Of Kinetic Liquid Fraction

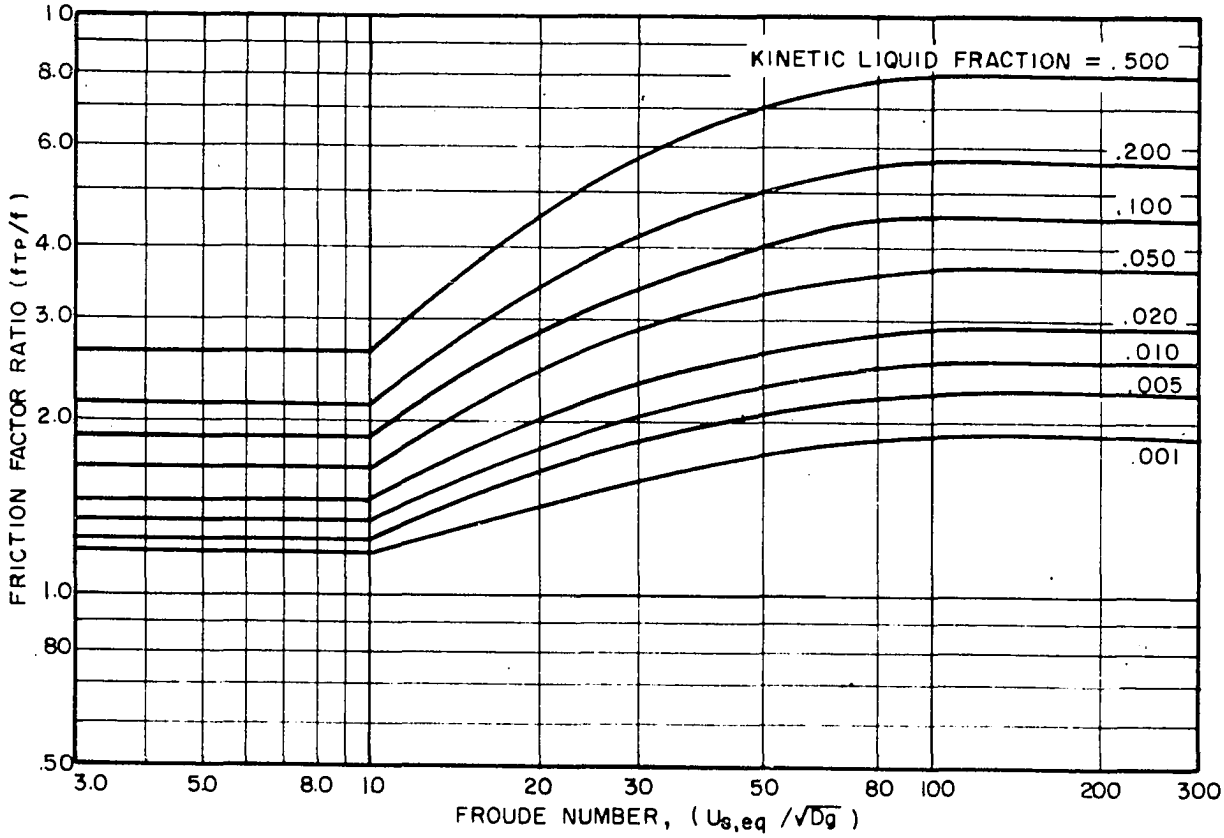

FIG. XIII CORRELATION OF TWO-PHASE PRESSURE DROP
Friction Factor Ratio (fTP/f)
As A Function Of Froude Number

This correlation only extends to a K.L.F. of 0.50. When the liquid fraction was somewhat higher than 0.50, the Intermediate (or Slug) Flow mechanism was still evident, but the correlation was no longer valid. Apparently between a K.L.F. of 0.15 and 0.50 the flow behavior is close enough to the Continuous Flow model that the validity of this correlating approach is not seriously harmed by the presence of the slugs, while above 0.50 this is no longer true.

The Froude Number. For closer scrutiny, one of the lines of Figure XIII is replotted as the solid line of Figure XIV. The friction factor ratio (f_{TP}/f) is plotted against the Froude Number at a K.L.F. of 0.100. In the correlation it was assumed that the friction factor ratio remains constant at a Froude Number above 100. This assumption appears reasonable from the curve of Figure XIV, for the curve becomes horizontal as the Froude Number nears 100. The data also validated this assumption, for at some of the highest flow rates the Froude Number ranged above 200.

At the lower left end of the curve there is a slope discontinuity at a Froude Number of 10.0. Below 10.0 it was assumed that the ratio f_{TP}/f was independent of the Froude Number. This is implied by the horizontal solid line extending to the left at f_{TP}/f equal to 1.88. The data indicated the true curve may be more nearly like the dashed line in Figure XIV; however, at these low flow rates the data were not accurate enough to attempt a further refinement of the correlation. The friction factor ratio is probably a smooth continuous function of the Froude Number, as implied by the dashed line; but the solid curves of Figure XIII were quite adequate in correlating the data.

Correlation in Equation Form. The design engineer often has a

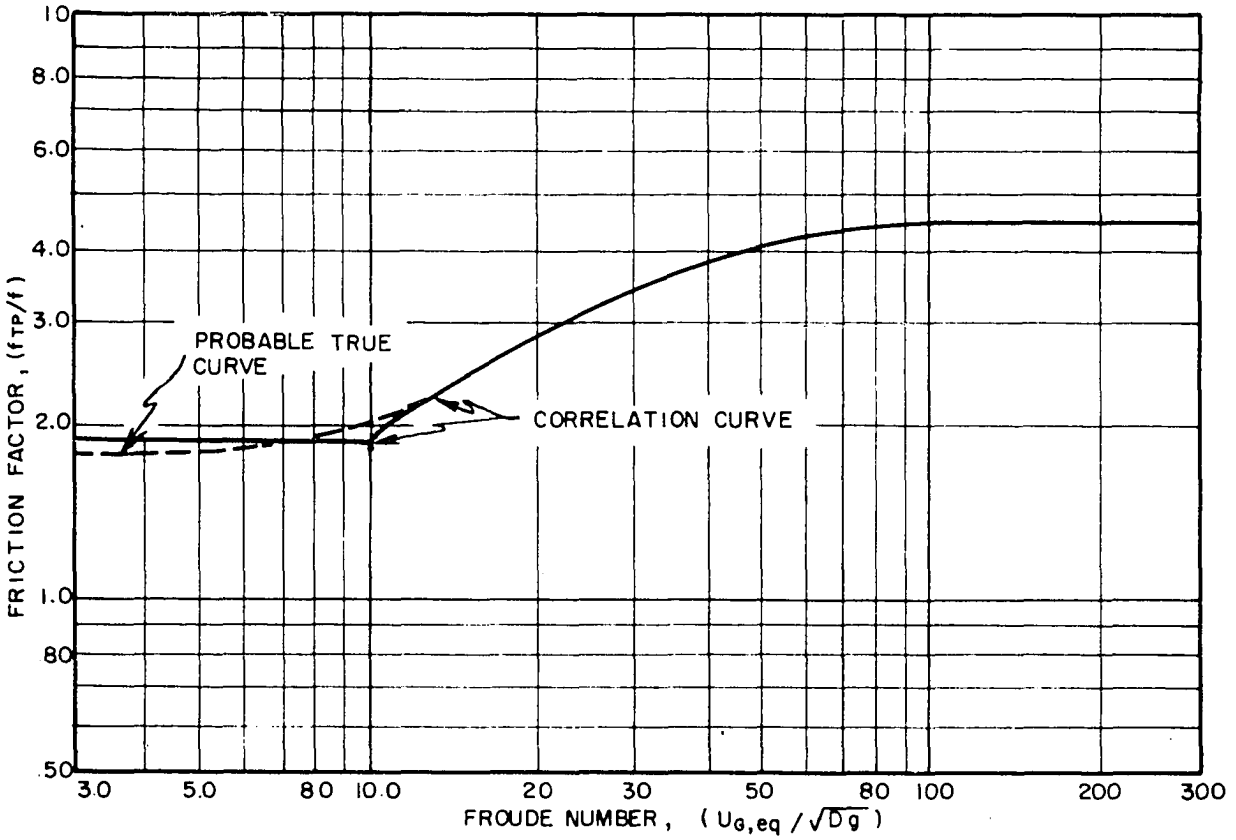

FIG. XIV FRICTION FACTOR RATIO AT KINETIC LIQUID FRACTION EQUAL TO .100

computer available when making his calculations. Since it is much more desirable to have an equation rather than a set of curves for computer input, a power equation was assumed for the curves of Figures XII and XIII, and a least-squares fit of the data was made using the following equation form.

$$z = A_1 + B_1x + C_1x^2 + A_2y + B_2xy + C_2x^2y + A_3y^2 + B_3xy^2 + C_3x^2y^2 \qquad (48)$$

where $x = \ln (Fr.No.)$
$y = \ln (1000 \times K.L.F.)$
$z = \ln (f_{TP}/f)$

The values for the constants of Equation (48) were calculated on the Continental Oil Company IBM 650 computer using a regression analysis program. The program determines the constants by the usual least-squares method and at the same time calculates the standard deviation of the data from from the curves. The constants were:

$A_1 = -0.85377650$ $B_1 = 0.55026605$ $C_1 = -0.048616989$

$A_2 = -0.16950800$ $B_2 = 0.11382944$ $C_2 = -0.014042873$

$A_3 = -0.0063980830$ $B_3 = 0.013921857$ $C_3 = -0.0014182368$

It should be emphasized that no theoretical significance can be attributed to either the exponents or the constants in Equation (48). The equation is merely a least-squares fit of the data using the correlation parameters of Figures XII and XIII. The constants are carried to more places than the accuracy of the data warrants; but the computer has an eight-place output, so all the digits were included.

The regression analysis program also runs an error analysis on the data. It showed that the data fit the correlating curves with a

standard deviation of ±15 per cent. This is equivalent to ±32 per cent at the 95 per cent confidence level (1.96σ). A further discussion of the accuracy of the correlation will be presented later in the chapter; but first equations will be presented for the other flow regions.

Prediction of Pressure Drop — Plug Flow

In the preceding chapter, two equations were presented for prediction of the Plug Flow pressure drop. The first was based on the assumption that the liquid and gas flow as if they are completely mixed. The result is,

$$Re.No. = \frac{D(G_L + G_G)}{\mu_L} \tag{32}$$

and

$$f_{TP} = \frac{2g_c D}{(G_L + G_G)(U_L + U_G)} \left(\frac{dP}{dL}\right)_{TP} \tag{33}$$

The second assumption was that the liquid and gas flow in separate plugs; and separate Reynolds Numbers and friction factors must be calculated for each phase. The resulting equations for this assumption were:

$$(Re.No.)_L = \frac{DG_L}{\mu_L}\left(\frac{U_L + U_G}{U_L}\right) \tag{34}$$

$$(Re.No.)_G = \frac{DG_G}{\mu_L}\sqrt{\frac{\rho_L}{\rho_G}}\left(\frac{U_L + U_G}{U_G}\right) \tag{38}$$

$$\left(\frac{dP}{dL}\right)_{TP} = \left(\frac{dP}{dL}\right)_G + \left(\frac{dP}{dL}\right)_L = \frac{f_G G_G (U_G + U_L)}{2g_c D} + \frac{f_L G_L (U_G + U_L)}{2g_c D} \tag{39}$$

An analysis of the visual data along with a calculation of flow rates showed that Plug Flow existed at K.L.F.'s greater than about 0.85. Below this value, Intermediate (or Slug) Flow was the mechanism. Again

the change from one flow mechanism to the other was rather gradual, and the division at a K.L.F. of 0.85 was somewhat arbitrary. The selection was based on the point where the velocity of the liquid plugs became appreciably higher than bulk liquid velocity. So once again it proved to be a simple matter to determine the flow region. Above a K.L.F. of 0.85 the mechanism is Plug Flow; between a K.L.F. of 0.15 and 0.85 the mechanism is Intermediate (or Slug) Flow; and below 0.15 the mechanism is Continuous Flow.

In processing the data, it soon became apparent that the gas term in Equation (39) was negligible. In no case did it exceed 5 per cent of the liquid term, and for the data at higher pressure it was even smaller. So Equation (38) was eliminated, and Equation (36) could be used rather than Equation (39).

$$\left(\frac{dP}{dL}\right)_{TP} = \left(\frac{dP}{dL}\right)_{L} = \frac{f_L G_L (U_G + U_L)}{2 g_c D} \qquad (36)$$

For correlation, the actual pressure drop data were compared with the predictions of Equations (33) and (36). The data fell midway between the two equations, as predicted in Chapter IV; and the best fit was simply to add the two predicted pressure drops and divide by two. This fit was quite satisfactory. The standard deviation was ±14 per cent which is equal to an error of ±29 per cent at the 95 per cent confidence level.

Correlation of Pressure Drop — Intermediate Flow

The correlations developed above successfully predicted the pressure drop when operating below a K.L.F. of 0.500 and above a K.L.F. of 0.85. It only remained to bridge the intermediate gap between 0.50

and 0.85. No theoretical treatment was attempted for Intermediate Flow. It appeared that the flow mechanism was so complex that the most effective method would be to simply interpolate between the Continuous the Plug Flow correlations.

At a K.L.F. of 0.50 the Plug Flow equation is in error. The magnitude of this error can be calculated by using the Continuous Flow correlation as a reference. At a K.L.F. of 0.85 the Plug Flow equation is correct. One simple interpolation scheme is to assume that the amount of error in the Plug Flow equation is a linear logarithmic function of the K.L.F.

An example of this interpolation method is shown in Figure XV. To make this graph, the pressure drop is calculated at a K.L.F. of 0.50 using both the Plug Flow and the Continuous Flow equations. For this example, at a liquid fraction of 0.50 the Plug Flow prediction was found to be double the correct Continuous Flow prediction. This point is plotted at a K.L.F. of 0.50 in Figure XV. At a K.L.F. of 0.15 the Plug Flow equation is correct. This point was also plotted on the graph and a straight line was drawn between. As seen from Figure XV, if the actual flow was at a liquid fraction of 0.67, the Plug Flow equation would be in error by a factor of 1.58. So if the K.L.F. is between 0.50 and 0.85 it is necessary to make three different pressure drop calculations: (1) at a K.L.F. of 0.50 using the Plug Flow equation, (2) at a liquid fraction of 0.50 using the Continuous Flow equation, and (3) at the actual flowing K.L.F. using the Plug Flow equation. Then, according to the errors found in the first two calculations, an interpolation is made to correct the third calculation.

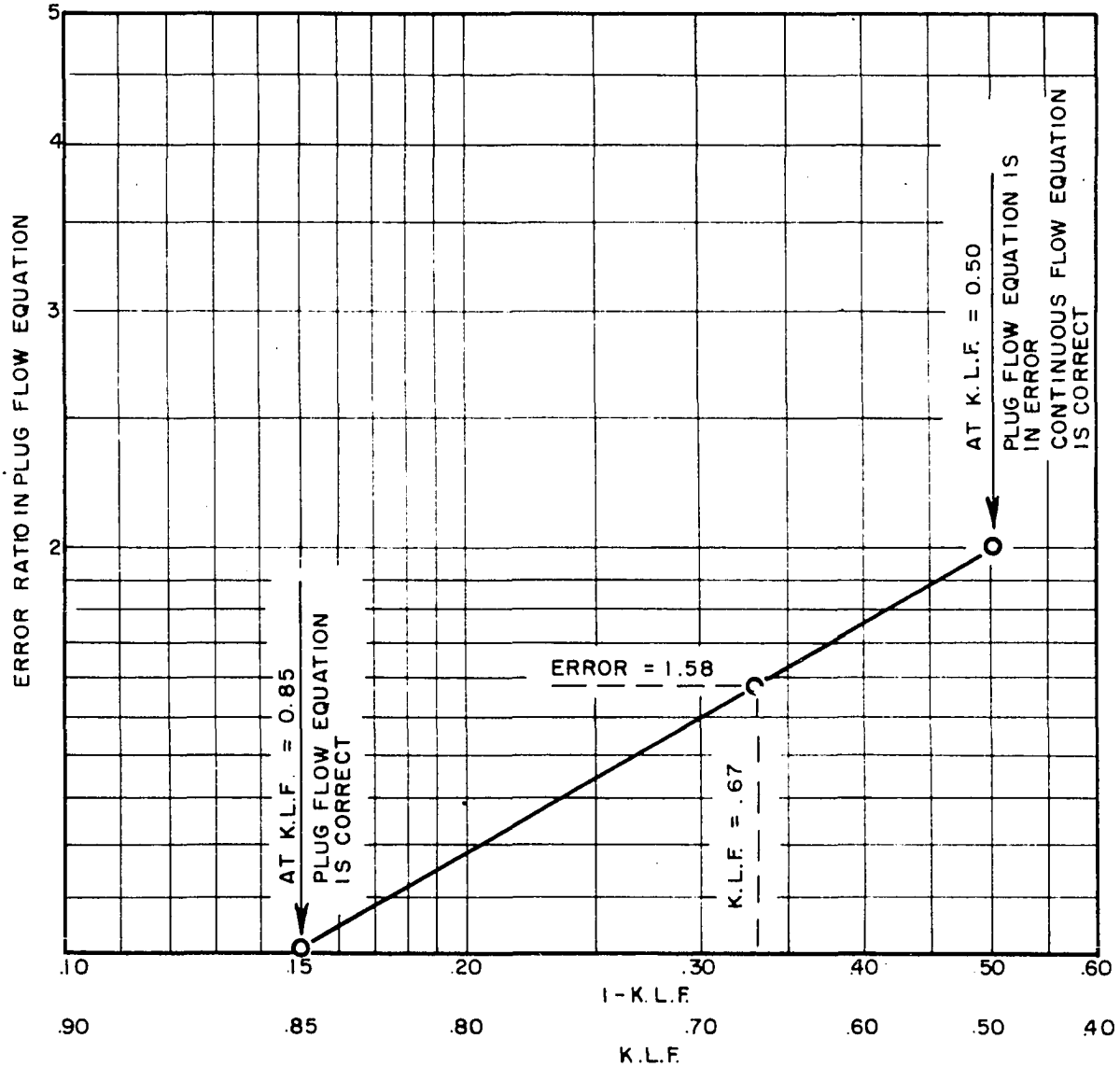

FIG. XV SAMPLE INTERPOLATION GRAPH FOR INTERMEDIATE FLOW BETWEEN KFL OF 0.50 AND 0.85

Using this interpolation scheme, the standard deviation was found to be ±16 per cent or an error of ±34 per cent at the 95 per cent confidence level. This error is slightly greater than found in the other two flow regions. But this was not unexpected, for in this region the violence of the slugs caused great pressure fluctuations, and even duplicate points sometimes differed by more than 34 per cent.

Accuracy of the Pressure Drop Predictions

In Figures XVI and XVII the data are plotted showing the actual pressure drops compared to the predicted pressure drops. In Figure XVI are the writer's water-air, oil-air and glycol-air data, and in Figure XVII the Chenoweth and Martin water-air data. Considering the inherent errors in measuring two-phase pressure drops, the fit is excellent. The average absolute error is ±12 per cent. With a normal Gaussian distribution, the average error can be related to the standard deviation ($3\sigma_b$) using the factor $\sqrt{\pi/2}$. So the standard deviation is ±15 per cent. This gives an error of ±32 per cent at the 95 per cent confidence level (1.96σ). The 95 per cent confidence limit lines are shown in Figures XVI and XVII.

This correlation covers a broad range of data. The liquid mass velocities ranged from 1,942 lb/hr-sq ft to 2,258,000 lb/hr-sq ft. The gas mass velocities ranged from 73 lb/hr-sq ft to 225,800 lb/hr-sq ft. The Kinetic Liquid Fraction ranged from 0.0012 (almost 100 per cent gas flow) to 0.994 (almost pure liquid). The pressure drops ranged from 0.105 lb/sq ft-ft of pipe to 83.4 lb/sq ft-ft of pipe. There were 642 points used in all — 352 from the writer's data and 290 from Chenoweth and Martin.

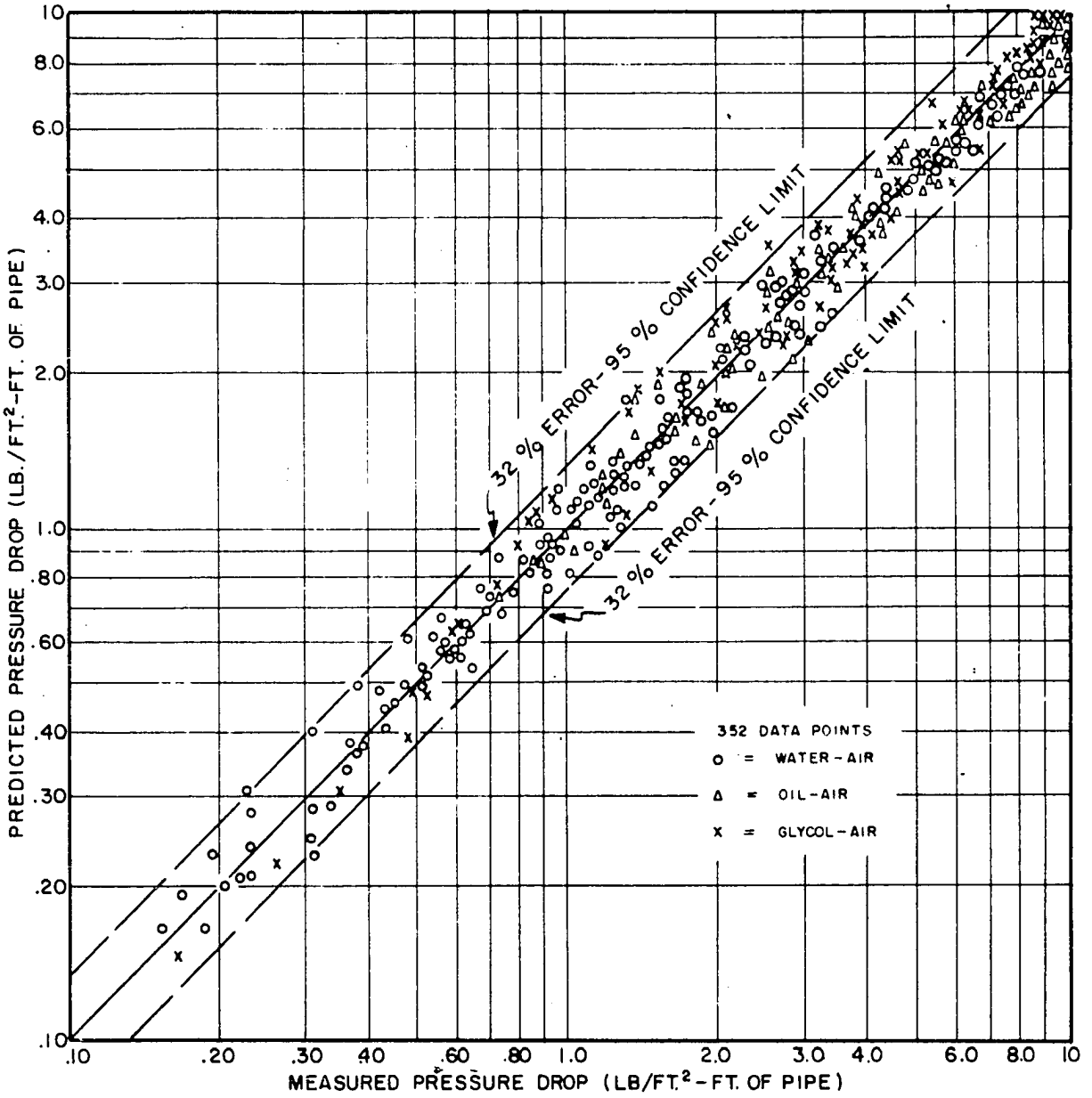

FIG. XVI

COMPARISON OF PREDICTED VERSUS MEASURED PRESSURE GRADIENT BRIGHAM DATA

FIGURE XVII
COMPARISON OF PREDICTED PRESSURE GRADIENT
VERSUS
MEASURED PRESSURE GRADIENT
Chenoweth and Martin data
Air-Water flow in 1½" & 3" pipe
290 Data Points

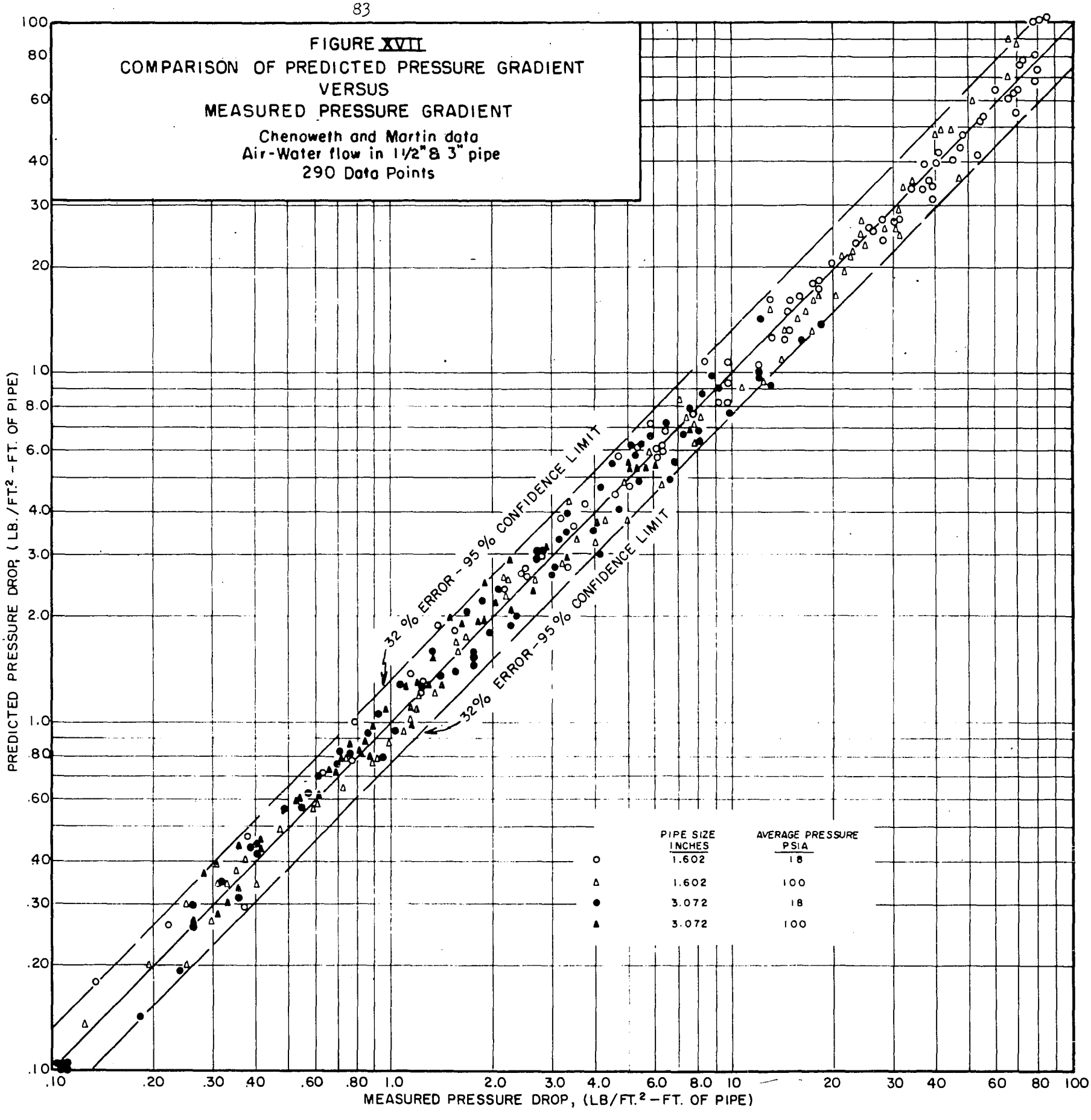

As a test of the correlation, the accuracy of fit may be compared to Chenoweth and Martin's correlation of their own data. Their correlation had an average absolute error of ±19 per cent, which is equivalent to a standard deviation of ±24 per cent and a 95 per cent confidence level of ±53 per cent. This is roughly half again as much error as in Figures XVI and XVII. In addition, Chenoweth and Martin only included 264 of their data points. The others fell considerably below their correlating lines.

Comparison with Other Laboratory Data. The correlation was also tested against the data of Green (37) on the water-air and gas oil-air systems in 2-inch pipe, and the data of Reid, et. al. (62) on water and air in 4-inch and 6-inch pipes. Since Green's data were taken in the same kind of tubing as the writer's, Equation (2) was used for calculating his single-phase friction factors. The comparison with these data is shown in Figure XVIII. As can be seen, the fit is outstandingly good — even better than the writer's data in Figure XVI. This excellent fit is primarily due to better control of flow rates in Green's data. The standard deviation was found to be only ±11 per cent, and the corresponding error at a 95 per cent confidence level only ±25 per cent.

Green (37) has tested his data against White's correlation. He found for his Wave, Cresting and Annular flow data, that the accuracy of White's fit was about the same as in Figure XVIII. This is not surprising, since White's correlation has always been found to fit the laboratory data in these flow regions. However, none of Green's Slug Flow data fit White's correlation. On the other hand, the slug data are included in Figure XVIII, and are found to fit exceedingly well. Green's data ranged from

FIGURE XVIII
TEST OF PRESSURE DROP CORRELATION
AGAINST THE DATA OF GREEN & REID et. al.
118 Data Points

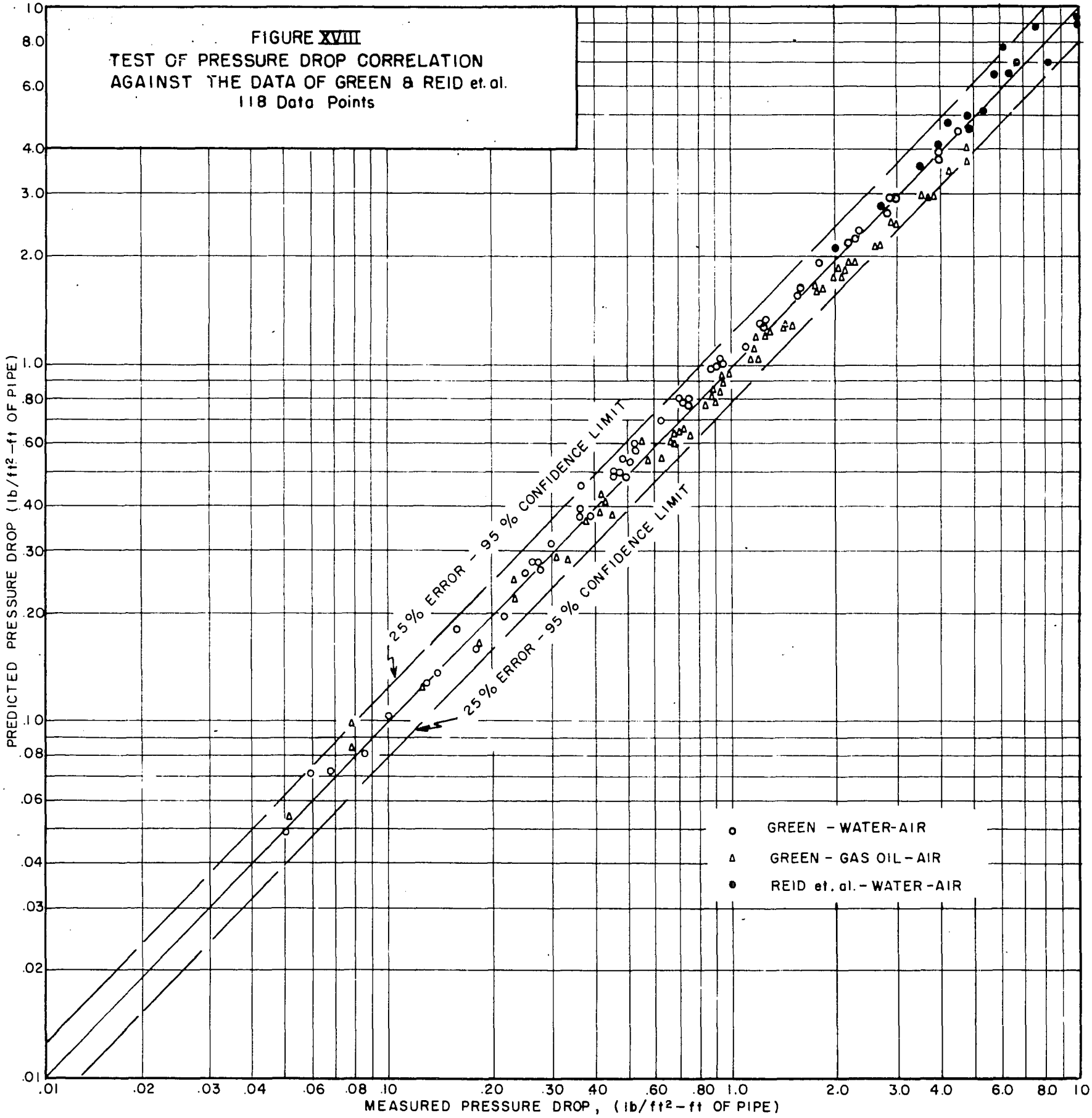

a K.L.F. of 0.0070 to 0.50, thus he includes both the Continuous and the Intermediate Flow regions.

Only a portion of the data of Reid, et. al., are included in Figure XVIII. This is due to some obvious errors in their original data. The reported single-phase friction factors are not internally consistent for their 6-inch pipe. The two-phase data on this pipe were found to fit the predictions closely; but, due to the cloud of doubt raised by the single-phase data, this portion of the two-phase data was not included in Figure XVIII. The 4-inch pipe data are reliable, and the fit was excellent on these, as seen in Figure XVIII. The data ranged over a liquid fraction of 0.50 to 0.96, so the flow was in both the Intermediate and Plug regions.

Comparison with Field Data. When the major constituent in a flowing two-phase system is liquid, the K.L.F. is high (>0.85) and the flow mechanism is Plug Flow. The most reliable field data in this region is reported by Baxendell (12,13). He correlated his data within ±15 per cent using a pseudo-friction factor based on the average density of the flowing fluids. This pseudo-friction factor equation is equivalent to Equation (33) presented in the previous chapter.

$$f_{TP} = \frac{2g_c D}{(G_L+G_G)(U_L+U_G)}\left(\frac{dP}{dL}\right)_{TP} \qquad (33)$$

According to the correlation results found in Plug Flow, Equation (33) would predict slightly too high a pressure drop for Baxendell's data -- or, in other words, the two-phase friction factors calculated by Equation (33) would be lower than the single-phase friction factors. At the conditions of Baxendell's flow lines this error should be a factor of about

0.80 to 0.90. In Figure XIX Baxendell's correlation of his data is compared to the single-phase Fanning friction factor. It can be seen that the two-phase data is slightly below the single-phase equation, and thus the Plug Flow correlation in this text is well validated by the data.

When the most of the flowing fluid is gas, the K.L.F. approaches zero. One might expect the correlation to predict the single-phase gas pressure drop under this condition, but the actual Continuous Flow correlation of Figure XII shows (at a Froude Number below 10.0 -- the usual range in pipelines) the two-phase friction factor is roughly 20 per cent higher than the single-phase friction factor. Field pipeline data exhibit the same behavior. Baker (10) and Flanigan (32) both point out that an almost infinitesimal amount of liquid will cause roughly a 10 per cent loss in pipeline efficiency. Apparently it is only necessary for the pipe wall to be damp with liquid for this loss to occur. A 10 per cent drop in pipeline efficiency is equivalent to a 20 per cent increase in friction factor, thus the correlation appears valid at very low values of K.L.F.

Baker (8) and Van Wingen (73) have presented field data in the 4-inch to 10-inch pipes ranging in K.L.F. from 0.021 to 0.75. There are 29 data points between a K.L.F. of 0.021 and 0.35; 18 from Baker's data and 11 from Van Wingen's data. Using the Continuous Flow correlation of Figure XII, the data from 0.021 to 0.35 were predicted with an average absolute error of ±31 per cent. This is certainly not an outstanding match of the data, but Baker's and Van Wingen's correlations of these same data gave an average absolute error of ±44 per cent, which is considerably worse. Also the correlation of Figure XII is much easier to

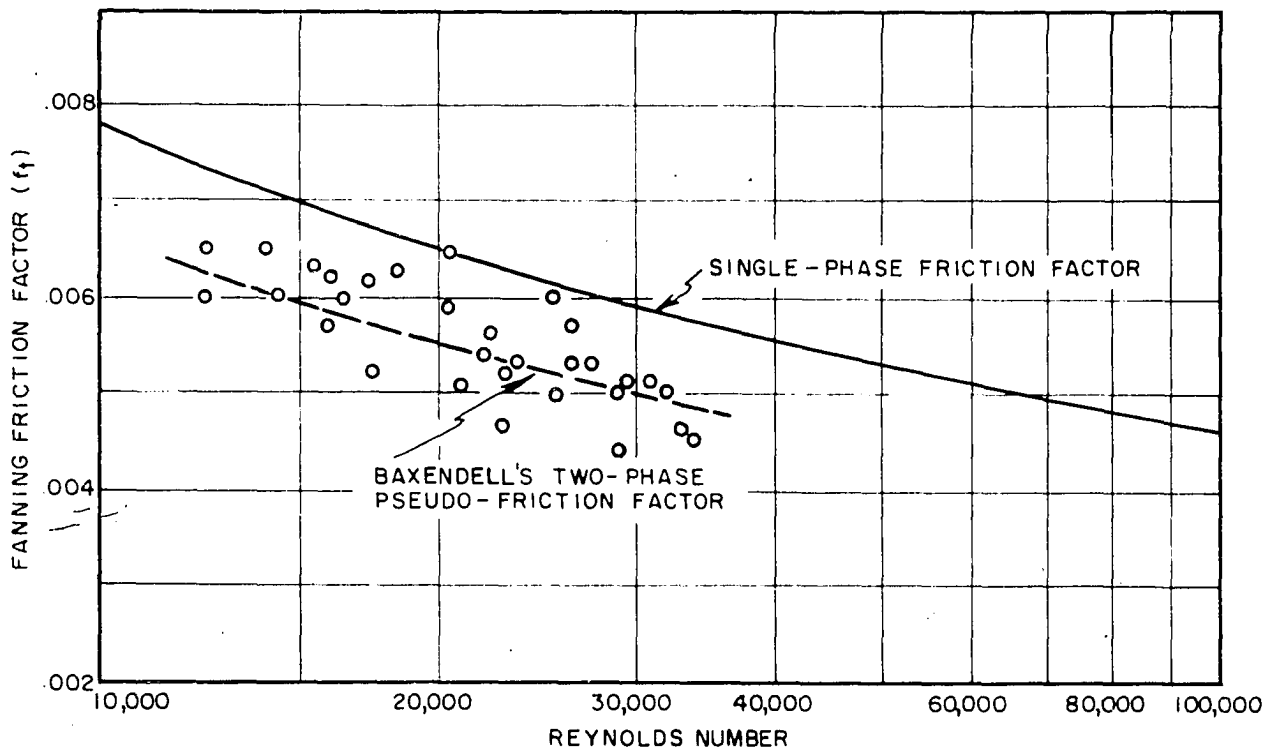

FIG. XIX COMPARISON OF BAXENDELL'S TWO-PHASE FRICTION FACTOR WITH THE SINGLE-PHASE FRICTION FACTOR

use, for only one calculation method is needed, while four different equations were used by Baker and Van Wingen depending on the flow pattern of the data. It is not really reasonable to expect much greater accuracy of prediction on these data; for some of the Van Wingen data were undoubtedly at unsteady-state conditions, and some of the Baker data showed pressure drops as low as 0.50 and 1.0 psi.

The data of Baker and Van Wingen at K.L.F.'s ranging from 0.35 to 0.75 were also checked against the correlations in this chapter. In this range, the actual pressure drops were found to be two to four times higher than predicted. This result was somewhat puzzling, especially considering the good match found with all other data. The probable reason for the poor correspondence is the violent slugging that occurs in this range of liquid fraction. The slugging may cause an extra pressure drop in field pipelines due to the hills and valleys. Also the slugging may cause a greater pressure gradient in long lines due to the very nature of the flow process itself. This is explained below.

The laboratory data definitely show that the most violent slugs occur in the region between K.L.F.'s of about 0.35 to 0.75. In this region the pressure drop jumps to a very high level as a slug goes by and then drops drastically. The investigator has to filter out these variations and try to read an "average" value. However, in the shorter laboratory tubing, the slugs are not always present. That is, they form, then are swept out, then re-form again. During the time after one slug has been swept out and before the formation of another slug, the pressure drop is much lower and thus the average is lowered. This happened in the relatively long laboratory tubing used by this writer, so it

surely must have occurred in the shorter tubing of the other laboratory investigators. On the other hand, in long field lines the slugs are always present, and the average pressure gradient is likely to be higher than found in shorter tubing.

The reason for Baker's and Van Wingen's higher pressure drops cannot be stated for sure. This answer will have to come by taking careful data in long exactly-horizontal lines. In the meantime, however, we must predict the gradients in two-phase systems in the region of K.L.F. from about 0.35 to 0.75. From the results shown, it looks as if the pressure drops in short two-phase tubing (such as heat-exchangers, condensers, and tubular reactors) will be correctly predicted by the correlations presented here; while the pressure gradients in long field lines will be greater by a factor of two to four. At higher or lower K.L.F.'s the correlations will correctly predict the pressure drop in all horizontal two-phase systems.

Correlation of Shut-In Ratio

In the preceding chapter, it was predicted that the liquid fraction shut-in (F.S.I.) would be a function of the Kinetic Liquid Fraction (K.L.F.) and the Reynolds Number. The Reynolds Number was defined in Equation (46).

$$Re.No. = \frac{D G_{L,eq.}}{\mu_L} \left(\frac{\mu_L}{\mu_G}\right)^{0.30} \tag{46}$$

and the K.L.F. from Equation (23) is,

$$K.L.F. = \frac{G_L \sqrt{\Delta P_L}}{G_L \sqrt{\Delta P_L} + G_G \sqrt{\Delta P_G}} \tag{23}$$

Using these parameters, the writer's shut-in data on the

water-air, oil-air and glycol-air systems were correlated along with the water-air and gas-oil-air data of Green (37). The resulting correlation is presented in Figure XX. In Figure XXI the calculated shut-in fraction from the correlation of Figure XX is compared with the actual shut-in fraction to show the accuracy of fit. The standard deviation is ±19 per cent, which is equivalent to ±40 per cent at the 95 per cent confidence level. This is not as close as the pressure drop correlations, but is still quite good considering the scatter of the basic data.

As seen in Figure XX, the correlation qualitatively follows the theoretical curves in Figure IX of Chapter IV. The shut-in fraction increases with an increase in Kinetic Liquid Fraction, and it decreases with an increase in Reynolds Number. Also, the correlation curves are seen to fall below and to the right of the theoretical curves of Figure IX, as predicted.

The errors in this correlation are mainly due to the inaccurate shut-in data. There are several points at duplicate flow conditions which differ from each other by two standard deviations. It seems likely, as more accurate shut-in data become available in piping of various diameters and at different pressures, that the Froude Number will be necessary to improve the correlation. The data available at the present time, however, are basically not accurate enough to warrant the addition of this term.

Conclusions

There are three major flow regions in horizontal two-phase gas-liquid turbulent flow; Continuous Flow, Intermediate (or Slug) Flow,

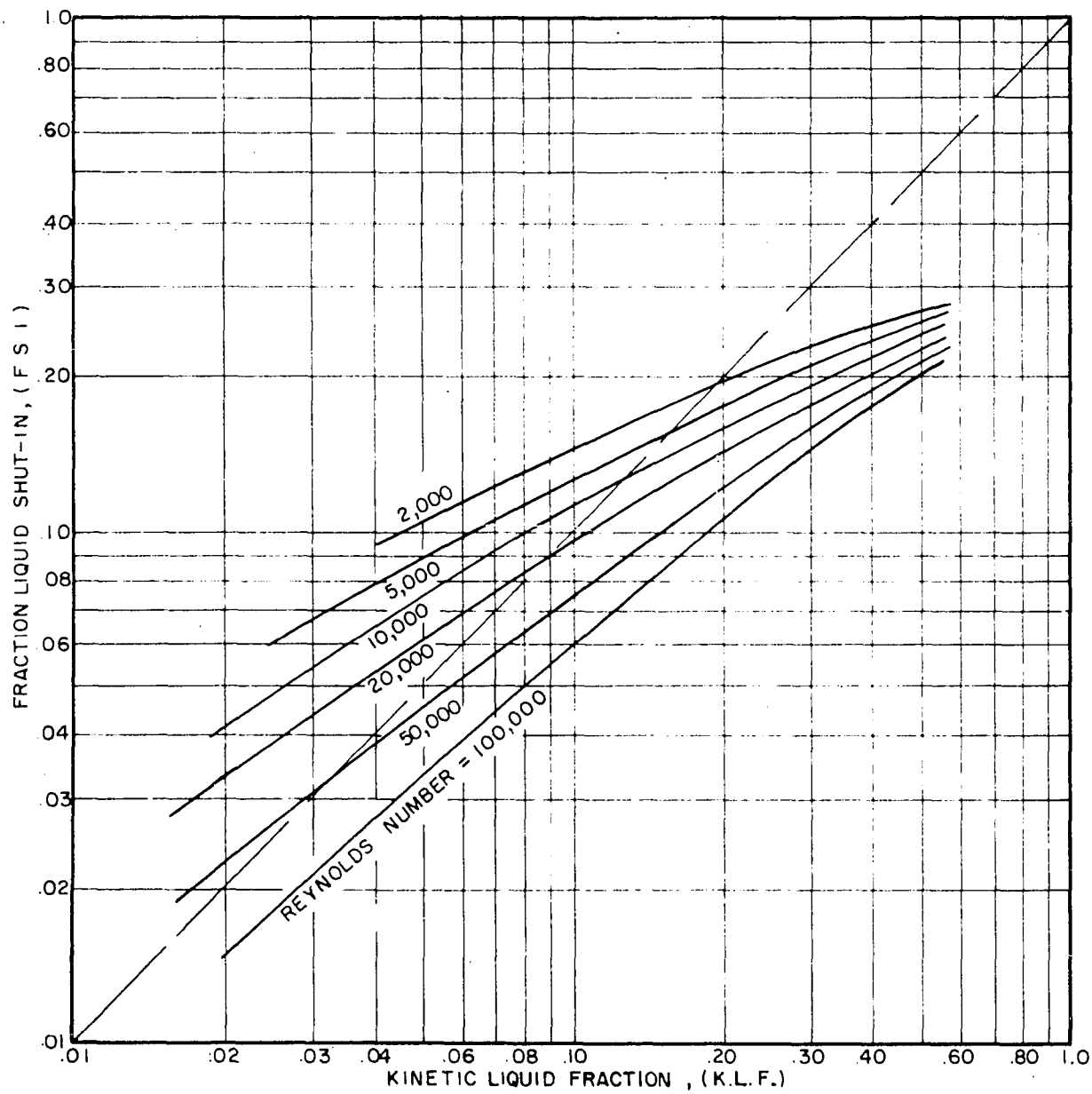

FIG. XX CORRELATION OF SHUT-IN FRACTION
VERSUS
KINETIC LIQUID FRACTION AND TWO-PHASE REYNOLDS NUMBER

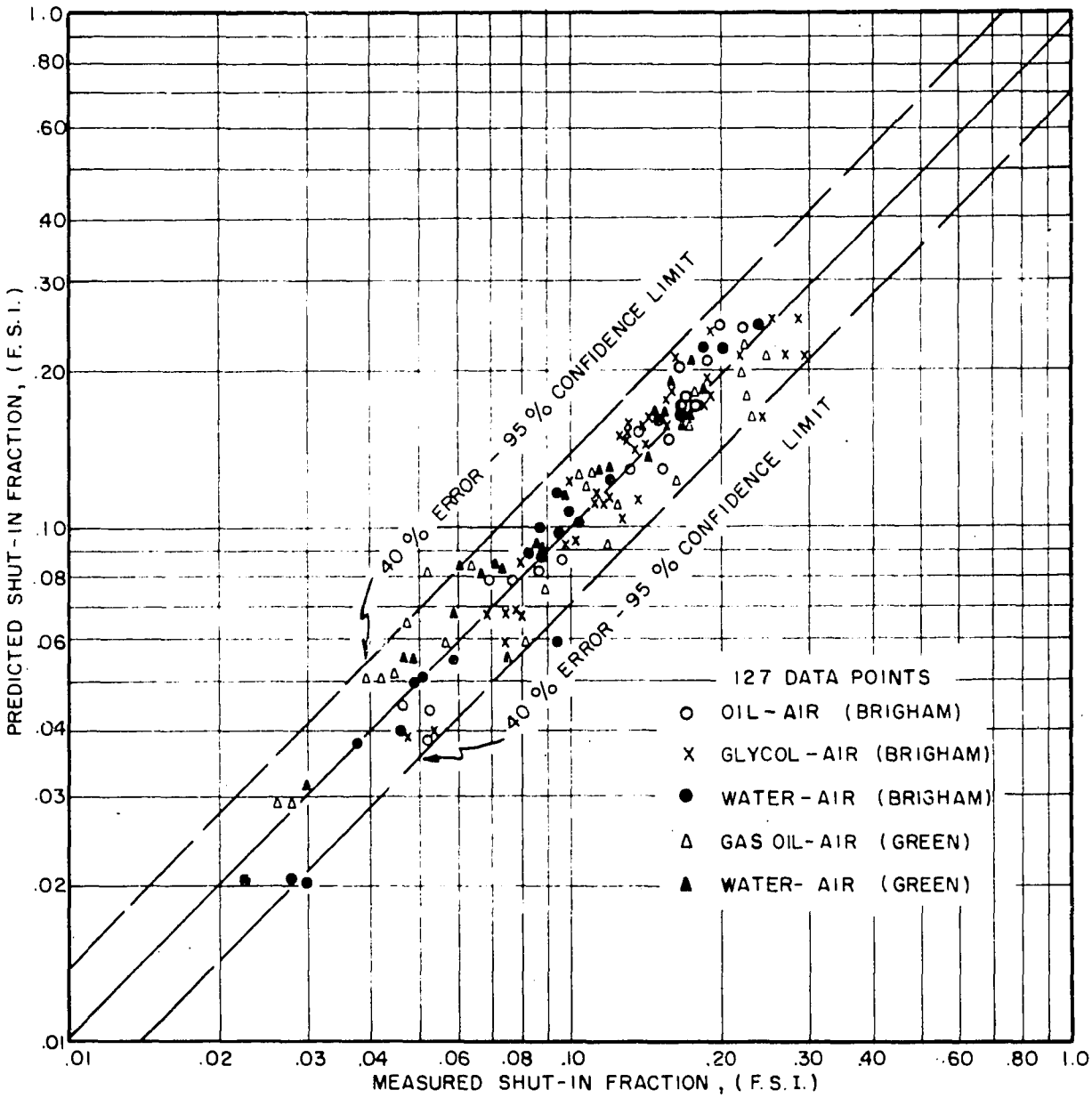

FIG. XXI COMPARISON OF PREDICTED FRACTION SHUT-IN VERSUS ACTUAL SHUT-IN FRACTION

and Plug Flow. Continuous Flow occurs when the gas is predominant in determining the flow mechanism. Intermediate (or Slug) Flow occurs when the liquid and gas are more or less equally important. Plug Flow occurs when the liquid is the predominant flowing fluid, with the gas being of secondary importance.

A dynamic flowing ratio, the Kinetic Liquid Fraction (K.L.F.) is defined which relates the relative kinetic energies of the flowing fluids and which can be used to determine the flow mechanism. When the K.F.L. lies between 0.00 and 0.15 the mechanism is Continuous Flow; from 0.15 to 0.85 the mechanism is Intermediate (or Slug) Flow; and from 0.85 to 1.0 the mechanism is Plug Flow.

The pressure drop in the Continuous Flow region was correlated using five dimensionless parameters; the friction factor, the Reynolds Number, the ratio of the gas and liquid viscosities, the Kinetic Liquid Fraction and the Froude Number. These parameters were chosen by analogy with the accepted theories of single-phase turbulent flow. The correlating technique is applicable from a K.L.F. of 0.00 to 0.50 and at all ranges of the other parameters. Although the flow mechanism is Intermediate (or Slug) Flow in the K.F.L. range of 0.15 to 0.50, the pressure drop is apparently caused predominately by the Continuous Flow mechanism and the correlating technique is valid in this range.

For the Plug Flow region, two theoretical equations were defined; one assuming the liquid and gas flow completely mixed, and the other assuming they flow as completely separate plugs. The actual pressure drop was found to lie midway between these two equations. The Plug Flow equation is valid between K.L.F.'s of 0.85 and 1.00.

The Intermediate Flow region (K.L.F. from 0.50 to 0.85) was successfully correlated using a simple logarithmic interpolation between the Continuous and the Plug Flow equations.

The laboratory pressure drop data presented herein and the data of Chenoweth and Martin (29) were correlated with a standard deviation of ±15 per cent. The laboratory data of Green (37) and Reid, et al. (62) were correlated with a standard deviation of ±12 per cent. Thus the pressure drop correlations appear to be more accurate than any presented heretofore.

The pressure drop data in long field lines were found to be adequately predicted by the above equations in the K.L.F. ranges of 0.00 to 0.35 and from 0.75 to 1.00. However, at K.L.F's from 0.35 to 0.75 the pressure drop was two to four times as high as predicted. The reason for this discrepancy may be due to the hills and valleys in long field lines or may be due to the basic nature of the flow process. This question probably can only be cleared up by taking accurate data in exactly horizontal lines of several hundred feet in length.

The volume of liquid in-place (fraction shut-in) in the line was correlated as a function of the Kinetic Liquid Fraction (K.L.F.) and the two-phase Reynolds Number. The correlation standard deviation was ±19 per cent. The Froude Number may also be important in determining the shut-in conditions; but the data were not accurate enough, and the pipe diameter and pressure ranges not broad enough, to warrant an attempt to further refine the correlation.

SUMMARY

Two-phase pipe flow of liquid and gas is becoming a problem of considerable interest to engineers. In the producing of petroleum, for instance, the problem of predicting two-phase pressure drops frequently arises. Also in the processing industries predictions are needed in heat exchangers, boilers and reactors where both the pressure drop and the ratios of fluids in-place are important. Correlations are available for design of these systems, but their accuracy leaves much to be desired.

Flow data were run in 2-inch clear plastic tubing on the oil-air, glycol-air and water-air systems. These data represented a wide range of liquid properties and gas/liquid flowing ratios. Data published by Messrs. Chenoweth and Martin of the C. F. Braun Company were also used in the correlative work to extend the range of pipe diameters and operating pressures.

Visual data were recorded on 16 mm film and are available through Dr. R. L. Huntington of the Department of Chemical Engineering. These studies gave the clue to the understanding of the two-phase flow mechanism so that the flow could be divided into three major regions: (1) Continuous (or Annular) Flow, in which the gas is predominant in the flow mechanism; (2) Intermediate (or Slug) Flow, in which the liquid and gas are both important; and (3) Plug Flow, in which the liquid is the predominant flowing fluid and the gas is of secondary importance.

These data also showed that Stratified Flow, which has been discussed at length in the literature, is primarily a laboratory phenomenon caused by the short lengths of tubing used. A flowing ratio, termed the Kinetic Liquid Fraction, is developed which determines the flow region.

An analogy with the single-phase theories of Prandtl and von Karman is used to develop correlating paramaters for the pressure drops and shut-in ratios in Continuous Flow. For the pressure drop prediction, five dimensionless parameters are important. They are: the friction factor, the Reynolds Number, the gas/liquid viscosity ratio, the Kinetic Liquid Fraction and the Froude Number. For the shut-in ratio, the Reynolds Number and the Kinetic Liquid Fraction were found to be adequate correlating terms; although the Froude Number may also be found necessary in systems at higher pressures and different diameters.

Two theoretical equations are developed for the Plug Flow region. The pressure drop data in this region was found to fall midway between these equations with a good accuracy of fit.

In the Intermediate Flow region no theoretical analysis was attempted. It was found that a simple logarithmic interpolation between the Continuous and the Plug Flow equations was quite adequate for correlating these data.

The correlations were compared with published laboratory and field data and in most cases fit remarkably well. The lone exception was in Intermediate (or Slug) Flow in long field pipelines. It appears that this discrepancy can only be resolved with accurate data in exactly-horizontal lines of several hundred feet in length.

BIBLIOGRAPHY

1. Abramson, A. E. "Investigation of Annular Liquid Flow with Co-current Air Flow in Horizontal Tubes," Jour. of Appl. Mech. (Sept., 1952), 267-74.

2. Alves, G. E. "Cocurrent Liquid-Gas Flow in a Pipe-Line Contactor," Chem. Engr. Prog. (Sept., 1954) 50, No. 9, 449-56.

3. Angel, R. F. "Volume Requirements for Air or Gas Drilling," AIME Paper No. 873-G, Presented at 32nd Annual Fall Meeting, SPE, Dallas, Texas (Oct., 1957).

4. Aziz, M. F. "Annular Flow of Gas and Liquid in Smooth Pipes," Paper No. 60-WA-161 presented at Winter Meeting of ASME, New York, N. Y. (Nov. 1960).

5. Baker, O. "Experience with Two-Phase Pipelines," Can. Oil and Gas Ind. (March, 1961) 43-53.

6. Baker, O. "Multiphase Flow in Pipelines," Oil and Gas Jour. (Nov. 19, 1958) 156-57.

7. Baker, O. "Discussion of 'How Uphill and Downhill Flow Affect Pressure Drop'," Oil and Gas Jour. (Nov. 11, 1957) 150-52.

8. Baker, O. "Design of Pipelines for the Simultaneous Flow of Oil and Gas," Oil and Gas Jour. (July 26, 1954).

9. Baker, O. "Speed-Up Flow Calculations for Design of Gas Gathering Systems," Oil and Gas Jour. (May 16, 1955)

10. Baker, O. "Designing Pipelines for Simultaneous Flow of Oil and Gas," Pipeline Engr., Handbook Section (Feb., 1960) H-67.

11. Bakhmeteff, Boris A. The Mechanics of Turbulent Flow, Princeton University Press, Princeton, New Jersey (1941).

12. Baxendell, P. B. and Thomas, R. "The Calculation of Pressure Gradients in High Rate Flowing Wells," Paper presented at 43rd National Meeting of AIChE, Tulsa, Okla. (Sept., 1960).

13. Baxendell, P. B. "Pipeline Flow of Oil and Gas Mixtures," Proc. Fourth World Petr. Cong. - Section II E (1955), 343-351.

14. Begell, W. and Hoopes, J. A., Jr. "Acceleration Pressure Drops in Two-Phase Flow," U. S. Atomic Energy Comm., AEC Bulletin CU-18-54-AT-DP-Ch. E. (April, 1954).

15. Benjamin, M. W. and Miller, J. G. "The Flow of Flashing Mixtures of Water and Steam Through Pipes," Trans. ASME, (1942) 64, 657.

16. Bergelin, O. P. and Gazley, C., Jr. "Co-Current Gas-Liquid Flow, I. Flow in Horizontal Tubes," Heat Transfer and Fluid Mechanics Inst., Berkeley, Calif. Meeting, Published by ASME (1949), 5-18.

17. Bergelin, O. P. "Flow of Gas-Liquid Mixtures," Chem. Engr. (1949) 56, 104.

18. Berry, A. L. and Moreau, B. L. "The Peace River and Alaska Highway Gas Gathering System," Presented at the Annual Gen'l. and Prof. Meeting, Engr. Inst. of Canada, Banff, Alberta (June, 1957).

19. Bertuzzi, A. F., Tek, M. R. and Poettman, F. H. "Simultaneous Flow of Liquid and Gas Through Horizontal Pipes," Trans. AIME, 207 (1956) 17-24.

20. Buckley, S. E. and Leverett, M. C. "Mechanism of Fluid Displacement in Sands," Trans. AIME, (1942) 146, 107-116.

21. Brigham, W. E., Holstein, E. D. and Huntington, R. L. "How Uphill and Downhill Flow Affect Pressure Drop," Oil and Gas Jour. (Nov. 11, 1957), 145-152.

22. Brigham, W. E. "Two-Phase Flow of Oil and Air Through Inclined Pipe," M. Ch. E. Thesis, Univ. of Okla. (1956).

23. Calvert, S. and Williams, B. "The Upward Co-Current Annular Flow of Air and Water in Smooth Tubes," AIChE Jour. (March, 1955) 1, No. 1, 78-86.

24. Campbell, J. M. "Problems of Multiphase Pipeline Flow," Oil and Gas Jour., (Nov. 4, 1957) 55, No. 44, 151-2.

25. Campbell, J. M. "How to Calculate Multiphase Flow Systems," Oil and Gas Jour. (Dec. 9, 1957) 55, No. 49, 126-7.

26. Charles, M. E. "The Reduction of Pressure Gradients in Oil Pipelines: Experimental Results for the Stratified Pipeline Flow of a Heavy Crude Oil and Water," Paper presented at First Joint Meeting of CIM and the Rocky Mtn. Sect. of SPE of AIME, Calgary, Alberta (May, 1960).

27. Charles, M. E., Govier, G. W. and Hodgson, G. W. "The Horizontal Pipeline Flow of Equal Density Oil-Water Mixtures," Can. Jour. of Ch. E. (Feb., 1961) 27-36.

28. Chavez, J. A. "New Correlation for Two-Phase Pipeline Flow," Oil and Gas Jour. (Aug. 24, 1959) 57, No. 35, 100-102.

29. Chenoweth, J. M. and Martin M. W. "Turbulent Two-Phase Flow," Petr. Ref. (Oct., 1955), 151-55.

30. Coldiron, A. L. "The Inclined Two-Phase Flow of Diethylene Glycol and Air," M.Ch.E. Thesis, Univ. of Oklahoma (1950).

30a. Davis, W. J. "The Effect of the Froude Number in Estimating Vertical Two-Phase Gas-Liquid Friction Losses," Paper presented at 46th Nat'l. AIChE Meeting, Los Angeles, (Feb. 4-7, 1962).

30b. Dixon, W. J. and Massey, F. J., Jr. Introduction to Statistical Analysis, McGraw Hill Book Co., New York, N. Y. (1951) 233.

31. Dittus, F. W. and Hildebrand, A. "A Method of Determining the Pressure Drop for Oil-Vapor Mixtures Flowing Through Furnace Coils," Trans. ASME (1942) 64, 185.

32. Flanigan, O. "Affect of Uphill Flow on Pressure Drop in Design of Two-Phase Gathering Systems," Oil and Gas Jour. (March 10, 1958) 132-41.

33. Gazley, C., Jr. "Co-Current Gas-Liquid Flow — III, Interfacial Shear and Stability," Heat Transfer and Fluid Mechanics Inst., Berkeley, Calif. Meeting, Published by ASME (1949), 29-40.

34. Gazley, C., Jr. and Bergelin, O. P. "Discussion of "Proposed Correlation for Isothermal Two-Phase, Two-Component Flow in Pipes"," Chem. Engr. Prog. (Jan., 1949) 45, No. 1, 45-48.

35. Gilbert, W. E. "Flowing and Gas Lift Well Performance," API Drill. and Prod. Practice (1954).

36. Gray, K. E. "The Cutting Carrying Capacity of Air at Pressures Above Atmospheric," AIME Paper No. 874-G, Presented at 32nd Annual Fall Meeting, SPE, Dallas, Texas (Oct., 1957).

37. Green, D. W. "Concurrent Two-Phase Flow of Liquids and Air Through Inclined Pipe," M.Ch.E. Thesis, Univ. of Okla. (1959).

38. Green, D. W. and Huntington, R. L. "Velocities are Critical in Two-Phase Gathering Systems," Ref. Engr. (May, 1959) C-29.

39. Govier, G. W. and Omer, M. M. "The Horizontal Flow of Air-Water Mixtures," Preprint No. 7 presented at joint AIChE-CIC Meeting, Cleveland, Ohio (May, 1961).

40. Hanratty, T. J. and Enzen, J. M. "Interaction Between a Turbulent Air Stream and a Moving Water Surface," AIChE Jour. (Sept. 1957) 3, No. 3, 299-304.

41. Holstein, E. D. "Two-Phase Flow of Water and Air Through Inclined Pipe," M.Ch.E. Thesis, Univ. of Okla. (1955).

42. Hoogendorn, C. J. "Gas-Liquid Flow in Horizontal Pipes," Chem. Engr. Sci. (1959) 9, 205-17.

43. Isbin, H. S., Moen, R. H. and Mosher, D. R. "Two-Phase Pressure Drops," U. S. AEC Bull. AECU-2994 (Nov., 1954).

44. Isbin, H. S., Rodriguez, H. A., Larson, H. C. and Pattie, B. D. "Void Fractions in Two-Phase Flow," AIChE Jour. (Dec. 1959) 417-32.

45. Isbin, H. S., Moen, R. H., Wickey, R. O., Mosher, D. R. and Larson, F. W. "Two-Phase Steam-Water Pressure Drops," Chem. Engr. Prog. Symposium Series (1959) 5, No. 23, 75-84.

46. Jeffreys, H. "On the Formation of Water waves by Wind," Proc. Roy Soc. A-107 (1925) 189-206.

47. Jenkins, R. "Two-Phase, Two-Component Flow of Air and Water," M. S. Thesis, Univ. of Dela. (1947).

48. Johnson, H. A. and Abou-Sabe, A. H. "Heat Transfer and Pressure Drop for Turbulent Flow of Air-Water Mixtures in Horizontal Pipe," Trans. AIME (1954) 76, 561.

49. Kosterin, S. I. "An Investigation of the Influence of the Diameter and Inclination of a Tube in the Hydraulic Resistance and Flow Structure of Gas-Liquid Mixtures," Izvest. Akad. Nauk. U.S.S.R. — Otdel Tekh Nauk No. 12, (1949), 1864.

50. Krasiaskova, L. I. "Some Characteristic Flows of a Two-Phase Mixture in a Horizontal Pipe," Zhurn. Tech. Fiz. (1952) 22, No. 4, 656.

51. Lamb, H. Hydrodynamics, Sixth Edition, Dover Publications, New York, N. Y. (1945).

52. Lockhart, R. W. and Martinelli, R. C. "Proposed Correlation of Data for Isothermal Two-Phase, Two-Component Flow in Pipes," Chem. Engr. Prog. (Jan., 1949) 45, No. 1, 39-45.

53. Martinelli, R. C., Boelter, L. M. K., Taylor, T. H. M., Thomsen, E. G. and Morrin, E. H. "Isothermal Pressure Drop for Two-Phase, Two-Component Flow in a Horizontal Pipe," Trans. ASME (Feb., 1944), 139-51.

54. Martinelli, R. C., Putnam, J. A. and Lockhart, R. W. "Two-Phase, Two-Component Flow in the Viscous Region," AIChE Jour. (1946) 681-705.

55. Martinelli, R. C. and Nelson, D. B. "Prediction of Pressure Drop During Forced-Circulation Boiling of Water," Trans. ASME (1948) 70, 695.

56. McAdams, W. H., Woods, W. K. and Heroman, L. C., Jr. "Vaporization Inside Horizontal Tubes — II, Benzene-Oil Mixtures." Trans. ASME (1942) 64, 193-200.

57. McAfee, R. V. "The Evaluation of Vertical Lift Performance in Producing Wells," AIME Paper No. 1557-G, Presented at 35th Annual Fall Meeting, SPE, Denver (Oct., 1960).

58. Moody, L. F. "Friction Factors for Pipe Flow," Trans. ASME (1944) 66, 671-684.

59. Nikuradse, J. "Laws of Fluid Flow in Rough Pipes (Part 4)," Petr. Engr. (July 4, 1940) 38-42.

60. Perry, J. H., Editor. Chemical Engineer's Handbook Third Edition, McGraw Hill Book Co., New York, N. Y. (1950).

61. Poettman, F. H. and Carpenter, Paul G. "The Multiphase Flow of Gas, Oil, and Water Through Vertical Flow Strings with Application to the Design of Gas-Lift Installations," API Drill. and Prod. Practice (1952).

62. Reid, R. C., Reynolds, A. B., Diglio, A. J., Spiewak, I. and Klipstein, D. H. "Two-Phase Pressure Drops in Large Diameter Pipes," AIChE Jour. (Dec., 1956) 2, No. 4, 536-8.

63. Rogers, J. D. "Two-Phase Flow of Hydrogen in Horizontal Tubes," AIChE Jour. (Dec. 1956) 2, No. 4, 536-8.

64. Rouse, H. and Howe, J. W. Basic Mechanics of Fluids, John Wiley and Sons, Inc., New York, N. Y. (1953).

65. Russell, J. S. "Report on Waves," Brit. Assn. Rep. (1844).

66. Russell, T. W. F. and Charles, M. E. "The Effect of the Less Viscous Liquid in the Laminar Flow of Two Immiscible Liquids," Can. Jour. of Chem. Engr. (1959) 37, No. 1, 18-24.

67. Schneider, F. N. "Some Aspects of Simultaneous Horizontal Two-Phase Flow," M. P. E. Thesis, Univ. of Okla. (1953).

68. Schneider, F. N., White, P. D. and Huntington, R. L. "Horizontal Two-Phase Oil and Gas Flow," Pipe Line Ind. (Oct., 1954).

69. Scott, J. O. "How Much Air to Put Down the Hole in Air Drilling," Oil and Gas Jour. (Dec. 16, 1957) 104-7.

70. Tek, M. R. "Multiphase Flow of Water, Oil and Natural Gas Through Vertical Flow Strings," Chem. and Met. Engr. Dept., Univ. of Michigan, Ann Arbor, Mich. (Sept., 1960).

71. Tek, M. R. and Chan, W. J. "Simultaneous Flow of Liquid and Gas Through Vertical Pipe," Paper presented at AIChE Annual Meeting, San Francisco, Calif. (Dec., 1959).

72. Uren, L. C., Gregory, P. P., Hancock, R. A. and Feskov, G. V. "Flow Resistance of Gas-Oil Mixtures," Oil and Gas Jour. (Oct. 3, 1960) 28, No. 20, 148-49.

73. Van Wingen, N. "Pressure Drop for Oil-Gas Mixtures in Horizontal Flow Lines," World Oil (1949) 129, No. 7, 156.

74. Vogt, E. G. and White, R. R. "Friction in the Flow of Suspensions," Ind. Eng. Chem. (1948) 40, 1731-8.

75. Von Karman, T. "The Analogy Between Fluid Friction and Heat Transfer," Trans ASME. (1939), 61, 705-710.

76. White, P. D. "Horizontal Co-Current Two-Phase Two-Component Flow," Ph. D. Thesis, Univ. of Okla. (1954).

77. White, P. D. and Huntington, R. L. "Horizontal Co-Current Two-Phase Flow of Fluids in Pipe Lines," Petr. Engr. (Aug., 1955) D-40.

78. Wicks, Moye, III and Dukler, A. E. "Entrainment and Pressure Drop in Concurrent Gas-Liquid Flow: I. Air-Water in Horizontal Flow," AIChE Jour. (Sept., 1960) 6, No. 3, 463-8.

APPENDIX A

NOMENCLATURE

NOMENCLATURE

A	Multiplication constant in the Blazius equation, dimensionless
A	Area, sq ft
A_L	Cross-sectional area of pipe through which liquid is flowing, sq ft
A_1	Constant found by Nikuradse in the "universal velocity profile" equation, dimensionless
D	Pipe diameter, ft
$\Delta P/\Delta L$	Pressure gradient, lb/sq ft-ft of pipe
$(\Delta P/\Delta L)_G$	Term used by Martinelli, the pressure gradient if only the gas were flowing in the pipe, lb/sq ft-ft of pipe
$(\Delta P/\Delta L)_G$	Average pressure drop per length of pipe due to the gas plugs in Plug Flow, lb/sq ft-ft of pipe
$(\Delta P/\Delta L)_L$	Average pressure drop per length of pipe due to the liquid plugs in Plug Flow, lb/sq ft-ft of pipe
$(\Delta P/\Delta L)_{TP}$	Actual two-phase pressure gradient, lb/sq ft-ft of pipe
du/dy	Velocity gradient across pipe, 1/sec
e	Wall roughness height, ft
$F.S.I.$	Fraction of liquid shut-in in the pipe. The fraction of the pipe filled with liquid, dimensionless
Fr_{NO}	Froude Number, defined by Equation (27), dimensionless
f	Moody friction factor, dimensionless
f_c	Fanning friction factor, $f/4$, dimensionless
f_G	Moody friction factor for the gas plugs, dimensionless
f_L	Moody friction factor for the liquid plugs, dimensionless
f_{TP}	Two-phase Moody friction factor, defined by Equation (22), dimensionless

G	Mass velocity, lb/hr-sq ft
G_G	Superficial gas mass velocity, based on the total pipe cross sectional area, lb/hr-sq ft
G_L	Superficial liquid mass velocity, based on the total pipe cross sectional area, lb/hr-sq ft
$G_{L,eq.}$	Total equivalent liquid mass velocity, $G_L + G_G\sqrt{\rho_L/\rho_G}$, lb/hr-sq ft
g	Gravitational acceleration, ft/sec^2
g_c	Conversion factor in Newton's laws of motion, ft-lb mass/ lb force-sec^2
K.L.F.	Kinetic Liquid Fraction. The fraction of the kinetic energy of the system which is attributable to the liquid, defined in Equation (23), dimensionless
K	Constant in the Prandtl "universal profile" equation, dimensionless
L	Pipe length, ft
l	Prandtl mixing length, ft
m	Constant of exponentiation on the Reynolds Number in the Blazius equation, dimensionless
n	Constant of exponentiation on the liquid/gas viscosity ratio, equal to 0.30, dimensionless
P	Pressure, lb/sq ft
R	Ratio of the pressure drops predicted by the two Plug Flow equations, dimensionless
Re.NO.	Reynolds Number, dimensionless
r	Radius, ft
r_i	Radius at the gas-liquid interface, ft
r_o	Pipe radius, ft
U	Average or bulk velocity, ft/sec
U_G	Gas bulk velocity, based on the total cross-sectional area of pipe, ft/sec

$U_{G,eq.}$	Total equivalent gas bulk velocity, $U_G + U_{L\to G}$, ft/sec
U_L	Liquid bulk velocity, based on the total cross-sectional area of pipe, ft/sec
$U_{L\to G}$	Gas equivalent of the liquid bulk velocity, $U_L\sqrt{\rho_L/\rho_G}$, ft/sec
u	Local or point velocity, ft/sec
u_L	Liquid point velocity, ft/sec
u_w	Velocity at the wall where the laminar layer ends and the turbulent layer begins, ft/sec
u'	Velocity difference between neighboring layers in turbulent flow, ft/sec
u^*	Friction velocity, $\sqrt{\tau_0 g_c/\rho}$, ft/sec
u^+	u/u*, dimensionless
V_c	Volumetric flow rate in the center core of the pipe, cu ft/sec
V_G	Volumetric gas flow rate, cu ft/sec
$V_{G,eq.}$	Total equivalent volumetric gas flow rate, $V_G + V_{L\to G}$, cu ft/sec
V_L	Volumetric liquid flow rate, cu ft/sec
$V_{L\to G}$	Gas equivalent of the liquid volumetric flow rate, $V_L\sqrt{\rho_L/\rho_G}$, cu ft/sec
V_T	Total volumetric flow rate in the pipe, cu ft/sec
v'	Prandtl's interchange or eddy velocity, ft/sec
W_G	Gas mass flow rate, lb/hr
W_L	Liquid mass flow rate, lb/hr
y	Radial distance from pipe wall toward the center, ft
y_w	Thickness of the laminar layer, ft
y^+	$yu^*\rho/\mu$, dimensionless

Greek Letters

α	Martinelli liquid hydraulic radius term, accounts for the non-circular cross-section of the flow, dimensionless
μ	Viscosity, lb/ft-hr
μ_G	Gas viscosity, lb/ft-hr
μ_L	Liquid viscosity, lb/ft-hr
ρ	Density, lb/cu ft
ρ_G	Gas density, lb/cu ft
ρ_L	Liquid density, lb/cu ft
σ	Standard deviation, dimensionless
τ	Shear stress lb/sq ft
τ_o	Shear stress at the pipe wall, lb/sq ft

APPENDIX B

DERIVATION OF FRACTION SHUT-IN VERSUS KINETIC LIQUID FRACTION

DERIVATION OF FRACTION SHUT-IN VERSUS KINETIC LIQUID FRACTION

The Karman equation for the velocity profile may be simplified to two parts; the laminar layer

$$u^+ = y^+ \qquad y^+ < 11.62 \tag{1}$$

and the turbulent core

$$u^+ = 5.5 + 2.5 \ln y^+ \qquad y^+ > 11.62 \tag{2}$$

where $u^+ = u/u^*$
$y^+ = yu^*\rho/\mu$

The value of 11.62 for y^+ at the laminar-turbulent boundary was found by eliminating u^+ from the two equations and solving for y^+. When the definitions for u^+ and y^+ are inserted into Equation (2), the result is

$$u = 5.5u^* + 2.5u^* \ln(yu^*\rho/\mu) \tag{3}$$

The friction velocity, u^* may be related to the bulk velocity, U, and the friction factor, f.

$$u^* = U\sqrt{f/8} \tag{4}$$

So, substituting in Equation (3), the result is

$$u = 5.5\ U\sqrt{f/8} + 2.5\ U\sqrt{f/8} \ln\ (yU\sqrt{f/8}\ \rho/\mu) \tag{5}$$

Notice that the term, $y\rho U/\mu$, in the logarithm is in the form of a Reynolds Number. This can be expressed in terms of the usual pipe Reynolds Number ($DU\rho/\mu$) by multiplying and dividing by double the pipe radius ($2r_o$). The result is,

$$u = 5.5\ U\sqrt{f/8} + 2.5\ U\sqrt{f/8} \ln\ (Re\sqrt{f/32}\ y/r_o) \tag{6}$$

If a fluid is flowing at a given velocity, the Reynolds Number and the friction factor are constants, so these may be separated out, leaving only the dimensionless variable, y/r_o.

$$u = 5.5\ U\sqrt{f/8} + 2.5\ U\sqrt{f/8}\ \ln\left(Re\sqrt{f/32}\right) + 2.5\ U\sqrt{f/8}\ \ln(y/r_o) \quad (7)$$

In deriving the Continuous Flow shut-in equation, the liquid is assumed to be flowing only in the concentric annular ring and the gas only in the symmetrical cylindrical core. The radius at the interface between the two will be called r_i. We are interested in the fraction of the flow coming from the outer ring (the liquid fraction), however, this is most conveniently calculated indirectly, by calculating the flow in the inner cylinder and subtracting from the total flow. The flow in the inner cylinder, V_c, is,

$$V_c = \int_0^{r_i} 2\pi r u\, dr \quad (8)$$

Substituting for "u" from Equation (7), the result is,

$$V_c = 2\pi U\sqrt{f/8}\left[5.5\int_0^{r_i} r\,dr + 2.5\ln\left(Re\sqrt{f/32}\right)\int_0^{r_i} r\,dr + 2.5\int_0^{r_i} r\ln(y/r_o)\,dr\right] \quad (9)$$

The first two integrals are easily evaluated on sight. To evaluate the third integral it is necessary to remember that "y" is equal to $(r_o - r)$. To make the equation easier to integrate, the variable y/r_o can be changed to y'. The third integral in Equation (9) then becomes,

$$\int_0^{r_i} r \ln(y/r_o)\, dr = r_o^2 \int_0^{y_i'} (y'-1) \ln y'\, dy' \quad (10)$$

which, when evaluated at the limits, is

$$\int_0^{r_i} r\ln(y/r_o)\,dr = r_o^2\left[(y_i'/2)(2-y_i')\ln(1/y_i') - 1/4\,(3-y_i')(1-y_i')\right]$$

$$= r_o^2\left\{\left[1-(r_i/r_o)^2\right]\ln\left[r_o/(r_o-r_i)\right] - 1/2\left[2+(r_i/r_o)\right](r_i/r_o)\right\} \quad (11)$$

Thus Equation (9) when integrated, becomes

$$V_C = \pi r_i^2 (U\sqrt{f/8})\left[5.5 + 2.5 \ln (Re\sqrt{f/32})\right] + 2.5\pi r_o^2 (U\sqrt{f/8})\left\{\left[1-(r_i/r_o)^2\right]\ln\left[r_o/(r_o-r_i)\right] - \tfrac{1}{2}\left[2+(r_i/r_o)\right](r_i/r_o)\right\} \quad (12)$$

It is also necessary to calculate the total flow volume V_T. This includes the flow in the laminar layer as well as the turbulent core, so the volume integral will have to be divided into two parts. The radius at the boundary between the laminar and turbulent regions will be called r_b, and the total flow, V_T, is

$$V_T = \int_0^{r_b} 2\pi r u_T\, dr + \int_{r_b}^{r_o} 2\pi r u_L\, dr \quad (13)$$

where u_L = Laminer layer velocity, Equation (1).
u_T = Turbulent core velocity, Equation (2).

The first integral in this equation is evaluated in the same manner as Equations (8) and (9), and it becomes

$$\int_0^{r_b} 2\pi r u_T\, dr = \pi r_b^2 (U\sqrt{f/8})\left[5.5 + 2.5 \ln (Re\sqrt{f/32})\right] + 2.5\pi r_o^2 (U\sqrt{f/8})\left\{\left[1-(r_b/r_o)^2\right]\ln\left[r_o/(r_o-r_b)\right] - \tfrac{1}{2}\left[2+(r_b/r_o)\right](r_b/r_o)\right\} \quad (14)$$

For the second integral in Equation (13) the laminar layer velocity (Equation (1)) must be used. However, u^+ and y^+ can be related to the friction factor and the Reynolds Number, so Equation (1) may be rewritten,

$$u = U\sqrt{f/8}\,(Re\sqrt{f/32})(r_o-r)/r_o \quad (15)$$

Thus the second integral of Equation (13) is,

$$\int_{r_b}^{r_o} 2\pi r u_L\, dr = 2\pi U\sqrt{f/8}\,(Re\sqrt{f/32})\int_{r_b}^{r_o} (r/r_o)(r_o-r)\, dr = \pi U\sqrt{f/8}\,(Re\sqrt{f/32})(r_o^2/3)\left\{1-(r_b/r_o)^2\left[3-2(r_b/r_o)\right]\right\} \quad (16)$$

The total volume, V_T, is the sum of Equations (14) and (16).

$$V_T = \pi r_6^2 (U\sqrt{f/8}) \{5.5 + 2.5 \ln (Re\sqrt{f/32}) + \pi (r_6^2/3)(U\sqrt{f/8})(Re\sqrt{f/32}) \{1 - (r_6/r_0)^2 [3 - 2(r_6/r_0)]\} + 2.5\pi r_0^2 (U\sqrt{f/8}) \{[1 - (r_i/r_0)^2] \ln [r_0/(r_0 - r_i)] - 1/2 [2 + (r_i/r_0)](r_i/r_0)\} \quad (17)$$

The result desired from these computations is the Kinetic Liquid Fraction (K.L.F.) which is defined as follows.

$$K.L.F. = \frac{V_T - V_C}{V_T}$$

$$= \frac{\text{Equation (17)} - \text{Equation (12)}}{\text{Equation (17)}} \quad (18)$$

It can be seen that the term, $\pi(U\sqrt{f/8})$, is common to both Equations (12) and (17) so this term can be cancelled to simplify the expression of Equation (18). The equation is still long and unwieldy to write, so for convenience, the numerator and denominator will be listed separately.

$$\text{Numerator} = (r_6^2 - r_i^2)[5.5 + 2.5 \ln (Re\sqrt{f/32})] + r_6^2/3 (Re\sqrt{f/32}) \{1 - (r_6/r_0)^2 [3 - 2(r_6/r_0)]\} + 2.5 r_6^2 \{[1 - (r_i/r_0)^2] \ln [r_0/(r_0 - r_i)] - 1/2 [2 + (r_i/r_0)](r_i/r_0)\} - 2.5 r_6^2 \{[1 - (r_6/r_0)^2] \ln [r_0/(r_0 - r_6)] - 1/2 [2 + (r_6/r_0)](r_6/r_0)\} \quad (19)$$

$$\text{Denominator} = r_6^2 [5.5 + 2.5 \ln (Re\sqrt{f/32})] + r_6^2/3 (Re\sqrt{f/32}) \{1 - (r_6/r_0)^2 [3 - 2(r_6/r_0)]\} + 2.5 r_6^2 \{[1 - (r_6/r_0)^2] \ln [r_0/(r_0 - r_6)] - 1/2 [2 + (r_6/r_0)](r_6/r_0)\} \quad (20)$$

For any given Reynolds Number and friction factor, the thickness of the laminar layer, y_b, can be calculated from Equations (1) and

(2); thus the radius to the boundary, r_b, is known. Then the denominator (Equation (20)) can be evaluated as a constant; and it merely remains to evaluate the numerator at various gas-liquid interface radii, r_i. The Kinetic Liquid Fraction is,

$$K.L.F. = \frac{V_T - V_c}{V_T} = \frac{\text{Numerator (Equation (19))}}{\text{Denominator (Equation (20))}} \qquad (21)$$

and the fraction shut-in (F.S.I.) is equal to,

$$F.S.I. = \frac{r_o^2 - r_i^2}{r_o^2} \qquad (22)$$

Equations (21) and (22) have been evaluated at various Reynolds Numbers and interface radii and the results plotted in Figure IX.

APPENDIX C

PRESSURE DROP DATA

TABLE I

PRESSURE DROP DATA - WATER AND AIR

RUN NO. - - - = RUN NUMBER
G LIQUID - - = MASS VELOCITY OF THE LIQUID, LB/HR SQ.FT. OF PIPE
G GAS - - - - = MASS VELOCITY OF THE GAS, LB/HR-SQ.FT. OF PIPE
T - - - - - - = FLOWING TEMPERATURE, DEGREES RANKINE
PRESS AVE - - = AVERAGE PRESSURE, INCHES OF MERCURY
K.L.F.- - - - = KINETIC LIQUID FRACTION
DP/DL ACTUAL= ACTUAL PRESSURE GRADIENT, LB/SQ.FT.-FT. OF PIPE
DP/DL PRED = PREDICTED PRESSURE GRADIENT, LB/SQ.FT-FT. OF PIPE

RUN NO.	G LIQUID	G GAS	T	PRESS AVE	K.L.F.	DP/DL ACTUAL	DP/DL PRED
148	26,600	5,660	538	29.45	.1384	.154	.165
1	26,600	6,100	543	29.80	.1298	.168	.191
5	26,600	7,810	539	30.15	.1052	.224	.305
298	26,600	9,720	553	29.81	.0849	.379	.491
153	26,600	9,810	538	30.00	.0856	.421	.478
2	26,600	10,100	542	31.05	.0843	.505	.489
127	26,600	10,920	540	29.69	.0770	.477	.598
4	26,600	13,530	540	32.55	.0659	.813	.805
24	26,600	14,600	542	32.50	.0612	.870	.937
132	26,600	15,220	540	30.84	.0575	.954	1.07
3	26,600	16,810	541	33.75	.0546	1.23	1.16
25	26,600	23,200	538	36.20	.0416	1.74	1.94
133	26,600	28,200	540	35.14	.0340	2.75	2.85
26	26,600	40,300	534	46.40	.0276	3.98	4.00
138	26,600	40,500	540	40.54	.0256	4.88	4.67
10	37,100	8,270	536	30.50	.1351	.309	.395
7	37,100	10,250	537	31.35	.1132	.561	.571
9	37,100	13,300	536	32.60	.0913	.954	.884
8	37,100	16,530	537	34.05	.0762	1.23	1.25
149	45,300	5,680	538	29.55	.215	.196	.231
152	45,300	9,780	538	30.25	.1383	.533	.608
128	45,300	11,080	540	30.19	.1238	.673	.767
27	45,300	15,240	530	33.65	.0986	1.07	1.18
131	45,300	15,330	540	31.59	.0945	1.21	1.31
30	45,300	15,960	523	35.25	.0972	1.35	1.20
28	45,300	22,900	527	37.40	.0716	2.02	2.16
134	45,300	28,300	540	36.74	.0576	3.20	3.28
29	45,300	40,500	525	48.75	.0474	4.71	4.46
137	45,300	40,600	540	43.24	.0441	5.78	5.19
15	52,500	7,830	544	30.50	.1882	.449	.448
12	52,500	10,130	536	31.55	.1551	.561	.667
14	52,500	13,150	546	32.95	.1253	.870	1.03
13	52,500	17,210	548	35.20	.1015	1.54	1.55
17	64,100	10,320	543	32.10	.1807	.729	.778
19	64,100	13,400	541	33.40	.1479	.954	1.16

TABLE I

RUN NO.	G LIQUID	G GAS	T	PRESS AVE	K.L.F.	DP/DL ACTUAL	DP/DL PRED
18	64,100	17,000	542	35.40	.1234	1.51	1.64
150	82,300	5,600	538	29.75	.336	.365	.379
151	82,300	10,080	538	30.90	.222	.898	.922
22	82,300	10,400	546	32.56	.220	.898	.930
129	82,300	11,170	540	31.19	.2060	1.01	1.08
23	82,300	13,300	546	34.16	.1843	1.12	1.32
130	82,300	15,380	540	32.79	.1615	1.51	1.73
31	82,300	24,400	536	40.86	.1198	2.47	2.95
135	82,300	30,000	540	40.09	.0983	4.32	4.27
297	82,300	37,800	553	45.56	.0836	5.97	5.64
32	82,300	38,900	533	51.96	.0881	5.22	5.01
136	82,300	40,500	540	46.64	.0803	6.59	6.03
144	127,000	5,770	538	30.40	.433	.617	.637
147	127,000	10,290	538	32.35	.307	1.40	1.31
139	127,000	10,850	540	32.19	.294	1.46	1.43
44	127,000	12,740	530	37.55	.279	1.96	1.51
33	127,000	15,740	531	37.56	.239	2.02	2.08
141	127,000	15,780	540	34.69	.230	2.47	2.30
142	127,000	21,800	540	37.99	.1843	3.31	3.44
34	127,000	25,400	529	44.66	.1749	3.14	3.66
154	127,000	30,500	538	43.05	.1467	4.96	5.12
35	127,000	35,100	528	52.61	.1431	5.33	5.17
36	127,000	40,300	528	49.46	.1235	6.68	6.83
156	127,000	43,100	538	51.75	.1178	8.02	7.40
40	203,000	39,100	528	56.46	.1988	8.70	7.69
536	212,000	124	536	29.28	.9832	.187	.167
537	212,000	221	536	29.28	.9703	.220	.208
538	212,000	395	536	29.38	.9484	.310	.276
539	212,000	608	536	29.38	.9227	.374	.361
540	212,000	815	536	29.68	.8995	.433	.437
541	212,000	1,053	536	29.78	.8741	.517	.527
542	212,000	1,371	536	29.93	.8425	.635	.628
543	212,000	1,646	536	30.03	.8169	.749	.682
544	212,000	2,100	536	30.33	.778	.920	.761
545	212,000	2,420	534	30.98	.756	1.01	.807
546	212,000	2,910	534	31.18	.721	1.13	.892
547	212,000	3,560	534	31.28	.678	1.27	.997
548	212,000	4,240	532	31.78	.641	1.47	1.09
549	212,000	4,910	532	31.98	.608	1.54	1.20
550	212,000	5,880	530	32.18	.565	1.69	1.35
551	212,000	7,930	530	33.58	.496	1.84	1.62
552	212,000	8,780	528	34.18	.474	2.10	1.78
553	212,000	10,230	528	34.98	.439	2.31	2.06
554	212,000	13,000	528	36.18	.385	2.94	2.66
145	223,000	5,730	538	32.15	.582	1.51	1.45
140	223,000	10,700	540	34.99	.437	2.92	2.36

TABLE I

RUN NO.	G LIQUID	G GAS	T	PRESS AVE	K.L.F.	DP/DL ACTUAL	DP/DL PRED
146	223,000	11,020	538	35.35	.431	2.86	2.42
143	223,000	24,100	540	44.49	.279	5.58	5.29
38	223,000	30,700	528	49.11	.245	7.01	6.60
155	223,000	31,800	538	50.75	.239	7.18	6.87
39	223,000	32,200	528	50.61	.239	7.29	6.88
505	245,000	75	536	30.25	.99117	.386	.370
504	245,000	108	536	30.25	.98744	.204	.200
501	245,000	125	536	30.25	.98544	.231	.207
503	245,000	192	536	30.35	.9779	.231	.237
502	245,000	292	536	30.45	.9666	.231	.278
507	280,000	73	536	29.73	.99238	.306	.230
508	280,000	105	536	29.76	.98913	.306	.246
509	280,000	182	536	29.81	.98142	.335	.285
510	280,000	282	536	29.83	.9715	.363	.336
511	280,000	425	536	29.93	.9578	.435	.406
526	280,000	606	542	29.85	.9405	.471	.498
527	280,000	817	542	29.95	.9215	.580	.598
528	280,000	1,112	542	30.25	.8666	.698	.735
529	280,000	1,370	542	30.45	.8760	.820	.852
530	280,000	1,437	542	30.55	.8710	.933	.879
531	280,000	2,120	542	31.15	.8221	1.11	1.12
532	280,000	2,410	542	31.25	.8030	1.14	1.20
533	280,000	2,750	542	31.55	.782	1.29	1.28
534	280,000	3,430	540	31.95	.743	1.50	1.45
535	280,000	4,030	539	32.35	.713	1.68	1.60
514	345,000	385	534	30.56	.9690	.517	.507
512	345,000	471	531	30.66	.9625	.587	.554
515	345,000	524	535	30.66	.9584	.604	.587
513	345,000	581	534	30.66	.9541	.617	.619
516	345,000	694	536	30.86	.9458	.694	.681
517	345,000	808	537	30.96	.9375	.781	.743
518	345,000	975	537	31.11	.9257	.858	.833
519	345,000	1,134	538	31.26	.9147	.938	.917
520	345,000	1,306	537	31.51	.9034	1.03	1.01
521	345,000	1,556	537	31.66	.8873	1.14	1.13
522	345,000	1,701	537	31.91	.8785	1.30	1.20
523	345,000	1,988	537	32.11	.8613	1.42	1.35
524	345,000	2,550	537	32.51	.8298	1.64	1.58
525	345,000	2,730	536	32.71	.8203	1.81	1.64
				5.5 DEGREE INCLINE			
85	26,600	5,500	538	29.80	.1427	.589	
299	26,600	5,640	552	29.56	.1375	.617	
82	26,600	9,800	536	30.12	.0859	.701	
73	26,600	10,450	536	30.12	.0810	.645	.536
56	26,600	11,450	528	30.31	.0752	.617	.621

TABLE I

RUN NO.	G LIQUID	G GAS	T	PRESS AVE	K.L.F.	DP/DL ACTUAL	DP/DL PRED
57	26,600	15,910	529	31.41	.0562	1.04	1.11
58	26,600	21,900	530	33.21	.0426	1.68	1.88
59	26,600	29,300	531	35.41	.0331	2.69	2.97
74	26,600	29,300	536	35.52	.0330	2.66	2.98
60	26,600	37,400	531	38.91	.0274	4.10	4.17
61	26,600	44,100	528	41.87	.0242	5.39	5.13
62	41,600	39,400	528	41.87	.0416	5.33	4.83
300	45,300	5,770	552	29.76	.210	.743	
86	45,300	5,880	538	29.95	.210	.729	
83	45,300	9,850	536	30.37	.1378	.813	
303	45,300	9,880	551	30.31	.1358	.813	
67	45,300	10,530	528	30.27	.1308	.898	
66	45,300	15,260	528	31.57	.0959	1.29	1.27
65	45,300	21,100	528	33.37	.0732	2.02	2.11
75	45,300	29,300	536	37.42	.0563	3.39	3.38
64	45,300	30,800	528	38.07	.0545	3.81	3.58
63	45,300	39,400	528	42.07	.0452	5.39	4.97
301	78,100	5,580	552	30.06	.323	.925	
87	78,100	6,060	538	30.40	.309	.981	
302	78,100	9,960	551	31.06	.214	1.18	
68	78,100	10,080	528	31.17	.216	1.24	
84	78,100	10,390	536	31.32	.210	1.12	.913
76	78,100	11,360	536	31.27	.1952	1.23	1.06
69	78,100	15,190	528	33.07	.1582	1.57	1.59
77	78,100	15,980	536	32.97	.1505	1.71	1.77
78	78,100	22,400	536	36.12	.1176	2.75	2.82
70	78,100	22,500	528	36.57	.1178	2.69	2.76
79	78,100	30,100	536	39.87	.0938	4.35	4.17
71	78,100	30,400	528	40.57	.0941	4.26	4.11
80	78,100	38,200	536	44.87	.0795	5.92	5.53
72	78,100	39,800	528	45.37	.0775	5.83	5.76
81	78,100	43,100	536	47.52	.0731	7.01	6.37
304	127,000	5,790	551	30.71	.431	1.23	
88	127,000	5,910	538	31.05	.430	1.29	
90	127,000	10,250	538	32.65	.308	1.63	1.29
49	127,000	11,050	535	31.99	.291	2.13	
50	127,000	16,020	533	34.79	.228	2.24	2.32
51	127,000	18,480	532	38.99	.214	3.37	2.57
52	127,000	30,900	531	43.19	.1461	4.82	5.14
53	127,000	39,300	530	49.49	.1260	6.96	6.60
54	198,000	40,900	530	52.49	.1821	8.42	8.65
89	223,000	6,090	538	32.55	.568	2.13	
91	223,000	11,150	538	35.55	.429	3.20	2.44
55	223,000	33,900	527	48.71	.2260	7.85	7.64

TABLE I

12.4 DEGREE INCLINE

RUN NO.	G LIQUID	G GAS	T	PRESS AVE	K.L.F.	DP/DL ACTUAL	DP/DL PRED
308	26,600	5,410	551	30.16	.1439	1.29	
96	26,600	6,000	533	30.83	.1339	1.21	
101	26,600	9,930	533	30.58	.0857	1.15	
313	26,600	10,090	551	30.41	.0830	1.23	
102	26,600	10,660	533	30.73	.0805	1.09	
107	26,600	15,300	537	31.25	.0577	1.21	1.06
106	26,600	21,300	537	32.95	.0432	1.74	1.84
113	26,600	30,000	537	35.95	.0325	2.92	3.09
114	26,600	36,900	534	38.87	.0276	4.04	4.09
117	26,600	43,500	534	42.57	.0246	5.39	4.99
309	45,300	5,160	551	30.46	.232	1.46	
97	45,300	5,510	533	30.56	.223	1.43	
100	45,300	10,260	533	31.08	.1348	1.37	
312	45,300	10,490	551	30.96	.1301	1.43	
103	45,300	10,750	533	30.93	.1291	1.40	
108	45,300	15,610	537	31.95	.0937	1.63	1.33
109	45,300	21,900	537	34.10	.0709	2.24	2.24
112	45,300	30,000	537	37.35	.0550	3.48	3.54
115	45,300	36,600	534	41.17	.0478	4.29	4.50
118	45,300	42,800	534	44.87	.0429	6.40	5.42
310	78,100	4,940	551	30.96	.354	1.77	
98	78,100	6,000	533	31.08	.315	1.68	
99	78,100	10,170	533	31.78	.215	1.68	
311	78,100	10,250	551	31.86	.2112	1.88	
104	78,100	11,520	533	32.18	.1958	1.79	
105	78,100	15,340	533	33.23	.1566	1.91	1.63
110	78,100	22,600	537	36.30	.1158	3.00	2.86
111	78,100	30,200	537	40.25	.0938	4.26	4.16
116	78,100	39,200	534	45.72	.0785	6.20	5.63
119	78,100	42,400	534	47.92	.0746	7.12	6.13
305	127,000	5,920	551	31.51	.428	2.05	
92	127,000	6,090	544	31.33	.422	2.20	
307	127,000	10,390	551	33.31	.305	2.38	
94	127,000	10,820	541	33.03	.298	2.52	
122	127,000	11,860	534	33.52	.282	2.24	
121	127,000	16,410	534	35.52	.226	2.58	2.36
120	127,000	22,700	534	38.77	.1805	3.67	3.55
123	127,000	31,400	534	44.32	.1456	5.41	5.16
124	127,000	40,800	534	50.42	.1226	7.26	6.91
306	223,000	5,870	551	33.16	.577	2.80	
93	223,000	5,900	542	32.63	.575	2.80	
95	223,000	10,740	540	35.83	.439	3.70	
126	223,000	23,900	534	43.92	.281	5.95	5.24
125	223,000	31,900	534	51.02	.240	7.74	6.81

TABLE II

PRESSURE DROP DATA - NO. 10 S.A.E. OIL AND AIR

RUN NO. - - = RUN NUMBER
G LIQUID - - = MASS VELOCITY OF THE LIQUID, LB/HR-SQ.FT. OF PIPE
G GAS - - - = MASS VELOCITY OF THE GAS, LB/HR-SQ.FT. OF PIPE
T - - - - - = FLOWING TEMPERATURE, DEGREES RANKINE
PRESS AVE - = AVERAGE PRESSURE, INCHES OF MERCURY
K.L.F. - - - = KINETIC LIQUID FRACTION
DP/DL ACTUAL= ACTUAL PRESSURE GRADIENT, LB/SQ.FT.-FT. OF PIPE
DP/DL PRED = PREDICTED PRESSURE GRADIENT, LB/SQ.FT-FT. OF PIPE

RUN NO.	G LIQUID	G GAS	T	PRESS AVE	K.L.F.	DP/DL ACTUAL	DP/DL PRED
157	18,500	9,700	539	30.38	.0664	.729	.734
166	18,500	10,470	537	30.22	.0618	.898	.854
173	18,500	15,490	538	31.12	.0432	1.35	1.76
181	18,500	21,100	538	33.27	.0331	2.52	2.90
182	18,500	30,200	538	37.87	.0249	5.08	4.86
189	18,500	36,400	535	40.84	.0216	6.76	6.24
190	18,500	40,600	534	42.49	.01981	7.74	7.28
158	26,500	9,740	538	30.53	.0924	.842	.846
167	26,500	10,530	537	30.52	.0862	.962	.978
174	26,500	15,360	538	31.47	.0615	1.51	1.92
180	26,500	22,000	538	34.57	.0458	3.25	3.36
183	26,500	30,200	538	38.52	.0355	5.47	5.31
188	26,500	39,100	536	44.04	.0297	8.05	7.27
191	26,500	40,400	533	44.64	.0290	8.47	7.57
210	42,000	18,410	540	34.68	.0833	2.86	2.90
159	46,700	10,130	538	31.08	.1483	1.18	1.18
168	46,700	10,590	537	31.82	.1444	1.18	1.24
175	46,700	15,300	538	32.17	.1050	1.96	2.37
179	46,700	22,300	538	35.72	.0781	3.76	4.12
184	46,700	30,200	538	40.47	.0624	6.00	6.13
187	46,700	40,000	538	45.64	.0507	9.06	8.80
192	46,700	40,600	533	46.84	.0509	9.31	8.70
160	70,500	10,150	538	32.53	.212	1.80	1.48
169	70,500	10,270	537	32.52	.210	1.96	1.49
176	70,500	16,170	538	33.42	.1459	2.55	3.11
177	70,500	22,400	538	36.87	.1147	4.18	4.85
185	70,500	30,400	538	42.37	.0928	6.70	7.03
186	70,500	38,700	540	47.54	.0783	8.81	9.42
193	70,500	41,800	532	48.80	.0743	10.1	10.3
170	95,000	11,190	537	33.52	.250	2.83	2.09
171	95,000	16,400	537	35.72	.1902	3.59	3.58
209	95,000	18,340	540	37.68	.1770	3.81	4.08
178	95,000	22,200	538	38.87	.1530	4.71	5.35

TABLE II

5.5 DEGREE INCLINE

RUN NO.	G LIQUID	G GAS	T	PRESS AVE	K.L.F.	DP/DL ACTUAL	DP/DL PRED
224	6,500	5,420	540	29.36	.0421	.421	
206	18,500	5,200	540	29.58	.1157	.841	
245	18,500	5,750	541	30.08	.1065	.813	
250	18,500	9,750	541	30.63	.0663	1.09	
194	18,500	10,750	538	30.35	.0604	1.04	.901
220	18,500	13,640	540	31.16	.0487	1.29	1.38
225	18,500	15,060	537	31.80	.0449	1.63	1.62
230	18,500	22,300	537	34.90	.0321	3.23	3.06
235	18,500	29,300	537	38.60	.0259	5.13	4.49
239	18,500	38,800	537	44.35	.0211	7.85	6.46
204	18,500	39,100	540	44.73	.0209	8.05	6.55
246	26,500	5,500	541	30.08	.1516	.897	
211	26,500	7,330	540	30.28	.1186	.897	
251	26,500	9,720	541	30.73	.0926	1.21	
195	26,500	10,580	538	30.85	.0861	1.26	
199	26,500	11,250	542	30.06	.0802	1.23	1.14
219	26,500	13,540	540	31.56	.0692	1.37	1.52
226	26,500	15,890	537	32.50	.0606	2.05	1.98
213	26,500	17,530	540	33.08	.0555	2.13	2.33
231	26,500	22,400	537	35.90	.0459	3.34	3.32
236	26,500	29,200	537	39.35	.0372	5.55	4.86
242	26,500	38,500	537	45.65	.0306	8.33	6.86
243	26,500	41,500	537	47.75	.0291	9.28	7.47
215	37,500	5,200	540	29.68	.210	.729	
207	37,500	5,270	540	30.08	.209	1.15	
203	37,500	31,700	542	41.21	.0487	6.17	6.09
223	42,000	15,450	540	33.16	.0958	2.08	2.23
247	46,700	5,420	541	30.33	.2427	1.23	
252	46,700	9,650	541	31.28	.1546	1.51	
196	46,700	10,730	538	31.50	.1420	1.74	
214	46,700	11,860	540	31.68	.1304	1.63	1.54
218	46,700	13,530	540	32.26	.1171	1.85	1.91
227	46,700	15,900	537	33.50	.1034	2.52	2.42
232	46,700	21,900	537	37.10	.0808	4.18	3.83
237	46,700	30,000	537	41.95	.0639	6.06	5.83
241	46,700	39,700	537	49.15	.0530	9.37	8.06
244	46,700	41,700	537	50.85	.0514	10.15	8.46
222	60,500	12,880	540	32.36	.1530	2.13	2.01
248	70,500	5,890	541	30.88	.3101	1.65	
253	70,500	10,200	541	32.48	.210	2.24	
197	70,500	10,570	538	32.00	.204	2.24	
200	70,500	11,830	542	31.91	.1852	2.47	1.94
217	70,500	14,260	540	33.56	.1623	2.64	2.53
228	70,500	16,650	537	35.50	.1461	3.56	3.37

TABLE II

RUN NO.	G LIQUID	G GAS	T	PRESS AVE	K.L.F.	DP/FL ACTUAL	DP/FL PRED
221	70,500	20,030	540	37.26	.1269	3.67	3.99
233	70,500	23,200	537	39.30	.1144	5.13	4.82
238	70,500	31,600	537	45.05	.0921	7.35	7.36
205	70,500	38,900	540	49.23	.0792	9.54	9.20
249	95,000	5,960	541	31.48	.3767	1.99	
212	95,000	7,780	540	31.68	.317	2.08	
254	95,000	10,210	541	33.18	.266	2.83	
198	95,000	11,760	538	33.40	.240	3.03	2.28
201	95,000	12,100	542	32.71	.233	2.81	2.46
216	95,000	14,090	540	35.16	.213	3.48	2.88
202	95,000	16,070	542	34.91	.1908	3.65	3.58
229	95,000	16,680	537	35.90	.1880	4.26	3.65
240	95,000	20,800	537	39.55	.1630	5.13	4.73
234	95,000	22,900	537	41.00	.1528	5.78	5.33
			12.4 DEGREE INCLINE				
255	18,500	5,600	544	30.66	.1097	1.40	
286	18,500	10,030	537	31.18	.0653	1.60	
260	18,500	11,380	537	31.48	.0582	1.77	
269	18,500	16,170	537	32.68	.0425	2.02	1.86
270	18,500	23,200	538	35.40	.0312	3.48	3.27
278	18,500	30,200	534	39.70	.0256	5.30	4.59
279	18,500	38,200	534	44.30	.0214	7.74	6.25
283	18,500	42,500	534	47.30	.01997	9.20	7.09
256	26,500	5,340	544	30.86	.1566	1.94	
287	26,500	9,910	537	31.48	.0923	1.55	
261	26,500	11,440	537	31.88	.0815	1.76	
268	26,500	16,000	537	32.98	.0606	2.33	
271	26,500	23,200	538	36.30	.0446	3.84	3.49
277	26,500	30,200	535	40.50	.0366	5.55	5.01
280	26,500	39,000	534	45.90	.0304	8.30	6.90
284	26,500	42,200	534	48.30	.0288	9.37	7.58
257	46,700	5,680	544	31.36	.237	1.82	
288	46,700	10,620	537	32.48	.1453	2.38	
262	46,700	11,300	537	32.38	.1376	2.41	
267	46,700	15,860	537	34.28	.1047	3.06	
272	46,700	22,900	537	37.90	.0784	4.57	4.04
276	46,700	31,600	535	43.60	.0621	6.79	6.12
281	46,700	39,600	534	48.90	.0531	9.26	8.03
285	46,700	42,000	534	50.60	.0510	10.9	8.57
258	70,500	5,890	544	31.86	.313	2.30	
289	70,500	10,640	537	33.28	.206	2.97	
263	70,500	11,280	537	33.68	.1975	3.03	
266	70,500	16,140	537	35.58	.1502	3.76	
273	70,500	23,100	537	39.60	.1154	5.33	4.73

TABLE II

RUN NO.	G LIQUID	G GAS	T	PRESS AVE	K.L.F.	DP/DL ACTUAL	DP/LL PRED
275	70,500	31,700	536	45.90	.0928	7.85	6.93
282	70,500	39,300	534	51.30	.0804	9.87	8.88
259	95,000	6,200	544	32.41	.370	2.66	
290	95,000	10,590	537	34.08	.262	3.48	
264	95,000	11,420	537	34.48	.249	3.59	
265	95,000	16,520	537	36.98	.1917	4.54	
274	95,000	23,000	536	40.90	.1522	5.95	5.36

TABLE III

PRESSURE DROP DATA - DIETHYLENE GLYCOL AND AIR

RUN NO. - - = RUN NUMBER
G LIQUID- - = MASS VELOCITY OF THE LIQUID, LB/HR-SQ.FT. OF PIPE
G GAS - - - = MASS VELOCITY OF THE GAS, LB/HR-SQ.FT. OF PIPE
T - - - - - = FLOWING TEMPERATURE, DEGREES RANKINE
PRESS AVE - = AVERAGE PRESSURE, INCHES OF MERCURY
K.L.F.- - - = KINETIC LIQUID FRACTION
DP/DL ACTUAL= ACTUAL PRESSURE GRADIENT, LB/SQ.FT.-FT. OF PIPE
DP/DL PRED = PREDICTED PRESSURE GRADIENT, LB/SQ.FT-FT. OF PIPE

RUN NO.	G LIQUID	G GAS	T	PRESS AVE	K.L.F.	DP/DL ACTUAL	DP/DL PRED
569	26,500	4,180	540	29.04	.1693	.164	.148
570	26,500	5,460	540	29.19	.1351	.260	.222
571	26,500	7,280	540	29.44	.1053	.479	.392
676	26,500	8,110	546	29.73	.0956	.492	.485
572	26,500	9,340	539	29.84	.0847	.593	.627
573	26,500	11,490	539	30.34	.0705	.797	.917
677	26,500	12,420	546	30.73	.0655	.864	1.06
574	26,500	14,690	538	31.14	.0567	1.12	1.42
678	26,500	16,580	546	31.83	.0507	1.31	1.76
575	26,500	17,950	536	31.94	.0475	1.50	1.98
590	26,500	25,600	526	34.05	.0352	2.53	3.47
591	26,500	34,600	525	37.95	.0278	4.56	5.29
592	26,500	40,700	527	40.95	.0245	6.21	6.58
593	26,500	48,400	528	45.25	.0217	8.32	8.10
567	46,500	5,420	535	29.53	.218	.360	.304
566	46,500	6,940	535	29.93	.1800	.521	.469
565	46,500	9,030	534	30.33	.1453	.716	.748
564	46,500	11,620	534	31.03	.1179	.937	1.16
563	46,500	14,800	534	31.93	.0962	1.34	1.73
562	46,500	18,820	535	33.53	.0789	2.07	2.53
594	46,500	19,400	532	33.85	.0773	2.07	2.63
595	46,500	27,200	528	37.55	.0595	3.80	4.22
596	46,500	38,500	528	44.85	.0465	6.94	6.48
597	46,500	44,700	528	48.35	.0418	8.69	7.80
598	46,500	50,100	528	51.75	.0387	10.1	8.90
680	78,000	8,190	546	31.33	.240	1.18	.889
558	78,000	9,340	534	31.53	.219	1.34	1.06
559	78,000	12,130	534	32.63	.1804	1.66	1.59
681	78,000	12,640	546	32.53	.1725	1.70	1.75
560	78,000	15,090	537	33.73	.1521	2.11	2.22
682	78,000	16,850	546	34.53	.1388	2.46	2.66
561	78,000	18,770	536	35.43	.1289	2.85	3.05
599	78,000	20,300	528	35.55	.1215	2.95	3.40
600	78,000	28,500	528	40.15	.0946	4.71	5.33
601	78,000	37,100	528	45.95	.0791	7.02	7.36

TABLE III

RUN NO.	G LIQUID	G GAS	T	PRESS AVE	K.L.F.	DP/DL ACTUAL	DP/DL PRED
602	78,000	43,700	528	50.35	.0709	8.88	8.72
603	78,000	49,900	528	54.25	.0649	10.2	10.1
580	135,000	13,930	532	36.10	.259	3.18	2.67
674	135,000	16,060	546	36.80	.232	3.62	3.32
581	135,000	17,770	532	38.10	.220	4.07	3.65
585	135,000	20,400	529	37.93	.1969	4.08	4.49
582	135,000	20,700	530	40.20	.1989	4.57	4.37
604	135,000	22,800	540	40.65	.1839	4.74	5.09
586	135,000	28,000	527	42.03	.1589	5.39	6.61
605	135,000	29,000	538	45.85	.1583	6.21	6.57
606	135,000	36,200	537	51.65	.1381	7.93	8.28
587	135,000	38,000	523	49.13	.1310	7.53	7.13
607	135,000	44,200	537	56.85	.1209	9.74	10.4
588	135,000	44,700	524	54.33	.1188	9.19	10.7
608	135,000	46,500	537	58.75	.1173	10.3	10.9
584	210,000	17,440	530	42.80	.321	5.92	4.62
583	210,000	20,400	530	45.30	.294	6.58	5.42
609	210,000	29,700	537	52.55	.234	8.17	8.10
610	210,000	34,100	537	56.35	.217	8.87	9.27
611	210,000	38,900	537	59.35	.1991	9.91	10.7
				1.5 DEGREE INCLINE			
612	26,500	3,470	546	29.25	.1965	.356	
613	26,500	6,190	546	29.25	.1207	.441	
614	26,500	9,330	546	29.95	.0844	.605	.633
615	26,500	12,210	546	30.65	.0665	.836	1.03
616	26,500	16,830	546	31.65	.0499	1.37	1.83
630	26,500	20,400	544	33.05	.0425	1.97	2.46
631	26,500	27,200	544	35.55	.0333	3.22	3.83
632	26,500	34,400	544	39.95	.0281	5.22	5.17
633	26,500	42,200	544	43.65	.0241	7.07	6.78
617	78,000	4,950	546	30.15	.339	.677	
618	78,000	7,570	546	30.85	.253	1.19	
619	78,000	10,400	546	31.85	.201	1.44	1.29
620	78,000	14,040	546	32.95	.1590	1.98	2.06
621	78,000	17,860	546	35.05	.1329	2.70	2.27
634	78,000	19,030	544	35.35	.1264	2.84	3.18
635	78,000	27,500	544	40.45	.0967	4.64	5.15
636	78,000	33,800	544	45.05	.0842	6.30	6.51
637	78,000	41,000	544	50.15	.0741	8.09	8.09
622	135,000	4,040	546	30.85	.524	1.15	
623	135,000	8,500	546	32.85	.350	2.18	
624	135,000	12,090	546	34.55	.280	2.76	2.32
625	135,000	15,650	548	36.65	.236	3.47	3.22
626	135,000	18,750	548	38.85	.210	3.98	4.00

TABLE III

RUN NO.	G LIQUID	G GAS	T	PRESS AVE	K.L.F.	DP/DL ACTUAL	DP/DL PRED
627	135,000	20,300	544	39.55	.1992	4.04	4.39
628	135,000	26,400	544	43.95	.1673	5.57	5.99
629	135,000	33,000	544	49.65	.1461	7.19	7.53
			12.4 DEGREE INCLINE				
648	26,500	4,730	545	30.45	.1549	1.57	
649	26,500	8,200	545	30.65	.0959	1.51	
650	26,500	11,220	545	31.05	.0724	1.51	
651	26,500	14,090	547	31.65	.0590	1.80	
652	26,500	17,030	547	32.35	.0498	2.00	1.82
638	26,500	20,100	546	33.35	.0432	2.41	2.37
639	26,500	26,700	546	35.55	.0339	3.31	3.71
640	26,500	33,800	546	39.35	.0284	5.12	5.07
641	26,500	40,700	546	43.25	.0247	6.88	6.45
653	78,000	5,150	547	31.45	.334	2.25	
654	78,000	8,390	547	31.95	.237	2.40	
655	78,000	11,350	547	32.85	.1892	2.52	
656	78,000	14,500	547	33.65	.1560	2.80	
657	78,000	18,320	547	35.45	.1305	3.36	2.99
642	78,000	19,270	546	36.15	.1261	3.56	3.18
643	78,000	27,600	546	40.85	.0968	4.94	5.12
644	78,000	36,500	546	47.05	.0800	7.04	7.10
658	135,000	5,380	550	32.45	.458	2.86	
659	135,000	9,280	550	33.55	.332	3.20	
660	135,000	12,580	550	35.05	.273	3.52	
661	135,000	15,490	550	36.85	.238	3.97	3.16
662	135,000	19,100	550	39.25	.207	4.47	4.09
645	135,000	20,700	546	39.85	.1965	4.61	4.50
646	135,000	27,600	546	44.85	.1624	6.17	6.31
647	135,000	35,300	546	51.25	.1397	8.06	8.13

APPENDIX D

SHUT-IN DATA

APPENDIX IV

SHUT-IN DATA - WATER AND AIR

RUN NO.- - - = RUN NUMBER
G LIQUID - - = MASS VELOCITY OF LIQUID, LB/HR-SQ.FT. OF PIPE
G GAS - - - = MASS VELOCITY OF GAS, LB/HR-SQ.FT. OF PIPE
K.L.F. - - - = KINETIC LIQUID FRACTION
RE. NO. T.P. = TWO-PHASE REYNOLDS NUMBER
F.S.I. ACTUAL= ACTUAL FRACTION LIQUID SHUT-IN
F.S.I. PRED. = PREDICTED FRACTION LIQUID SHUT-IN

RUN NO.	G LIQUID	G GAS	K.L.F.	RE. NO. T.P.	F.S.I. ACTUAL	F.S.I. PRED.
85	26,600	5,500	.1427	43,400	.103	.102
96	26,600	6,000	.1339	46,200	.0942	.0965
24	26,600	14,600	.0612	101,000	.0461	.0465
107	26,600	15,300	.0577	107,000	.0514	.0385
57	26,600	15,910	.0562	110,000	.0378	.0376
114	26,600	36,900	.0276	220,000	.0276	.0206
60	26,600	37,400	.0274	222,000	.0224	.0204
26	26,600	40,300	.0276	220,000	.0299	.0205
30	45,300	15,960	.0972	108,000	.0940	.0595
87	78,100	6,060	.309	56,800	.142	.160
69	78,100	15,190	.1582	115,000	.0884	.0885
105	78,100	15,340	.1566	116,000	.0819	.0880
80	78,100	38,200	.0795	225,000	.0506	.0510
116	78,100	39,200	.0785	227,000	.0498	.0505
21	82,300	6,150	.326	59,000	.166	.166
32	82,300	38,900	.0881	214,000	.0584	.0555
54	198,000	40,900	.1821	250,000	.0865	.0995
40	203,000	39,100	.1988	233,000	.0993	.107
93	223,000	5,900	.575	90,500	.183	.222
89	223,000	6,090	.568	91,500	.200	.221
125	223,000	31,900	.240	214,000	.119	.124
55	223,000	33,900	.226	227,000	.0938	.117
47	349,000	6,110	.717	114,000	.237	.249

TABLE V

SHUT-IN DATA - NO. 10 S.A.E. OIL AND AIR

RUN NO.- - - = RUN NUMBER
G LIQUID - - = MASS VELOCITY OF LIQUID, LB/HR-SQ.FT. OF PIPE
G GAS - - - = MASS VELOCITY OF GAS, LB/HR-SQ.FT. OF PIPE
K.L.F. - - - = KINETIC LIQUID FRACTION
RE. NO. T.P. = TWO-PHASE REYNOLDS NUMBER
F.S.I. ACTUAL= ACTUAL FRACTION LIQUID SHUT-IN
F.S.I. PRED. = PREDICTED FRACTION LIQUID SHUT-IN

RUN NO.	G LIQUID	G GAS	K.L.F.	RE. NO. T.P.	F.S.I. ACTUAL	F.S.I. PRED.
255	18,500	5,600	.1097	1,950	.136	.153
245	18,500	5,750	.1065	2,010	.156	.150
225	18,500	15,060	.0449	4,740	.0964	.0865
269	18,500	16,170	.0425	4,990	.0871	.0830
279	18,500	38,200	.0214	9,750	.0464	.0450
239	18,500	38,800	.0211	9,900	.0518	.0440
247	46,700	5,420	.243	2,220	.197	.211
257	46,700	5,680	.237	2,280	.166	.209
267	46,700	15,860	.1047	5,130	.132	.130
227	46,700	15,900	.1034	5,170	.152	.130
281	46,700	39,600	.0531	9,950	.0689	.0795
241	46,700	39,700	.0530	9,980	.0764	.0790
249	95,000	5,960	.377	2,910	.222	.243
259	95,000	6,200	.370	2,970	.196	.245
202	95,000	16,070	.1908	5,720	.164	.171
265	95,000	16,520	.1917	5,690	.166	.174
229	95,000	16,680	.1880	5,790	.177	.171

TABLE VI

SHUT-IN DATA -- DIETHYLENE GLYCOL AND AIR

RUN NO.- - - = RUN NUMBER
G LIQUID - - = MASS VELOCITY OF LIQUID, LB/HR-SQ.FT. OF PIPE
G GAS - - - = MASS VELOCITY OF GAS, LB/HR-SQ.FT. OF PIPE
K.L.F. - - - = KINETIC LIQUID FRACTION
RE. NO. T.P. = TWO-PHASE REYNOLDS NUMBER
F.S.I. ACTUAL= ACTUAL FRACTION LIQUID SHUT-IN
F.S.I. PRED. = PREDICTED FRACTION LIQUID SHUT-IN

RUN NO.	G LIQUID	G GAS	K.L.F.	RE. NO. T.P.	F.S.I. ACTUAL	F.S.I. PRED.
612	26,500	3,470	.1965	3,820	.184	.186
675	26,500	4,180	.1690	4,470	.240	.166
648	26,500	4,730	.1549	4,870	.133	.159
676	26,500	8,110	.0956	7,920	.138	.114
614	26,500	9,330	.0844	8,950	.127	.105
650	26,500	11,220	.0724	10,400	.102	.0940
677	26,500	12,420	.0655	11,500	.0800	.0870
678	26,500	16,580	.0507	14,900	.0750	.0685
616	26,500	16,830	.0499	15,100	.0689	.0680
652	26,500	17,030	.0498	15,200	.0810	.0680
638	26,500	20,100	.0432	17,300	.0741	.0600
630	26,500	20,400	.0425	17,500	.0783	.0590
640	26,500	33,800	.0284	26,200	.0541	.0403
632	26,500	34,400	.0281	26,400	.0472	.0398
617	78,000	4,950	.339	6,550	.219	.217
679	78,000	4,950	.340	6,530	.293	.217
653	78,000	5,150	.334	6,670	.163	.217
680	78,000	8,190	.240	9,260	.184	.178
619	78,000	10,400	.2005	11,100	.152	.160
655	78,000	11,350	.1892	11,700	.136	.153
681	78,000	12,640	.1725	12,900	.135	.143
682	78,000	16,850	.1388	16,000	.100	.123
621	78,000	17,860	.1329	16,700	.113	.117
657	78,000	18,320	.1305	17,100	.114	.116
634	78,000	19,030	.1264	17,400	.116	.114
642	78,000	19,270	.1261	17,500	.119	.114
635	78,000	27,500	.0967	22,600	.0977	.0925
671	135,000	3,980	.529	7,270	.284	.255
622	135,000	4,040	.524	7,350	.253	.253
658	135,000	5,380	.458	8,400	.191	.239
672	135,000	7,370	.383	10,000	.270	.217
673	135,000	10,260	.313	12,300	.187	.194
624	135,000	12,090	.2800	13,700	.159	.183
660	135,000	12,580	.273	14,100	.155	.177

TABLE VI

RUN NO.	G LIQUID	G GAS	K.L.F.	RE. NO. T.P.	F.S.I. ACTUAL	F.S.I. PRED.
674	135,000	16,060	.232	16,600	.143	.161
626	135,000	18,750	.2100	18,300	.128	.149
662	135,000	19,100	.207	18,600	.135	.147
645	135,000	20,700	.1965	19,400	.137	.143
628	135,000	26,400	.1673	22,800	.123	.127